

Fas Ligand interacting proteins:
New insights into complex signaling networks

Dissertation
Zur Erlangung des Doktorgrades
der Mathematisch-Naturwissenschaftlichen Fakultät
der Christian-Albrechts-Universität zu Kiel

vorgelegt von
Jing Qian
aus Hangzhou, Volksrepublik China
2004

1. Referent: Prof. Dr. Thomas C.G. Bosch

2. Referent: PD.Dr. Ottmar Janßen

Tag der mündlichen Prüfung: 08 Juni 2004

Zum Druck genehmigt: Kiel, 08 Juni 2004

Der Dekan

Index

1. Introduction	1-13
1.1 FasL: a death factor and signal transducer	1
1.2 Regulation of transcription and differential sorting of FasL	7
1.3 Structural characteristics of FasL	8
1.4. Identification of interacting proteins	11
2. Aims of the study	14-15
3. Materials and methods	16-50
3.1. Materials	16-34
Cell biology	
3.1.1. Cells	16
3.1.2. Media and buffers	16
3.1.3. Antibodies	20
3.1.4. Factors and other reagents	22
Molecular biology	
3.1.5. Primers	22
3.1.6. Vectors	24
3.1.7. Other constructs	24
3.1.8. Enzymes	25
3.1.9. Buffers and other reagents	26
3.1.10. Kits for molecular biology	26
Biochemistry	
3.1.11. Buffers and Reagents	27
3.1.12. Antibodies	32
3.1.13. Other material	32
3.1.14. Equipments	33
3.2 Methods	35-50
Cell biology	
3.2.1. Cell culture	35
3.2.2. Isolation of cells	35
3.2.3. Functional analysis of cells	37
3.2.4. Cell transfection and selection	38
3.2.5. FACS analysis	39

Molecular biology	
3.2.6. Reverse transcription-polymerase chain reaction-based cloning_____	40
3.2.7. Subcloning_____	43
Biochemistry	
3.2.8. Purification of FasFc fusion protein _____	44
3.2.9. GST fusion protein expression and purification_____	44
3.2.10. Protein “pull down” assays _____	45
3.2.11. Immunoprecipitation _____	46
3.2.12. Cell stimulation and anti-phosphotyrosine western blotting _____	46
3.2.13. SDS-PAGE and western blot_____	46
3.2.14. <i>In vitro</i> kinase assay_____	47
Immunostaining and confocal microscopy	
3.2.15. Coverslips and cell preparation _____	47
3.2.16. Fixation_____	48
3.2.17. Staining _____	49
3.2.18. Laser scan confocal microscopy _____	49
3.2.19. Observation of living cells and video recording_____	50
4. Results_____	51-85
4.1. Reverse signal transduction of FasL in human T cells_____	51
4.1.1. Generation and functionality of a FasFc fusion protein _____	51
4.1.2. Crosslinked but not soluble FasL inhibits proliferation of PBMC _____	52
4.1.3. Crosslinked FasL inhibits proliferation of T cell blasts in the absence of exogenously added rIL-2 _____	53
4.1.4. FasL-engagement inhibits proliferation of freshly isolated human peripheral T cells _____	55
4.1.5. FasL-engagement blocks cell-cycle progression of freshly isolated human peripheral T cells _____	57
4.1.6. Exogenous IL-2 does not counteract FasL-induced inhibition of T cells_____	60
4.1.7. Enhanced proliferation upon FasL-engagement in T cell clones_____	61
4.1.8. FasL-engagement blocks cell-cycle progression of T cell clones _____	61
4.1.9. Inhibition of TCR/CD3-induced tyrosine phosphorylation by FasL-engagement _____	62

4.1.10. <i>In vitro</i> phosphorylation of a casein kinase 1 motif present in the FasL cytoplasmic tail _____	63
4.2. Defining FasL interacting proteins _____	65
4.2.1. The interaction of FasL with FCH/SH3 proteins is mediated by SH3 domains _____	67
4.2.2. FasL coprecipitates with FCH/SH3 proteins _____	68
4.2.3. FasL co-localizes with FCH/SH3 proteins _____	70
4.2.4. FCH/SH3 proteins co-localize with FasL in the lysosomal compartment _____	71
4.3. FasL interacts with Nck1: linking FasL and the cytoskeleton to the TCR/CD3 complex? _____	75
4.3.1. Degranulation and surface expression of FasL in T cells _____	75
4.3.2. Interaction of FasL with Nck1 _____	78
4.3.3. Co-localization of FasL with Nck1 in activated cytotoxic T cells _____	81
4.3.4. Co-localization of Nck1, FasL and Cathepsin D in the contact region between cytotoxic CD8 ⁺ T and target cells _____	82
4.4. Other FasL interacting proteins and the potential role in the regulation of FasL expression _____	84
5. Discussion _____	86-97
5.1. Reverse signal transduction of FasL in T cells _____	86
5.2. Defining FasL interacting proteins: the FCH/SH3 family _____	90
5.3. FasL interacts with Nck1: linking the cytoskeleton and the TCR/CD3 complex? _____	92
5.4. Other FasL interacting proteins: FLAFs _____	96
6. Summary _____	98-99
7. References _____	100-112
8. Appendix _____	113-117
8.1. Publications _____	113
8.2. Acknowledgements _____	115
8.3. Curriculum Vitae _____	116
8.4. Erklärung/Statement _____	117

Abbreviations

Amino acids

A	Ala	Alanine	I	Ile	Isoleucine	R	Arg	Arginine
C	Cys	Cysteine	K	Lys	Lysine	S	Ser	Serine
D	Asp	Aspartic acid	L	Leu	Leucine	T	Thr	Threonine
E	Glu	Glutamic acid	M	Met	Methionine	V	Val	Valine
F	Phe	Phenylalanine	N	Asn	Asparagine	W	Trp	Tryptophan
G	Gly	Glycine	P	Pro	Proline	Y	Tyr	Tryrosine
H	His	Histidine	Q	Gln	Glutamine			

Nucleotide

A	Adenosin	C	Cytosine	G	Guanine	T	Thymidine
----------	----------	----------	----------	----------	---------	----------	-----------

Unit

k = kilo-	(10 ³)	m = milli-	(10 ⁻³)	μ = micro-	(10 ⁻⁶)	n = nano-	(10 ⁻⁹)
bp	base pair	Bq	Becquerel				
°C	degree centigrade	Ci	Curie				
g	gram	h	hour				
l	liter	M	molar				
min	minute (')	sec	second (")				
U	unit	V	voltage				
v/v	volume per volume	w/v	weight per volume				

aa	amino acid
Ab	antibody
mAb	monoclonal antibody
pAb	polyclonal antibody
AICD	activation-induced cell death
ALPS	autoimmune lymphoproliferative syndrome
APC	antigen presenting cells

ARP2/3	actin related protein 2/3 complex
ATCC	American Type Culture Collection
ATP	adenosine 5'-triphosphate
BAP2β	BAI1-associated protein 2 beta
BES	<i>N, N'</i> , -bis(2-hydroxyethyl)-2-aminoethanesulfonic acid
BLAST	Basic Local Alignment Research Tool
BSA	bovine serum albumin
CD	cluster of differentiation
CD2AP	CD2 associated protein
CD2BP1	CD2 binding protein 1
cDNA	complementary deoxyribonucleic acid
CIP4	cdc42 interacting protein 4
CK1	casein kinase 1
CRDs	cystein-rich domains
cpm	counts per minute
CTL	cytotoxic T lymphocyte(s)
CTSD	Cathepsin D
DMEM	Dulbeccos minimum essential medium
DNA	deoxyribonucleic acid
dNTP	deoxynucleoside triphosphate
EBV	Epstein-Barr virus
<i>E.coli</i>	<i>Escherichia coli</i>
EDTA	ethylenediaminetetraacetic acid
EGTA	ethylene glyco-bis(β -aminoethylether)- <i>N, N, N', N'</i> -tetraacetic acid
E/T	effector to target cell ratio
EtBr (EB)	ethidium bromide
FACS	fluorescence-activated cell sorting
FAP1	Fas-associated phosphatase 1
FasL	Fas ligand (=CD95L)
FBP	formin binding protein
FBS	fetal bovine serum
FCH	cdc15/Fes/CIP4 homology
FITC	fluorescein isothiocyanate
FLAF	Fas-ligand associated factor

c-FLIP	cellular FLICE-inhibitory protein
FSC	forward scatter
<i>g</i>	gravity
<i>gld</i>	generalized lymphoproliferative disease
GFP	green fluorescent protein
GST	glutathione-S-transferase
Grb2	growth factor-receptor binding protein 2
HEPES	<i>N</i> -2-hydroxyethylpiperazine- <i>N'</i> -2-ethanesulfonic acid
HRP	horseradish peroxidase
HYP A	huntingtin-interacting protein A
hrIL-2	human recombinant interleukin 2
IS	immunological synapse
LAMP1	lysosome-associated membrane glycoprotein 1
<i>lpr</i>	lymphoproliferation
LSM510	Zeiss laser scanning microscope 510
MALDI-TOF	matrix-assisted laser desorption ionization time-of-flight
β-ME	β -mercaptoethanol
MP	metalloproteinase
mRNA	messenger ribonucleic acid
MWCO	molecular weight cutoff
MW	molecular weight
NCBI	National Center for Biotechnology Information
NGF	nerve growth factor
NP-40	Nonidet-40
PAC SIN	protein kinase C and casein kinase substrate in neurons
PAGE	polyacrylamide gel electrophoresis
PBMC	peripheral blood mononuclear cell(s)
PBTC	peripheral blood T lymphocyte(s)
PBS	phosphate-buffered saline
PCR	polymerase chain reaction
PE	phycoerythrin
PHA	phytohemagglutinin
PHA blasts	phytohemagglutinin-activated lymphoblasts
RhoGAP C1	Rho-GTPase-Activation hematopoietic protein C1

PI	propidium iodide
PIPES	piperazine- <i>N,N'</i> -bis(2-ethanesulfonic acid)
PTK	protein-tyrosine kinases
PTP	protein-tyrosine phosphatase
PRD	proline rich domain
PSTPIP1	proline, serine, threonine phosphatase interacting protein
RNA	ribonucleic acid
RNase	ribonuclease
SDS-PAGE	sodium dodecyl sulfate polyacrylamide gel electrophoresis
SH	Src homology
SH3P12	sorbin and SH3 domain containing 1
Sos	Son of sevenless
SRBC	sheep red blood cell(s)
THDs	TNF homology domains
TIL	tumor-infiltrating lymphocytes
<i>T_m</i>	melting temperature
TCR	T cell receptor
TGN	trans-Golgi network
TNF	tumor necrosis factor
TNF-R	tumor necrosis factor receptor
TPA/PMA	Phorbol-12-myristate-13-acetate
WASP	Wiskott Aldrich Syndrome Protein
WAVE	WASP family Verprolin-homologous protein
WIP	WASP interacting protein

1. Introduction

Fas ligand (FasL, CD95L, Apo-1L, CD178, TNFSF6, APT1LG1) is the key death factor of receptor-triggered programmed cell death in immune cells. FasL/Fas-dependent apoptosis plays a pivotal role in activation-induced cell death, termination of immune responses, elimination of autoreactive cells, cytotoxic effector function of T cells and NK cells, and the establishment of immune privilege and tumor counterattack. A dysregulation of FasL expression has severe impact on the maintenance of immune homeostasis and defense. Moreover, it was recently shown that FasL serves as a costimulatory receptor for T cell activation. The molecular mechanisms underlying the multiple roles of FasL are completely unsolved. It is not known whether FasL ligation induces a "direct" signal, e.g. leading to a change in phosphorylation of the cytosolic part of the molecule, or whether the regulation of activation signals is a more "indirect" result of protein-protein-interactions. In the latter scenario, a unique polyproline region located in the membrane-proximal part of FasL was shown to be required for a directed transport and localization of FasL. Over the past few years, this group and others identified several FasL interacting molecules that all bind via Src homology 3 or WW domains to the proline-rich region of FasL. The detailed evaluation of cell-type or stimulation-dependent association of FasL with the numerous potential proline-rich region-interacting proteins will help to better position the molecule in the complex net work of signaling, cytoskeletal and transport elements.

1.1. FasL: a death factor and signal transducer

A death factor for immune cell cytotoxicity and immune system homeostasis

The Fas ligand is a 281 amino acid long (approximal 40 kDa) type II transmembrane protein of the TNF family of death factors¹. It was initially identified as the binding partner for CD95/Fas/Apo-1 with a primary death-inducing function. The binding of FasL to Fas transmits a signal to the cytoplasm that leads to activation of caspase 8 which in turn initiates a cascade of caspase activation leading to morphological changes of the cells and nuclei, as well as to degradation of the chromosomal DNA². The activity of FasL/Fas is best documented in the regulation of peripheral tolerance, associated with cytotoxic activity of T cells and NK cells and to terminate the immune response via activation-induced cell death (AICD) (Fig. 1.1.)

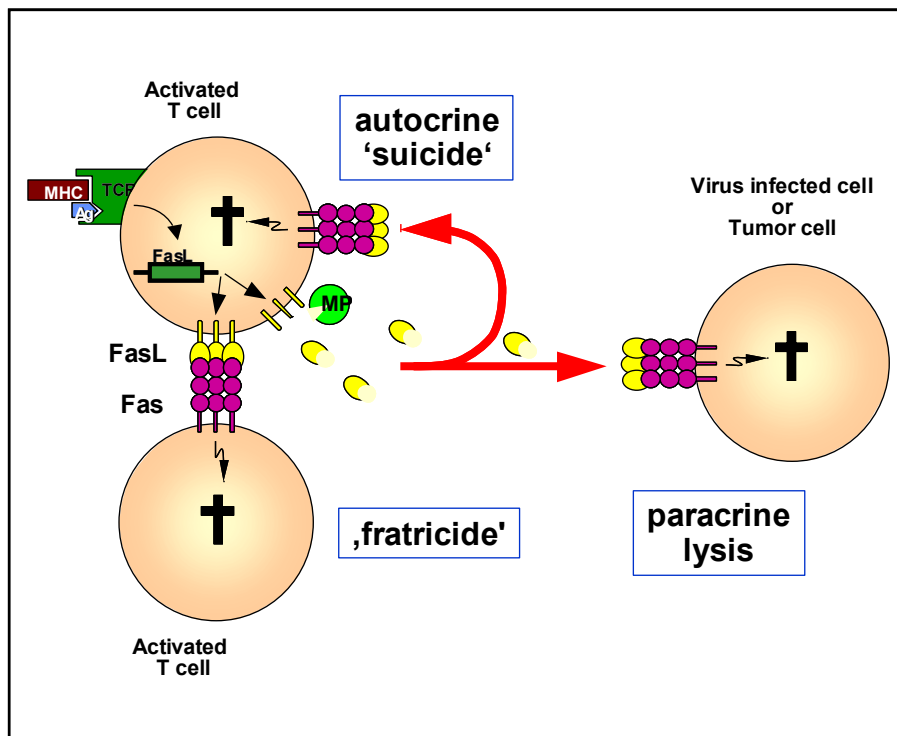


Fig. 1.1. FasL/Fas in immune system: cytotoxic effects and activation induced cell death of T cells. Stimulation of activated T cells through the TCR/CD3 complex results in the rapid up-regulation of FasL and Fas expression. FasL is used to destroy virus infected cells or tumor cells. The binding of FasL to the surface-expressed Fas molecule on the same or on neighboring cells triggers Fas dependent death signaling. Due to membrane folding or, alternatively, FasL cleaved by metalloproteases (MP), FasL/Fas interactions result in both autocrine "suicide" and paracrine "fratricide".

In mature T cells, FasL is expressed and regulated differentially in individual T cell subsets. On CD4⁺ cells, FasL appears as a transmembrane receptor of Thelper1 (and of some Thelper2) cells following T cell receptor (TCR) stimulation by antigen, anti-TCR/CD3 antibodies, mitogenic lectins, bacterial superantigens or other stimuli such as phorbol esters and calcium ionophore treatment^{3,4}. Since AICD can be efficiently blocked by using Fas-Fc fusion proteins in such cells, FasL was characterized as a major effector molecule in the AICD regulating the termination of T cell responses and preventing autoimmunity⁵⁻⁷. For CD4⁺ T helper2 cells, a reduced expression or absence of FasL under similar conditions was reported that explained resistance of such clones to AICD^{8,9}. However, further mechanisms at the level of transcription or beyond have been suggested to render these T helper2 cells unresponsive to Fas-mediated cell death^{4,10}. Thus, several reports indicate a role for PI-3 kinase modifying

Fas-associated caspase activity¹¹⁻¹³, for the Fas-associated phosphatase 1 (FAP1)¹⁴, or for a differential regulation of c-FLIP_{short}^{15,16} in the regulation of Th2-resistance.

Besides, FasL is expressed in Natural Killer cells where it can be further upregulated by CD16 engagement or cytokines including IL-2 and IL-12¹⁷⁻²⁰. Importantly, in cytotoxic T cells (and NK cells), FasL is expressed and synthesized upon primary stimulation and then directed to and stored in specialized secretory lysosomes/granules^{21,22}. Such secretory vesicles also contain cytotoxic proteins such as poreforming perforin and granzyme-type proteases. Upon contact with a (e.g. virally infected) target cell, the TCR-derived signal will lead to a redistribution of cytoskeletal elements and result in the release of these cytotoxic molecules into the immunological synapse²³. In theory this could be accompanied by a directed surface expression of FasL with binding to Fas on the target cell or, alternatively, shedding of FasL in the presence of a metalloproteinase. Similarly, although less well studied, high levels of intracellular FasL have been detected in monocytic cells with an inducible release upon activation by immune complexes, PHA, or superantigen²⁴.

During T cell development and maturation, FasL is discussed to be involved in negative selection in concert with other molecules including CD5, CD28 and CD43²⁵. In this context, FasL is supposed to act as an effector molecule leading to the deletion of autoreactive Fas-positive thymocytes²⁶. In contrast, other findings indicate that Fas/FasL effects are involved in peripheral but not thymic deletion of T lymphocytes²⁷ (reviewed in²⁸).

Immune privilege and tumor counterattack

Although still a matter of debate, FasL-expression has been associated with the establishment of immune privilege and tumor survival²⁹. As an indication of immune privilege, over the past years constitutive or inducible membrane expression of FasL was shown for numerous cell and tissue types including the eye^{30,31}, testis³² and/or mature spermatozoa³³, uterus and placenta^{34,35}, lung³⁶, thyrocytes^{37,38}, keratinocytes (upregulated by UV-B light)³⁹, CD68⁺-histiocytes in the dermis⁴⁰, neutrophils⁴¹, mature erythroblasts⁴², breast epithelial and vascular endothelial cells⁴³⁻⁴⁵, astrocytes (upregulated by IL-1, IL-6, TNF- α and IFN- γ)⁴⁶, microglia (downregulated by IFN- γ)⁴⁷ and intervertebral discs⁴⁸. The assumption, however, that FasL also confers immune

privilege and organ transplants^{32,49} has been challenged by studies indicating a differential pro- or anti-inflammatory effect of FasL depending on the microenvironmental context⁵⁰.

Moreover, the constitutive expression of relatively high levels of (trans)membrane (mFasL) or the secretion of soluble FasL (sFasL) is regarded as a mechanism to ensure tumor survival by blocking immune defense mechanisms⁵⁰⁻⁵⁶. Hahne and colleagues reported that although tumor-specific cytolytic T cells directed against well defined antigens are present in the population of tumor-infiltrating lymphocytes (TIL) or can even be detected in peripheral blood of melanoma patients, obviously the melanoma cells escape immune elimination⁵⁷. When melanoma cells were analyzed for the expression, both mFasL (40 kDa) and the sFasL(27 kDa) were detected whereas normal melanocytes did not express FasL. Since melanoma TIL mostly showed an activated phenotype (expressing Fas), it was proposed that transformed melanocytes induce apoptosis of Fas-sensitive TIL. As a proof of principle, FasL-positive mouse melanoma cells led to rapid tumor formation when injected into normal mice but to delayed tumor formation in Fas-deficient animals⁵⁷. In this regard, tumors could generate their immune privileged microenvironment.

Physiology and pathophysiology - genetic defects

Under physiological conditions, FasL is implicated in the control of erythroid differentiation⁵⁸, angiogenesis in the eye⁵⁹, skin homeostasis⁶⁰ and CTL-mediated killing of virally infected or transformed cells⁶¹. Furthermore, FasL expression can be induced in a variety of cell types by stress including heat shock, exposure to chemotherapeutic agents or radiation, growth factor withdrawal and viral infection⁶². If not controlled properly, many of these functions can lead to tissue destruction and on the long run to autoimmune diseases.

The lymphoproliferation (*lpr*) and generalized lymphoproliferative disease (*gld*) are naturally occurring mutations in mice^{63,64}. The *lpr* strain is characterized by an almost complete defect of Fas expression, the *lpr*^{cg} mutation allows the expression of a non-functional protein. In the *gld* mouse, a missense mutation in the extracellular domain of FasL abrogates its function. The phenotype of these mice is similar with developing nephritis, hypergammaglobulinemia and antinuclear antibodies in addition to

lymphadenopathy. With age, these mice accumulate CD4⁻CD8⁻TCR $\alpha\beta$ ⁺ T cells in the peripheral lymphocytes.

The phenotype of *Fas*^{-/-} mice, obtained by targeted mutation⁶⁵ is more severe than *gld* or *lpr* mice. In addition to massive production of lymphocytes, the Fas-null mice show substantial liver hyperplasia accompanied by the enlargement of nuclei in hepatocytes. Germline deletion of the FasL gene results in an unexpectedly severe phenotype⁶⁶. *FasL*^{-/-} mice exhibit an extreme splenomegaly and lymphadenopathy associated with lymphocytic infiltration into multiple organs and autoimmune disease that lead to the premature death at 4 months of age of >50% of the homozygous mice.

In human, direct defects in FasL/Fas result in specific forms of autoimmune lymphoproliferative syndrome (ALPS). ALPS is defined by functional analysis of lymphocyte sensitivity to Fas-induced apoptosis *in vitro*. T cells from ALPS patients can exhibit complete Fas-induced apoptosis (ALPS 0), consequence of a complete expression deficiency, partial Fas-induced apoptosis defect associated with normal or slightly reduced Fas expression (ALPS I and II), and finally normal Fas-induced apoptosis (ALPS III). Phenotype and genetic basis of these functional groups are diverse (See a summary in table 1.1, adapted from Rieux-Laucat et al.⁶⁷). Concerning FasL, loss of FasL gives rise to ALPS1b. This human genetic disease and its mouse model (*gld*) lead to a failure of apoptosis and aberrant T cell accumulation.

Table 1

ALPS	Genotype	Phenotype onset/ severity	Death-receptor defect	Mouse model
0	Homozygous Fas mutations	Prenatal/severe	Complete Fas expression and function defect	<i>lpr/lpr</i> ; Fas ko
Ia	Heterozygous Fas mutations	Childhood/moderate–severe, AI	Partial Fas function defect	<i>lpr^{tg}/lpr^{tg}</i>
Ib	Heterozygous FasL mutations	Adulthood/SLE	None	<i>gld/gld</i>
II	Caspase-10 mutations	Childhood/moderate, AI	Partial Fas, TNF RI, Trail R 1, 2, DR3. Function defect	Unknown
III	?	Childhood/moderate, AI	Unknown	Unknown

AI: autoimmunity; SLE: systemic lupus erythematosus.

Table. 1.1. Phenotype and genetic basis of ALPS patients.

A bidirectional signaling transducer in mature T cells and thymocytes

A series of reports employing mice defective for FasL (*gld*) or Fas (*lpr*; *lpr^{tg}*) recently suggested a costimulatory or modulatory function in the context of T cell activation for FasL in both CD8⁺ and CD4⁺ T cells⁶⁸⁻⁷¹. While CD4⁺ cells showed a reduction in

TCR/CD3-induced cell cycle progression and later entered apoptosis, CD8⁺ cells required the FasL-costimulation to rapidly progress through the cell cycle, resulting in proliferation and acquisition of cytolytic effector function⁶⁸⁻⁷¹. In all studies published so far, FasL reverse signaling seems to require a concomitant TCR engagement. Besides, Boursalian and Fink recently described Fas Ligand as an accessory molecule during positive selection⁷². They reported that in some (but not all) strains of TCR transgenic mice on a *gld*-background, T cell development is severely impaired. However, only positive selection seems to be altered whereas negative selection and death by neglect are not affected. The nature of the costimulatory signal delivered through FasL is unknown, although the structure of FasL suggests signaling capacity (as discussed in detail below). FasL could serve as a costimulatory molecule to either directly interfere with TCR triggered signal or by interfering with classical costimulatory molecules such as CD28 (Fig. 1.2).

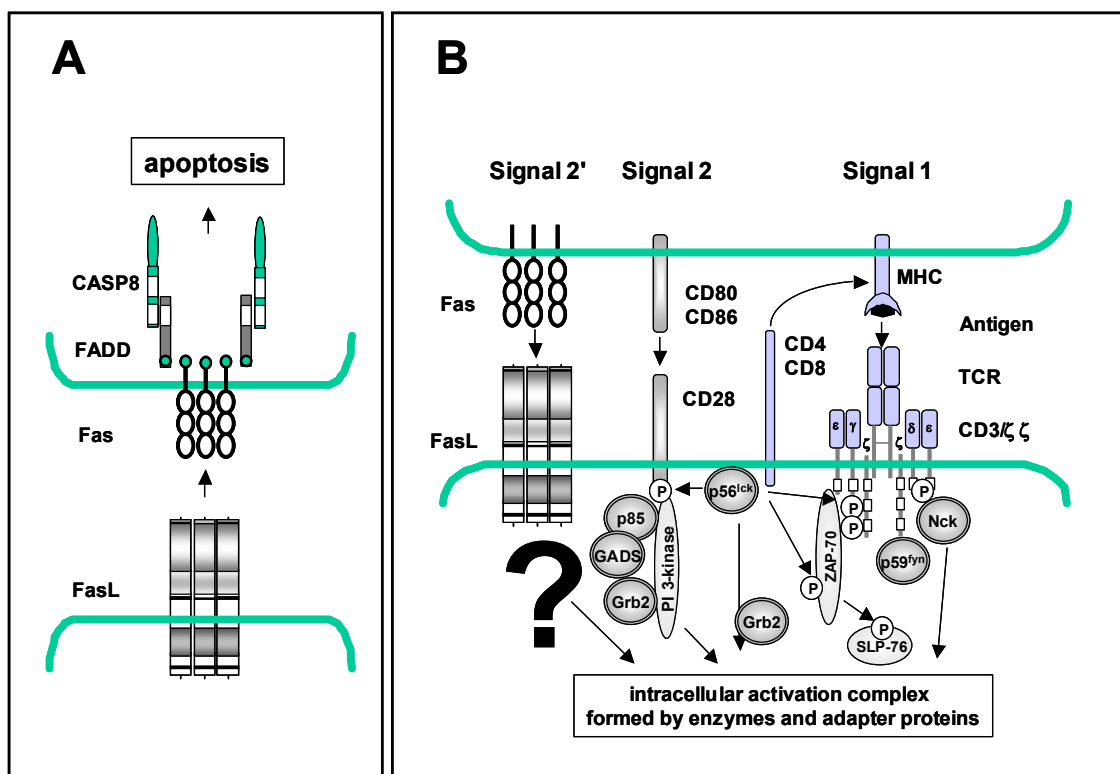


Fig. 1.2. FasL as a bifunctional membrane receptor. A. FasL trimers function as death factor to trigger Fas-induced apoptosis via FADD and caspase activation. This is the key event during activation-induced cell death, it plays a major role in target cell cytolysis, in the establishment of immune privilege, and during tumor counterattack. B. FasL as a costimulatory molecule? By virtue of assembling with a number of proteins (double-circled) required for TCR-dependent activation, FasL may alter the TCR/CD3 stimulus in different ways. In such a scenario, FasL could serve as a costimulatory molecule to either directly interfere with signal 1 given by the TCR or by interfering with signal 2 given by classical costimulatory molecules such as CD28.

1.2. Regulation of transcription and differential sorting of FasL

The signaling required for FasL message and protein induction in T cells follows the regular pathway of T cell activation with an early engagement of Src-type tyrosine kinases. In fact, inhibition of Src kinases blocks FasL expression in AICD-sensitive cells⁷³. The TCR-triggered induction of FasL may also be altered by costimulatory or accessory signals. In some T cell clones ligation of CD4 interferes with the composition of the regular TCR-associated signaling complex^{74,75}. As far as transcriptional regulation of FasL is concerned, many of the classical transcription factors have been shown to be involved under different conditions (see⁷⁶ for review). NFAT, NF- κ B, c-myc, IRF-1, Egr-3 mediate FasL induction upon T cell activation, e.g. in the context of AICD⁷⁷⁻⁸¹. Egr factors also contribute to FasL expression in double negative thymocytes⁸². These factors display different binding activities to Egr sites in the FasL promoter of Th1 and Th2 cells and thereby discriminate the two populations with regard to their AICD-sensitivities⁸³. The AP-1 complex increases FasL message following cellular stress⁸⁴ and forkhead transcription factors have been implicated upregulation and expression of FasL upon growth factor withdrawal^{76,85}.

In cytotoxic T cells and NK cells, newly synthesized FasL is targeted to so-called secretory lysosomes¹⁷. Upon recognition of an antigen presenting or target cell, those secretory lysosomes are transported to the immunological synapse, exhibiting their contents and membrane bound proteins to the site of interaction. In this regard the packaging of Fas ligand to secretory lysosomes ensures a rapid and accurate release of this protein to the immunological synapse²³. FasL is not only expressed in cells of the hematopoietic lineage, but also in a number of non-hematopoietic cell types. However in most non-hematopoietic cells FasL is expressed directly on the plasma membrane without being first sorted to lysosomes⁸⁶. The differential expression has important biological consequences i.e. in context of the establishment of immune privilege (see above).

Unlike other proteins that are sorted to the lysosomal compartment by di-leucine or tyrosine-based sorting motifs^{87,88}, Griffiths and colleagues convincingly showed that FasL is targeted to secretory lysosomes via the proline-rich domain (PRD)⁸⁶. Upon transfection, the presence of the PRD is sufficient to sort FasL to secretory lysosomes

whereas deletion of the PRD, but not of tyrosine or di-leucine motifs in the tail of FasL (7Y-9Y-13Y and 29V-30L), results in surface expression⁸⁶. A model of FasL sorting pathways in cells with secretory lysosomes versus conventional lysosomes is adapted⁸⁶ and shown in Fig. 1.3. Although in the meantime a number of possible interaction partners of FasL have been identified, the exact molecular mechanisms guiding FasL either to the secretory lysosomes or the plasma membrane remain unknown.

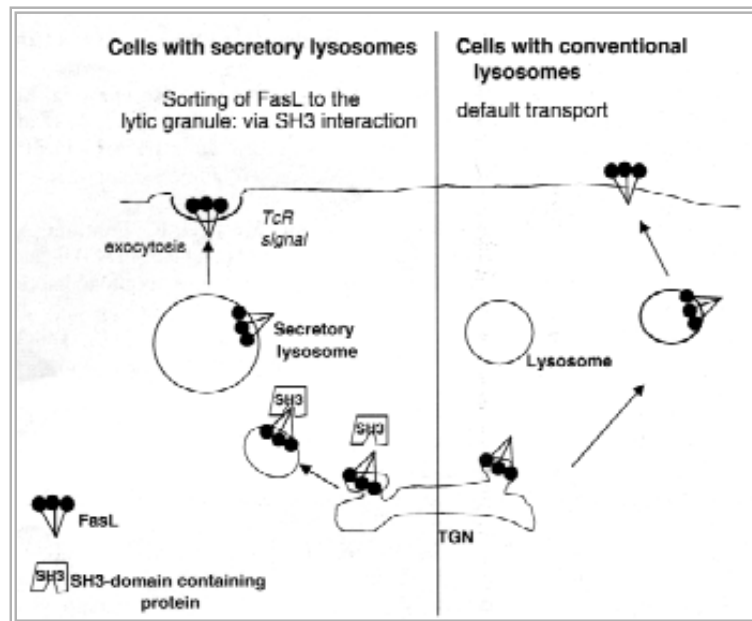


Fig. 1.3. Model of FasL sorting pathways in cells with secretory lysosomes versus conventional lysosomes. FasL exists the biosynthetic pathway at the trans-Golgi network (TGN). In secretory cells, a-SH3-domain-containing protein sorts FasL, via its proline-rich domain, to the secretory lysosomes. The absence of this interaction in non-secretory cells results in sorting of FasL to the plasma membrane via the default exocytosis pathway. Delivery of FasL to the plasma membrane in hematopoietic secretory cells only occurs during activation (e.g. stimulation via the TCR).

1.4. Structural characteristics

The Fas ligand is a 281 amino acids (278 in the mouse) containing type II transmembrane protein belonging to the tumor necrosis factor (TNF)/nerve growth factor (NGF) family which includes TNF, lymphotoxin, CD40L, 4-1BBL, TRAIL, OX40L, CD27L, CD30L, TRANCE and others⁸⁹. At the amino acid level, FasL is well conserved between species with the murine and human FasL being 76.9% identical and functionally interchangeable⁹⁰.

As mentioned before, the molecular basis for the postulated reverse signaling capacity of FasL and the exact regulatory molecules guiding FasL either to the secretory lysosomes or the plasma membrane still remain unknown. However, two motifs present in the cytoplasmic part of FasL are likely to be involved in the regulation of both processes: a casein kinase 1 (CK1) substrate motif and a proline-rich domain (PRD) (Fig 1.4.).

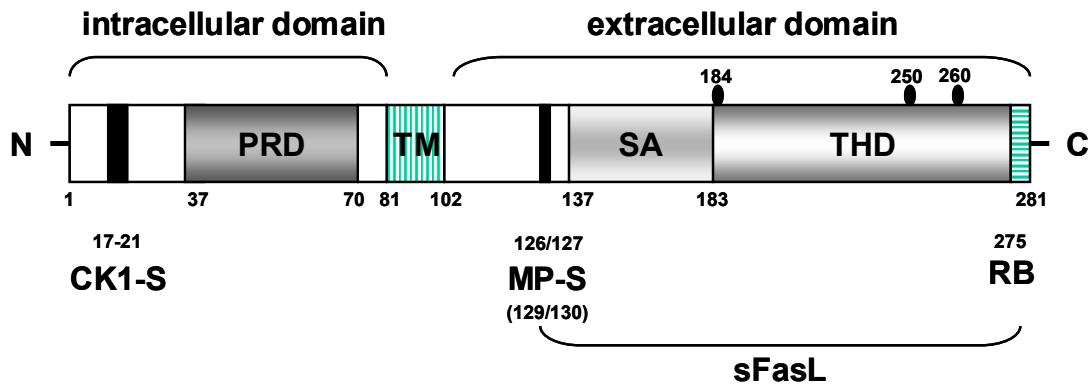


Fig. 1.4. Structural features of FasL. Human FasL is a type-II transmembrane molecule with 281 amino acids. The N-terminal cytoplasmic part (aa 1-81) contains a specific "double" CK1 substrate motif (CK1-S, aa 17-21). It also harbors the proline-rich domain (PRD, aa 37-70) which could function as a docking site for SH3 and WW domain proteins. The transmembrane region spans aa 81-102. Within the extracellular part, several metalloprotease substrate sites (MP-S) have been named to serve as cleavage sites for one or more metalloprotease (aa 109-115 (ELAELR), S126/127L and K129/130Q). These cleavage sites are located outside the region that is required for trimerization and self-assembly (SA). Thus, sFasL can also form trimers. The C-terminal TNF homology domain (THD, aa 183-281) contains several putative N-glycosylation sites (aa 184, 250, 260) and the very C-terminal receptor binding site (RB) with a critical phenylalanine residue at position 275.

FasL as a substrate for a casein kinase?

Most ligands of the tumor necrosis factor (TNF) superfamily are transmembrane proteins that share structurally related extracellular TNF homology domains (THDs) which bind to cysteine-rich domains (CRDs) of their specific receptors (of the TNF-receptor superfamily). Ligand/receptor interactions of these families orchestrate the organization and function of many facets of the immune system. In general, they regulate key events in cellular activation, proliferation, differentiation, cell death and survival of immune cells and other tissues⁹¹. Since most of the TNF-family-members act as membrane-bound factors and require direct cell-to-cell contact, it seems obvious that ligand/receptor engagement works as a bidirectional. Thus, ligand-transmitted costimulatory functions have been reported for several members of the

TNF superfamily in T cells, B cells and monocytes. In fact, the ligand-receptor-complexes of CD70/CD27 (TNFSF7/TNFRSF7)⁹², CD153/CD30 (TNFSF8/TNFRSF8)^{93,94}, CD154/CD40 (TNFSF5/TNFRSF5)⁹⁵⁻⁹⁸, 4-1BB-L/CD137 (TNFSF9/TNFRSF9)^{99,100}, OX40L/CD134 (TNFSF4/TNFRSF4)¹⁰¹, TRANCE/RANK (TNFSF11/TNFRSF11)¹⁰², LIGHT/LIGHTR (TNFSF14/TNFRSF14)¹⁰³⁻¹⁰⁵ and the death factors TNF¹⁰⁶, TRAIL (TNFSF10)¹⁰⁷ and FasL (TNFSF6)⁶⁸⁻⁷¹ were reported to convey such "retrograde" signals.

Importantly, a bidirectional signaling capacity has been associated with those six out of 16 TNF family members (CD27L, CD30L, CD40L, CD137L, TNF α and FasL) that contain a putative casein kinase 1 (CK1) substrate motif (-SXXS-). Since such phosphorylation sites are not present in any of the remaining TNF family members, it seems likely that reverse signaling involves a casein kinase. Moreover, a receptor-triggered and CK1-dependent serine phosphorylation of the corresponding residues within membrane-bound TNF has been experimentally proven¹⁰⁸. In case of FasL, the membrane distal N-terminus of the molecule in fact contains a unique "double" CK1 substrate site (amino acids 17-21 in man (-SSASS-) and 17-22 in mice (-SSATSS-)). The presence of such a double motif (-S(P)XXS-) indicates a role for an additional kinase to regulate the sensitivity of the site for CK1 by phosphorylation of the first serine residue¹⁰⁸. Clearly, so far no data are available that demonstrate the involvement of a kinase or phosphatase in the regulation of FasL reverse signal transduction.

The proline-rich domain (PRD) as a protein-docking site of FasL

The second striking feature of the cytoplasmic tail of FasL is a proline-rich domain (PRD) that spans amino acids 37-70 of the human FasL (Fig. 1.4.). In contrast to the CK1 motif, this PRD region is absolutely unique among all members of the TNF family, and thus may play a major role in the biology of FasL. Since proline-rich region bind to SH3- or WW-domain containing proteins¹⁰⁹, it seems likely that the PRD region of FasL functions as a docking site for proteins that regulate trafficking and expression and maybe signaling of FasL¹¹⁰. In fact, it was found several years ago that peptides corresponding to the PRD of the murine FasL (aa 40-77) were able to selectively interact with the SH3 domain of the Src-related kinase p59^{fyn(T)}¹¹¹. From this it was suggested that FasL membrane expression is primarily regulated through an

activation-independent SH3-mediated association with p59^{fyn(T)}. In 1996, Hachiya and coworkers deposited several protein fragments in the NCBI database that were found to interact with FasL in a yeast two-hybrid screen. Although these "Fas-ligand associated factors" (FLAF1-3 - AAB93495, AAB93496, AAB93497) contained either a WW domain (FLAF1) or one or more SH3 domains (FLAF2,3), no further results were published except a note that FLAFs might regulate FasL stability. Sequence comparison with novel entries in the databases reveals that FLAF-1 forms part of the formin binding protein 11 (FBP11, also called the huntingtin-interacting protein HYPA), FLAF2 is part of the c-Cbl-associated protein SH3P12 = "sorbin and SH3 domain containing 1" (containing 3 SH3 domains), and FLAF3 represents a portion of the BAI1-associated protein 2 (BAP2)-beta (with a single SH3 domain).

1.5. Identification of interacting proteins

Strategies to identify associated proteins with proline recognition domains

As mentioned, proline-rich regions are prerequisite to form binding sites for specific SH3- or WW-type proline recognition domains. Studies from this group clearly indicate that FasL might interact with several other molecules in addition to Fyn and the poorly characterized FLAFs¹¹². In order to identify proteins that interact with the FasL PRD, two different protein-based screening approaches were used.

First, a large panel of SH3 and WW domains expressed as GST fusion proteins were checked for their ability to precipitate FasL from stable transfectants and T lymphoblasts¹¹². These analyses revealed that in addition to the SH3 domain of p59^{fyn}, a number of other SH3 or WW modules are also capable to effectively and specifically interact with the full length FasL overexpressed in transfectants and inducibly expressed in stimulated human T lymphocytes. The identification of various other Src-related kinases and different SH3 adapter proteins of the Grb2-family, PI 3-kinase, Nck and Phox-47 and the WW domain proteins FE65, FBP11 and dystrophin as putative FasL-interacting molecules, opened new insights into the potential of FasL to regulate and modulate activation processes in T cells and other FasL expressing cells. In the context of reverse signaling, the long and - as we now know - by far not complete list of putative FasL interacting proteins opens the field for speculations and models.

As a second approach to identify FasL interactors, different variants of the intracellular region of human FasL were constructed as GST fusion proteins and used to precipitate binding partners from T cell lysates. The precipitates were separated by two dimensional gel electrophoresis and sequence information obtained by MALDI-TOF-based peptide finger print analyses. According to these analyses, Grb2, PACSIN2, FBP17 β -tubulin and actin were found in precipitates formed with fusion proteins containing the whole cytoplasmic region including the PRD¹¹³. Grb2 is a well-defined adapter protein that plays a pivotal role in growth factor receptor as well as TCR signaling. After TCR-activation the Grb2–Sos complex is recruited to the phosphorylated transmembrane adapter, linker for activated T-cells (LAT), thereby triggering the Ras/MAPK pathway and leading to transcription of a whole range of proteins needed for T-cell activation and differentiation¹¹⁴. The interaction of Grb2 and FasL was confirmed by this group¹¹³.

PACSIN2 and FBP17

As mentioned, with FBP17 and PACSIN2, we identified two new potential FasL binding partners in human T cells. PACSIN2 is a 53 kDa human splice variant of the rat Syndapin II, a member of a family of cytosolic adapter proteins that link clathrin-dependent-endocytosis to the actin cytoskeleton and are involved in the regulation of vesicular traffic¹¹⁵⁻¹¹⁹. To date, three PACSINs are known, all of which contain phosphorylation sites for casein kinase 2 and protein kinase C (the name PACSIN refers to "protein kinase C and casein kinase substrate in neurons"). In contrast to the ubiquitously expressed PACSIN2, PACSIN1 was previously not detected in cells other than neurons. In terms of function, PACSIN isoforms specifically interact with Sos, thereby regulating actin dynamics via MAP kinase signaling¹²⁰. In the context of FasL, PACSIN2 could be involved in the reorganization of the cytoskeleton and in trafficking of cytoplasmic vesicles leading to storage and regulation of extrusion of FasL. The potential association of PACSINs with the GEF Sos may also suggest a role in downstream signaling to MAP-Kinases¹²⁰.

Formin binding protein 17 (FBP17) is a 72 kDa protein that belongs to the large heterogeneous family of formin binding proteins. In association with the various formins, these proteins also regulate the organization and assembly of the actin cytoskeleton and are involved in orchestrating cell motility, adhesion and

cytokinesis¹²¹. Fuchs et al. showed that FBP17 is widely expressed in a variety of human tissues¹²². They demonstrated the interaction of FBP17 with sorting nexin (SNX2) and thus provided a link between MLL, a gene connected to myelogenous leukemia, and the epidermal growth factor receptor (EGFR) pathway. In general, SNX-proteins are crucial molecules involved in directed protein trafficking and lysosomal targeting¹²³. Therefore, association of FasL with FBP17 could represent once more an alternative mode of lysosomal transport of FasL and also point to a signaling crosstalk between the death factor and the EGFR-pathway.

Interestingly, PACSIN2 and FBP17 share an overall modular composition with an N-terminal FCH (Fes/CIP4 homology) domain, a central coiled-coil region and a C-terminal SH3 domain which interacts with FasL¹¹³. FCH domain was first identified in cell division control protein 15 from fission yeast where after the onset of mitosis, it forms a ring-like structure which co-localizes with the medial actin ring. From yeast to man in most cases it may mediate cytoskeletal rearrangements, vesicular transport and signal transduction¹²⁴⁻¹²⁶.

NCK

Nck-1 is a 47 kDa cytosolic adapter protein which is built of one N-terminal SH2 and three SH3 domains. The well known function of Nck-1 is the regulation of cytoskeletal assembly through interaction with the Wiskott-Aldrich syndrom protein WASP¹²⁷, the WASP interacting protein WIP¹²⁸, WASP-family verprolin homologous protein WAVE1¹²⁹, the Centaurin- α family of PIP3 binding proteins¹³⁰, the p21-activated kinase PAK1¹³¹, the ϵ -chain of CD3¹³² and others. This cytoskeletal association may also play a role in FasL transport to the cell membrane. In this context, Nck-1 seem to be a crucial regulator of protein assembly and cytoskeletal reorganisation during the formation of the immunological synapse upon TCR ligation¹³². Besides, Nck was shown to constitutively associate with the active $\gamma 2$ isoform of casein kinase 1 (CK1- $\gamma 2$)¹³³ and therefore could be involved in recruitment of the kinase into proximity of FasL as a putative substrate.

2. Aims of the study

Although FasL has been identified ten years back, we are still far from understanding the complex biology of the molecule. FasL is found in both immunologically active and immune privileged tissues and in immune cells as well as in tumor cells. The regulation of expression and the function seem to be cell-type-specific. This concerns both the cytotoxic potential and the putative co-stimulatory signaling capacity. In mature human T cells, the evidence of reverse signaling through FasL and the molecular mechanisms involved need to be identified. The analyses of FasL associated casein kinase activity may shed light on this function. In terms of FasL transport and storage, the identification of the PRD-interacting proteins will help to position the molecule in the complex cytoskeleton and transport network. Previous work from this group identified a relatively large numbers of putative interactors for FasL. The main focus of the present study was the detailed analysis of several of these interactions *in vitro* and *in vivo*.

1. Retrograde signaling of FasL in human T cells.

In order to analyze the retrograde signaling of FasL in human T cell populations, suitable culture and stimulation conditions had to be worked out and adapted for different T cell subpopulation. In order to mimic the FasL-ligation, a FasFc fusion protein had to be constructed and produced. Readout for effects of FasL-engagement were proliferation, cell cycle progression, expression of activation markers, cell death and others.

2. Storage of FasL in secretory lysosomes

When investigating the FasL expression in activated cells, it became obvious that this death factor was located in discrete subcellular compartment that could be later defined as lysosomes. Therefore, the role of the different proteins from the two screens for interactors needed to be exploited. In the context of organelle transport, since PACSIN2 and its relatives are known to be involved in vesicle transport in other system, the focus was set on the analysis of interaction of FasL and proteins of the FCH/SH3 family.

3. Leading FasL to the immunological synapse

Nck had been identified as an interactor of FasL. In 2002, it was described that Nck mediates recruitment of cytoskeletal elements to the TCR. Thus, we aimed at looking in detail into the association of Nck with FasL. To this end, co-transfection strategies as well as *in vivo* analyses of T cells encountering their target cells had to be established and investigated.

3. Materials and methods

3.1. Materials

Cell biology

3.1.1. Cells

Human peripheral blood mononuclear cells (PBMC) and T cell subpopulation were isolated from buffy coat preparations from healthy donors obtained from the department of Transfusion Medicine, UK-SH, Kiel. Staphylococcal enterotoxin (SE) superantigen A-reactive T cell clones (12603, 12623, 12632, 12625), CD8⁺ T cell lines (CD8-K, CD8-L), the $\gamma\delta$ T cell line (EP3) and EBV-transformed lymphoblastoid B cell lines (EBV-O, EBV-M) were established in this laboratory. We also used Jurkat leukemia cells (J16 or Je 6.1) and clones derived thereof. The variant clones mainly differed in the expression of Fas and FasL. JM301 was described earlier¹³⁴ as Fas⁺ but Fas-resistant. J16 Rapo is a Fas-lacking subclone of J16. Both Fas resistant variants were used to establish stable transfectants introducing the FasL molecule (see section 3.2.4.). KFL-9 is a FasL transfectant established from K562 human erythroleukemia cells by Dr. David Kaplan, OH, USA. For transient protein expression, 293T (human embryonic kidney, SV40 transformed, ATCC: CRL-1573), HeLa (human cervix adenocarcinoma, ATCC: CCL-2), HaCaT (human skin keratinocytes), HUT78 (human T lymphoma, ATCC: TIB-161) and RBL2H3 (Rat basophilic leukaemia) cells were selected on the basis of their tissue origin representing hematopoietic or non-hematopoietic cell types. For FasFc fusion protein production, human embryonic HEK293 cells were used. Besides, a human malignant melanoma fibroblast cell line MeWo was used as target cell in a cytotoxicity assay with $\gamma\delta$ T cells.

3.1.2. Media and buffers

Cell culture

Standard cell culture media

RPMI1640 (with 25 mM <i>N</i> -2-hydroxyethylpiperazine- <i>N'</i> -2-ethanesulfonic acid (HEPES) and L-Glutamine)	Invitrogen, Karlsruhe
DMEM (Dulbeccos minimum essential medium)	Invitrogen, Karlsruhe

Penicillin (10000 U)/Streptomycin (10000 µg) Biochrom AG, Berlin

FBS (fetal bovine serum) Invitrogen, Karlsruhe
(Inactivated for 30 min at 56°C, 0.22 µm filtered)

AB serum pool
(Inactivated for 30 min at 56°C, 0.22 µm filtered)

L-Glutamine (200 mM) Biochrom AG, Berlin

Media were supplemented with 1% (v/v) Penicillin/Streptomycin and 5-10% (v/v) FBS or AB serum pool as indicated in the respective section. To DMEM medium, additional 1% (v/v) L-Glutamine was added.

Serum free medium

FreeStyle™ 293T expression medium Invitrogen, Karlsruhe

Freezing medium

Culture medium with 20% FBS (v/v) and 10% (v/v) Dimethylsulfoxid (DMSO, Merck, Darmstadt)

Phosphate-buffered saline (PBS) Biochrom AG, Berlin

Trypsin-EDTA (0.5%/0.2% (w/v)) Biochrom AG, Berlin

Cell separation

Ficoll (1.077 g/ml) Biochrom AG, Berlin

Sheep red blood cells (SBRC) Invitrogen, Karlsruhe

Test Neuraminidase Dade Behring, Marburg

Rabbit Complement Cedarlane Lab, CA

Calcium-phosphate transfectionBES (2×)

N, N-bis (2-hydroxyethyl)-2-aminethanesulfonic acid (BES)	50 mM	Merck, Darmstadt
Sodium Chloride (NaCl)	280 mM	Merck, Darmstadt
Sodium phosphate dibasic (Na ₂ HPO ₄)	1.5 mM	Merck, Darmstadt
Adjusted to pH 6.95 and 0.22 μm filtered		

HBS (2×)

HEPES	50 mM	Merck, Darmstadt
NaCl	280 mM	Merck, Darmstadt
Na ₂ HPO ₄	1.5 mM	Merck, Darmstadt
Adjusted to pH 7.17 and 0.22 μm filtered		

Calcium chloride dihydrate (CaCl₂, 10×)

CaCl ₂	2.5 M	Merck, Darmstadt
ddH ₂ O		Braun, Melsungen

Immune cellular staining

<u>Poly-L-lysine (MW>300,000)</u>	Sigma, Munich
--------------------------------------	---------------

PEM buffer (2×)

Piperazine-N, N'-bis(2-ethanesulfonic acid), PIPES	200 mM	Merck, Darmstadt
Magnesium chloride (MgCl ₂)	2 mM	Merck, Darmstadt
Ethylene glyco-bis (β-aminoethylether)-N, N, N', N'-tetraacetic acid, EGTA	2 mM	Merck, Darmstadt
Adjusted to pH 6.5 and 0.22 μm filtered		

Borate buffer (2×)

Sodium borate	200 mM	Merck, Darmstadt
MgCl ₂	2 mM	Merck, Darmstadt
Adjusted to pH 11 and 0.22 μm filtered		

Triton X-100 stock solution

Triton[®]X-100 10% (v/v) Merck, Darmstadt
ddH₂O Braun, Melsungen

Fixation buffer- 3% paraformaldehyde (PFA)

3 g PFA (Merck, Darmstadt) were added to 50 ml ddH₂O with 1-2 drops 10 N NaOH and agitated in a 70°C water bath until the solution cleared. Upon cooling, pH was adjusted to pH 7.0. The same volume of 2× PEM buffer or 2× borate buffer was then added.

Permeabilization buffer- 1% (v/v) Triton X-100

1: 10 diluted from stock solution with PBS

Washing buffer- PBST

0.01% Triton (v/v) in PBS

Blocking buffer

0.2% (w/v) Bovine serum albumin (BSA, Carl Roth, Karlsruhe,) in PBST

Mounting medium

Solutions in Slowfade[®] Light Anti-Fade Kit (MoBiTec, Göttingen)

Immune surface stainingWashing buffer

1% BSA (w/v) in PBS with 0.1% sodium azide (NaN₃, w/v, Merck, Darmstadt)

Fixation buffer

1% PFA (w/v) in PBS, store at 4°C in the dark

DNA staining for cell cycling analysisStock solution

I. 0.5 M EthyleneDiamineTetraAcetic acid (EDTA)

Titriplex[®]III 186.1 g Merck, Darmstadt
ddH₂O Braun, Melsungen

Adjusted to pH 8.0

II. RNase A	1 mg/ml	Qiagen, Hilden
III. propidium iodide (PI)	1 mg/ml	Serva, Heidelberg

Washing buffer

PBS with 5 mM EDTA

Fixation buffer

100% Ethanol (Merck, Darmstadt)

Staining solution

50 µg/ml PI, 40 µg/ml RNase A in washing buffer

3.1.3. Antibodies (listed as final concentration or dilution factor)

Cell stimulation

α-CD3 (OKT3)	1-10 µg/ml	Janssen-Cilag, Neuss
α-CD28	5 µg/ml	BD Pharmingen, Heidelberg
α-FasL 5G51	10 µg/ml	Dr. K. Schulze-Osthoff, Düsseldorf

Crosslinking

Rabbit anti-mouse IgG	1 µg/ml	Jackson ImmunoResearch Laboratories, West Grive, PA
α-human IgG, Fc specific	2.5-5.0 µg/ml	Sigma-Aldrich, Munich

Cell separation

α-CD4	40 µg/ml	Dianova, Hamburg
α-CD8	40 µg/ml	Dianova, Hamburg
α-CD56	6 µg/ml	BD Pharmingen, Heidelberg

Immune cellular staining

I. Primary antibodies

α -FasL (CD178, NOK-1, IgG _{1a})	1:50	BD Pharmingen, Heidelberg
α -Nck (IgG _{2b})	1:50	BD Pharmingen, Heidelberg
α -myc (IgG ₁)	1:100	Invitrogen, Karlsruhe
α -myc (IgG _{2a})	1:200	Cell Signaling, Frankfurt
α -Lamp1 (IgG _{2b})	1:50	BD Pharmingen, Heidelberg
α -CathepsinD (rabbit polyclonal antibody, pAb)	1:75-1:100	Calbiochem, Bad Soden

II. Fluorescence conjugated secondary antibodies

goat anti-mouse/Alexa Fluor 488	1:500	MoBiTec, Göttingen
goat anti-mouse/Alexa Fluor 546	1:500	MoBiTec, Göttingen
goat anti-rabbit/Alexa Fluor 488	1:500	MoBiTec, Göttingen
donkey anti-mouse/CY5	1:75	Dianova, Hamburg
donkey anti-rabbit/Rhodamine	1:75	Santa Cruz, Heidelberg

Immune surface staining (concentration according to manufacturer's instructions)

I. Primary antibodies

α -CD3/Phycoerythrin (PE)		BD Pharmingen, Heidelberg
α -CD4/fluorescein isothiocyanate (FITC)		BD Pharmingen, Heidelberg
α -CD8/FITC		BD Pharmingen, Heidelberg
α -CD56/FITC		BD Pharmingen, Heidelberg
α -Fas (CD95)/ PE		BD Pharmingen, Heidelberg
α -FasL/biotin		BD Pharmingen, Heidelberg
α -FasL/PE		Caltag, Hamburg
α -CD25/PE		BD Pharmingen, Heidelberg
α -CD69/PE		BD Pharmingen, Heidelberg
IgG ₁ /PE		BD Pharmingen, Heidelberg
IgG _{2a} /FITC		BD Pharmingen, Heidelberg

II. Fluorescence-conjugated secondary antibodies/reagents

Goat anti-mouse/PE (gam-PE)		BD Pharmingen, Heidelberg
Streptavidin Phycoerythrin (SA-PE)		BD Pharmingen, Heidelberg
Avidin-FITC		BD Pharmingen, Heidelberg

3.1.4. Factors and other reagents (listed as final concentration)

Recombinant Interleukin-2 (rIL-2)	10 U /ml	Chiron GmbH, Marburg
Phytohemagglutinin (PHA)	0.5 µg/ml	Murex Biotech, England
Staphylococcal enterotoxin superantigen A, B, C, D, E (SEA, B, C, D, E)	0.5 ng/ml	Toxin Technologies, FL, USA
Phorbol-12-myristate-13-acetate (TPA/PMA)	5-10 ng/ml	Sigma-Aldrich, Munich
Ionomycin	500 ng/ml	Calbiochem, Darmstadt
Bacteria phospho-antigen, BrHPP	200 nM	Dr. Fournie, Toulouse, France
Cytochalasin D	10 µM	Calbiochem, Darmstadt
Latrunculin A	5 nM	Sigma-Aldrich, Munich
FasFc	25-50 µg/ml	See section 3.2.8
Human IgG-Fc fragment	25-50 µg/ml	Bethyl, TX, USA
Hygromycin B	300 mg/ml	Merck, Darmstadt
Lysotracker Red DND-99	50-100 nM	MoBiTec, Göttingen
Rhodamine phalloidin	1 unit	MoBiTec, Göttingen
Chromium-51 (⁵¹ Cr)	50 µCi	Amersham, Freiburg
Methyl ³ H thymidine (³ H TdR)	1 µCi	Amersham, Freiburg

Molecular Biology**3.1.5. Primers**

The primers were designed either encoding fragments of or full length target genes according to the sequence database in Gene Bank. The primers were used for regular or cloning PCR (as listed in **Table 3.1.1.**). For cloning purposes, flanking restriction sites were added to allow for unidirectional inserting.

Table 3.1.1. Primers used for PCR

1. Primers for regular PCR

Name	Sequence (5'-3')
FasL fragment (Exon1-Exon 4)	s: 5' Tgg CAg AAC TCC gAg AgT CTA 3' as: 5' CAC Tgg gAT TgA ACA CTg 3'
GAPDH fragment (codon 3199-4003)	s: 5' gAC CCC TTC ATT gAC CTC 3' as: 5' CCA AAg TTg TCA Tgg ATg 3'

2. Primers for cloning PCR

Name (GeneBank no.)	Sequence (5'-3')	RE	*
CIP4 (AJ000414)	s: CCCAAgCTT - gC ACC ATg gAT Tgg ggC ACT gAg as: ATAAgAATgCggCCgC - TT gAg CgT gAC TCg gAg gTA	HindIII NotI	(1)
CD2BP1 (AF038062/3)	s: CgggATCC - ACC ATg ATg CCC CAg CTg Cag as: CggAATTC - AAg CTT CTC CAg gTA ggA ACC	BamHI EcoRI	(1) (4)
PACSIN1 (AF242529)	s: CgggATCC - ACC ATg TCC AgC TCC TAC gAT g as: CggAATTC - gAT AgC CTC CAC gTA gTT ggC Ag	BamHI EcoRI	(1)
PACSIN2 (NM_00729)	s: CCggAATTC - gTC TgT CAC ATA TgA TgA TTC as: CgggATCC - gAA ATg TCT gTC ACA TAT g	EcoRI BamHI	(2)
PACSIN2P478L (NM_00729)	s: CCggAATTC - gTC TgT CAC ATA TgA TgA TTC as: CCggATCC-TCA CTg gAT CgC CTC CAC ATA ATT TgC gAg gTA TAg gCC	EcoRI BamHI	(2)
PACSIN3 (AF149825)	s: CggAATTC - ACC ATg gCT CCA gAA gAg gAC as: CCgCTCgAg - ggC ACC CAC ACA CTC CAC gTA g	EcoRI XhoI	(1)
SH3P12 (AF136381)	s: CCCAAgCTT - ACA CCA TgA gTT CTg AAT gTg ATg gTg as: CggAATTC - TAg ATA CAA Agg TTT TAC ATA gTT gC	HindIII EcoRI	(1)
BAP2-β (BC014020)	s: CgggATCC - ACC ATg TCT TTg TCT CgC as: CggAATTC - CAC TgT ggA CAC Cag CgT gC	BamHI EcoRI	(1)
FasL (NM_000639)	s: CggAATTC - TgC CAT gCA gCA gCC CTT CA as: CgggATCC - AgC TTA TAT AAg CCg AAA AA Cg	EcoRI BamHI	(3)
Fas (M67454) (extracellular)	s: CCCAAgCTT - ACA ACC ATg CTg ggC ATC Tgg ACC CTC as: CggAATTC - gTT AgA TCT ggA TCC TTC	HindIII EcoRI	(5)

no. number; s: sense; as: anti-sense; RE: restriction endonucleus enzyme * according to vector number in 3.1.6.

3.1.6. VectorsTA cloning

PCR2. 1 TOPO [®]	TA cloning	Invitrogen, Karlsruhe
---------------------------	------------	-----------------------

Bacteria expression

pGEX2T (4)	GST tag	Pharmacia, Sweden
------------	---------	-------------------

Mammalian expression

pcDNA3. 1/myc his A (1)	C-terminal myc/his tag	Invitrogen, Karlsruhe
pEGFP C1 (2)	C-terminal GFP tag	Invitrogen, Karlsruhe
pDsRed N1 (3)	N-terminal DsRed tag	BD Clontech, Heidelberg
pcDNA3-hFc (5)	C-terminal Fc tag	Dr. H. Wajant, Frankfurt
pEFBOS		Dr. B. Schraven, Magdeburg
Hygromycin resistant vector		Dr. B. Schraven, Magdeburg

3.1.7. Other constructs

We also used some constructs that were kindly provided by other laboratories for transfection or purification fusion protein. The information of those constructs is listed in **Table 3.1.2.** and also published elsewhere (see references).

Table 3.1.2. Constructs obtained from other laboratories

Insert	Vector	References
PACSIN1	pGEX 3X	Dr. M. Plomann, Köln ¹¹⁸
PACSIN2	pGEX 2T	Dr. M. Plomann, Köln ¹¹⁸
PACSIN2 p478I	pGEX 2T	Dr. M. Plomann, Köln ¹¹⁸
PACSIN3	pGEX 3X	Dr. M. Plomann, Köln ¹¹⁸
PACSIN2	pMyc-CMV	Dr. M. Plomann, Köln ¹¹⁸
PACSIN1	pEGFP C1	Dr. M. Plomann, Köln ¹¹⁸
PACSIN3	pEGFP C1	Dr. M. Plomann, Köln ¹¹⁸
FBP17	PDsRed1-N1	Dr. U. Fuchs, Giessen ¹²²
FBP17+myc	PCDNA3.1/V5-His TOPO	Dr. U. Fuchs, Giessen ¹²²
FBP17-SH3 +myc	PCDNA3.1/V5-His TOPO	Dr. U. Fuchs, Giessen ¹²²
Nck1	PCDNA3.1 Myc-His C	Dr. L. Larose, Montreal, CA ^{133,135}
Nck1 SH2 mutated	PCDNA3.1 Myc-His C	Dr. L. Larose, Montreal, CA ^{133,135}

Nck1 1 st SH3 mutated	PCDNA3.1 Myc-His C	Dr. L. Larose, Montreal, CA ^{133,135}
Nck1 2 nd SH3 mutated	PCDNA3.1 Myc-His C	Dr. L. Larose, Montreal, CA ^{133,135}
Nck1 3 rd SH3 mutated	PCDNA3.1 Myc-His C	Dr. L. Larose, Montreal, CA ^{133,135}
Nck1 all SH3s mutated	PCDNA3.1 Myc-His C	Dr. L. Larose, Montreal, CA ^{133,135}
Nck1	pGEX	Dr. L. Larose, Montreal, CA ^{133,135}
Nck1 SH2	pGEX	Dr. L. Larose, Montreal, CA ^{133,135}
Nck1 1 st SH3	pGEX	Dr. L. Larose, Montreal, CA ^{133,135}
Nck1 2 nd SH3	pGEX	Dr. L. Larose, Montreal, CA ^{133,135}
Nck1 3 rd SH3	pGEX	Dr. L. Larose, Montreal, CA ^{133,135}
Nck1 all SH3s	pGEX	Dr. L. Larose, Montreal, CA ^{133,135}
Nck1 1 st SH3 mutated	pGEX	Dr. L. Larose, Montreal, CA ^{133,135}
Nck1 2 nd SH3 mutated	pGEX	Dr. L. Larose, Montreal, CA ^{133,135}
Nck1 3 rd SH3 mutated	pGEX	Dr. L. Larose, Montreal, CA ^{133,135}
Nck1 all SH3s 1 st SH3 mutated	pGEX	Dr. L. Larose, Montreal, CA ^{133,135}
Nck1 all SH3s 2 nd SH3 mutated	pGEX	Dr. L. Larose, Montreal, CA ^{133,135}
Nck1 all SH3s 3 rd SH3 mutated	pGEX	Dr. L. Larose, Montreal, CA ^{133,135}
Nck1	CB6 GFP	Dr. M. Way, London, UK ¹³⁶
Nck1 W38K	CB6 GFP	Dr. M. Way, London, UK ¹³⁶
Nck1 W143K	CB6 GFP	Dr. M. Way, London, UK ¹³⁶
Nck1 W229K	CB6 GFP	Dr. M. Way, London, UK ¹³⁶
Nck1 R308K	CB6 GFP	Dr. M. Way, London, UK ¹³⁶

3.1.8. Enzymes

Restriction Endonucleus Enzymes

EcoRI	New England Biolabs, Frankfurt
BamHI	New England Biolabs, Frankfurt
XhoI	Promega, Mannheim
XbaI	New England Biolabs, Frankfurt
HindIII	New England Biolabs, Frankfurt

T4 ligase Promega, Mannheim

Pfu DNA polymerase Promega, Mannheim

Klenow fragment Boehringer, Mannheim

alkaline phosphatase (AP) Boehringer, Mannheim

3.1.9. Buffers and other reagents

Tris/acetate/EDTA (TAE, 50×)

tris (hydroxymethyl)aminomethane (Tris)	242 g	
Boric acid	55 g	
0.5 M EDTA	40 ml	Serva, Heidelberg
ddH ₂ O	up to 1 liter	Braun, Melsungen

1% agarose gel

Agarose	1% w/v	Merck, Darmstadt
1×TAE		

<u>Ethidium Bromide (EB, stock solution)</u>	5 mg/ml	Merck, Darmstadt
use 0.5 µg per ml agarose solution		

Agarose gel sample buffer (10×) Promega, Mannheim

DNA -Molecular weight Standards

1 Kb DNA ladder		Invitrogen, Karlsruhe
100 bp DNA ladder		Invitrogen, Karlsruhe
2-log DNA ladder with indicated concentration		New England Biolabs, Frankfurt

Competent cells

Subcloning Efficiency™ DH5α™ Invitrogen, Karlsruhe

3.1.10. Kits for molecular biology

RNeasy® Mini Kit	QIAGEN, Hilden
QIAquick PCR Purification Kit	QIAGEN, Hilden
QIAquick Gel Extraction Kit	QIAGEN, Hilden

QIAGEN® plasmid Mini and Maxi Kit	QIAGEN, Hilden
DyeEx spin Kit	QIAGEN, Hilden
Big-dye™ terminal sequencing kit	Applied biosystems, Darmstadt
GeneAmp® RNA PCR Kit	Applied biosystems, Darmstadt
PCR Master Mix	Promega, Mannheim

Biochemistry

3.1.11. Buffers and Reagents

FasFc fusion protein purification

Beads

Protein A Sepharose CL-4B Beads	Amersham, Freiburg
---------------------------------	--------------------

Start buffer (20 mM phosphate buffer, pH 7.0)

a) 1 M sodium phosphate monobasic (NaH₂PO₄) stock solution

NaH ₂ PO ₄ ·H ₂ O	68.995 g	Merck, Darmstadt
--	----------	------------------

ddH ₂ O	500 ml	Braun, Melsungen
--------------------	--------	------------------

1: 50 dilution before use (20 mM, pH 4.75-4.5), add 0.3M NaCl (8.766 g to 500 ml)

b) 1 M sodium phosphate dibasic (Na₂HPO₄) stock solution

Na ₂ HPO ₄ ·2H ₂ O	88.975 g	Merck, Darmstadt
---	----------	------------------

ddH ₂ O	500 ml	Braun, Melsungen
--------------------	--------	------------------

1: 50 dilution before use (20 mM, pH 9.3-8.9), add 0.3 M NaCl (8.766 g to 500 ml)

Mix 20 mM NaH₂PO₄/Na₂HPO₄ with NaCl to pH 6.5 (around 68.5/31.5 ml) or pH 7.0 (around 39/61 ml). Check by pH meter.

Elution buffer (0.1 M Glycine-HCl buffer, pH 2.7)

Glycine	3.275 g	Carl Roth, Karlsruhe
---------	---------	----------------------

Adjusted to pH 2.7 with HCl, filled to 500 ml with ddH₂O

Neutralization buffer (1 M Tris-HCl buffer, pH 9.0)

Tris	60.565 g	Carl Roth, Karlsruhe
------	----------	----------------------

Adjusted to pH 9.0 with HCl, filled to 500 ml with ddH₂O

To 1 ml elution fraction add 50 μ l

NaN₃ 0.1% (w/v) Merck, Darmstadt

Dialysis buffer

PBS

GST fusion protein purification

Beads

Glutathione Sepharose 4B Beads Amersham, Freiburg

Isopropyl-1-thio- β -D-galactopyranoside (IPTG) 1 mM Calbiochem, Darmstadt

Lysis buffer

Triton[®]X100 1% (v/v) Merck, Darmstadt

PBS

Elution buffer

Glutathione (reduced) 10 mM Sigma

Tris-buffer pH 8.0 50 mM

Dialysis buffer

PBS

Protein detection

Coomassie[®] protein assay reagent Pierce, IL, USA

Coomassie staining solution

Methanol 410 ml Sigma-Aldrich, Munich

Acetic acid 70 ml Merck, Darmstadt

ddH₂O 520 ml Braun, Melsungen

Coomassie brilliant blue G250 0.125 g Merck, Darmstadt

Coomassie destaining solution

Methanol	410 ml	Sigma-Aldrich, Munich
Acetic acid	70 ml	Merck, Darmstadt
ddH ₂ O	520 ml	Braun, Melsungen

Cell lysis

Lysis bufffer-1%NP40

Nonidet [®] P40 (NP40)	1% (v/v)	Merck, Darmstadt
Tris-buffer, pH 7.4	20 mM	Merck, Darmstadt
NaCl	150 mM	Merck, Darmstadt
EDTA	5 mM	Merck, Darmstadt

Inhibitors in lysis buffer (listed as final concentration)

Aprotinin (APR)	Inhibits serine proteases	2 µg/ml	Sigma
Leupeptin (LEU)	Inhibits trypsin-like serine and cysteine proteases	2 µg/ml	Sigma
Phenylmethyl sulfonyl Fluorid (PMSF)	Irreversible inhibition of serine proteases	1 mM	Sigma
Pepstatin A	Inhibits aspartic proteases	2 µg/ml	Sigma
Sodium orthovanadate (SOV)	Inhibits ATPase, phosphatase and tyrosine phosphatase	1 mM	Merck
EDTA	Broad spectrum metalloproteinase inhibitor	1-5 mM	Merck
Sodium fluoride (SF)	Enzyme inhibitor e.g. pyrimidine nucleoside monophosphate kinase	10 mM	Fluka
Sodium pyrophosphate (SPP)	Cdc2 kinase inhibitor	1 mM	Sigma

Sample buffer (3×)

Sodium dodecyl sulfate (SDS)	6% (w/v)	Calbiochem, Darmstadt
Glycine	30% (v/v)	Merck, Darmstadt
Tris-buffer pH 6.8	200 mM	Merck, Darmstadt
Bromophenol blue	0.005% (w/v)	Merck, Darmstadt
β-Mercapthoethanol (β-ME)	2-5% (v/v)	Merck, Darmstadt

SDS-PAGE (Sodium Dodecyl Sulfate-Polyacrylamid Gel Electrophoresis)

Running gel (30 ml per gel, 6%-12%)

30% Acrylamid/0.8% Bisacrylamid	6-12 ml	Carl Roth, Karlsruhe
Tris-buffer 1M pH 8.8	12.2 ml	Merck, Darmstadt
SDS 10%	300 µl	Merck, Darmstadt
ddH ₂ O	6.7-12.7 ml	Braun, Melsungen
Ammonium peroxodisulfate (APS) 20%	100 µl	Merck, Darmstadt
<i>N,N,N',N'</i> -Tetramethyldiamin (TEMED)	20 µl	Merck, Darmstadt

Stacking gel (10 ml per gel)

30% Acrylamid/0,8% Bisacrylamid	1.67 ml	Carl Roth, Karlsruhe
Tris-buffer 1M pH 6.8	1.25 ml	Merck, Darmstadt
SDS 10%	100 µl	Merck, Darmstadt
ddH ₂ O	7.03 ml	Braun, Melsungen
20% APS	50 µl	Merck, Darmstadt
TEMED	10 µl	Merck, Darmstadt

Electrophoresis buffer (10× stock solution)

Tris	30.3 g	Merck Darmstadt
Glycine	144 g	Merck Darmstadt
SDS	1 g	Calbiochem, Darmstadt
ddH ₂ O	up to 1 liter	Braun, Melsungen
Adjusted to pH 8.2-8.3		

Protein-Molecular Weight Standards

Precision Protein Standards	Bio-Rad, Munich
Protein Marker Low Range	Bio-Rad, Munich

Western blottingTransfer-buffer

Tris	25 mM	Merck, Darmstadt
Glycine	192 mM	Merck, Darmstadt
Methanol	20% (v/v)	Sigma-Aldrich, Munich
SDS	0.015% (v/v)	Merck, Darmstadt

Adjusted to pH8.0, stored at 4°C

Protein staining on membrane

Ponceau S solution
(0.1% Ponceau S (w/v) in 5% acetic acid (v/v))

Sigma, Munich

Washing buffer

I. Tris-buffered saline (TBS)

Tris	10 mM	Merck, Darmstadt
NaCl	150 mM	Merck, Darmstadt

Adjusted to pH 7.5-8.0

II. Tris-buffered saline containing Tween-20 (TBST)

Tween [®] 20	0.05%	Merck, Darmstadt
-----------------------	-------	------------------

TBS

Blocking solution

5% (w/v) BSA in TBST
0.22 µm filtered

Stripping solution

Tris pH 6.8	62.5 mM	Merck, Darmstadt
β-ME	2% (v/v)	Merck, Darmstadt
SDS	6.9% (v/v)	Merck, Darmstadt
ddH ₂ O		Braun, Melsungen

ECL[™] western blotting detection reagents

Amersham, Freiburg

***In vitro* kinase assay**

Kinase buffer

HEPES	25 mM	Merck, Darmstadt
MgCl ₂	10 mM	Merck, Darmstadt

Manganese chloride (MnCl ₂) Adjusted to pH 7.2	10 mM	Merck, Darmstadt
<u>Phosphor-32([γ-³²P]ATP)</u>	10 μ Ci	Amersham, Freiburg

3.1.12. Antibodies

A list of antibodies used for various biochemical analyses is given in **Table 3.1.3.** 1-5 μ g antibodies were used for immunoprecipitation, 1:1500 to 1:7500 (in TBST) dilutions were used for western blotting analysis.

Table 3.1.3. Antibodies used for biochemical analysis

Antibody	Isotope	Used for	Manufacturer
I. primary antibodies			
α -FasL (NOK-1)	IgG _{1a} mAb	IP	BD Pharmingen, Heidelberg
α -FasL (G247-4)	IgG _{1a} mAb	IP/WB	BD Pharmingen, Heidelberg
α -pTyr (4G10)	IgG _{2b} mAb	WB	Upstate Biotechnology, Hamburg
α -myc	IgG ₁ mAb	WB	Invitrogen, Karlsruhe
α -myc	IgG _{2a} mAb	IP	Cell Signaling, Frankfurt
II. Secondary antibodies			
goat anti-mouse/HRP	F(ab') ₂	WB	Amersham, Freiburg
goat anti-rabbit/HRP	F(ab') ₂	WB	Amersham, Freiburg

Abbreviations: WB, Western Blot; IP, Immunoprecipitation; mAb, monoclonal antibody; HRP, horseradish peroxidase

3.1.14. Other material

Nitrocellulose-membrane Hybond™-C extra	Amersham, Freiburg
Filter paper Whatman 3MM	Whatman, Maidstone, UK
Disposable filter unit 0.2 μ m	Schleicher & Schuell, Dassel
Disposable filter unit 0.45 μ m	Schleicher & Schuell, Dassel
Sterile vacuum filter 0.2 μ m	Millipore, Eschborn
Cellstar® TC flasks, plates (24 well)	Greiner bio-one, Frickenhausen
Nunc® TC plates (96 F, 96 U, 12 well, 6 well)	Nunc, Danmark
Falcon® TC dishes (10 cm, 20 cm)	Becton Dickison, France

Microcentrifuge tubes 1.5 ml	Sarstedt, Nümbrecht
Centrifuge tubes 15 ml, 50 ml	Sarstedt, Nümbrecht
Pipettes	Sarstedt, Nümbrecht
Tips with filter	Greiner bio-one, Frickenhausen
MicroAmp [®] reaction tubes	Applied biosystems, Darmstadt
Parafilm	American National Lab
Cuvette for spectrophotometer	Sarstedt, Nümbrecht
Gene pulser cuvette, 0.4 cm	Bio-Rad, Munich
Coverslips, round, 18 mm	Herenz, Hamburg
Lab-Tek II chambered coverslips	Nunc, Danmark
Microscope slides and coverslips	Sarstedt, Nümbrecht
Centricon [®] -30 concentrator 30,000 MWCO	Amicon, MA, USA
Slide-A Lyzer [®] dialysis cassette 10,000 MWCO	Pierce, IL, USA
Hyperfilm [™] ECL/MP	Amersham, Freiburg

3.1.15. Equipments

CO ₂ -humidified incubator	Heraeus, Osterode
Biosafety cabinet	Heraeus, Osterode
Radioactive shelter	Amersham, Freiburg
Centrifuge Type 5415C	Eppendorf, Hamburg
Centrifuge Type Biofuge 15R	Heraeus, Osterode
Centrifuge Type Megafuge 1.0	Heraeus, Osterode
Centrifuge Type J2MC (Rotor JA-14, JA-20)	Beckman, USA
Vortex mixers	Eppendorf, Hamburg
Rocky	Fröbel Labortechnik
Rotator	Heto, Danmark
Minishaker-MS1	IKA-Labortechnik
Waterbath	GFL, Burgwedel
Heatblock DB-2 und DB-3	Techne, Wertheim
Pipette	Eppendorf, Hamburg
Pipetus [®] Arkus Pipetting Aid	Hirschmann, Eberstadt
Hemocytometer	Fischer, Frankfurt/M
Dounce-homogenizier	Braun, Melsungen

Standard chromatography column C10	Pharmacia Biotech, Sweden
pH Meter Modell 537	WTW, Weilheim
Smart-Spec™ 3000-spectrophotometer	Bio-Rad, Munich
Hypercassette™	Amersham, Freiburg
Gel dryer	Bio-Rad, Munich
Power Pack 200/300/2000	Bio-Rad, Munich
Electrophoresis chamber Protean® II	Bio-Rad, Munich
Western-Blot transfer tank Trans-Blot®	Bio-Rad, Munich
Film developing machine Agfa-Curix60	Agfa, Germany
Digital imaging and microscopy with "gel imager" software	INTAS, Göttingen
Sonifier 250, Ultrasonics	Branson, USA
PE2400 thermocycler	Perkin-Elmer, Langen
GenePulser II, RF model	Bio-Rad, Munich
Inverse light microscope	Carl Zeiss, Jena
Zeiss laser scanning microscope LSM 510 with software	Carl Zeiss, Heiderburg
FACScan with cellquest software	Becton Dickinson
β scintillation counter	Inotech, Switzerland
γ scintillation counter	Inotech, Switzerland

3.2. Methods

Cell biology

3.2.1. Cell culture

Jurkat, HUT78 and KFL-9 cells were grown in RPMI1640 medium with 5% (v/v) FBS. RBL2H3 cells were maintained in RPMI1640 medium with 10% (v/v) FBS. HaCaT, HeLa, MeWo, 293T and HEK 293 cells were cultured in DMEM medium with 10% (v/v) FBS. Media were supplemented with 1% (v/v) Penicillin/Streptomycin and to DMEM medium, additional 1% (v/v) L-Glutamine was added. For passaging adherent cells, 0.05%/0.02% (w/v) Trypsin-EDTA solution was used to detach the cells.

Human T cell PHA blasts and T cell clones/lines were cultured in RPMI1640 with 10% (v/v) FBS, antibiotics supplemented with rIL-2 (10 U/ml). T cells were restimulated periodically (every 14 to 21 days) with irradiated PBMC (4000 rad) and EBV-transformed lymphoblastoid cell lines (6000 rad) in the presence of PHA (0.5 µg/ml) and rIL-2 (10 U/ml). After three days, dead cells were removed by Ficoll gradient centrifugation and T cells were further cultured in the presence of rIL-2.

Cells were grown in cell culture flasks or tissue culture (TC) plates at 37°C in a humidified atmosphere with 5% CO₂. All of the cells were routinely verified to be free of mycoplasma contamination by using a PCR-based mycoplasma detection kit (Minerva BioLabs, Berlin).

3.2.2. Isolation of cells

Human peripheral blood mononuclear cells (PBMC) were isolated from buffy coat preparations from healthy donors by Ficoll gradient centrifugation and were separated into NK-, T- cells (E⁺) by rosetting with neuraminidase-treated sheep erythrocytes (E) and subsequent gradient centrifugation. CD4⁺- or CD8⁺- T cells were further isolated by e.g. negative selection using complement-mediated lysis.

Isolation of PBMC and generation of PHA blasts

Buffy coat preparations diluted 1:2 in PBS were laid over Ficoll-Hypaque (density 1.077 g/ml) and centrifuged at 2000 rpm for 20 min without brake. PMBC at the interface were collected and washed twice before resuspended in RPMI1640 medium and 5% FBS.

To generate PHA blasts, 0.5 µg/ml PHA was added to freshly isolated PBMC for 3 days. Afterwards, dead cells were removed by Ficoll gradient centrifugation and 10 U/ml exogenous rIL-2 was added to the culture medium. The cells were used after 14-21 days.

Production of neuraminidase-treated sheep erythrocytes

20 ml sheep red blood cells (SRBC, 1:2 (v/v) in Alsever solution) were diluted with 20 ml PBS. Upon three times centrifugation at 2000 rpm for 5 min without brake and removing the supernatant and the lymphocyte interface, SRBC in the pellet were then resuspended in 20 ml RPMI1640 medium containing 10% FBS and 0.5 ml neuraminidase, incubated at 37°C for 30 min followed by three washes with PBS. The erythrocytes pellet was then diluted 1: 10 (v/v) in RPMI1640 medium containing 10% FBS to get 10% SRBC suspension.

Rosette-formation and isolation of (E⁺)T cells

20x10⁶ PBMC resuspension and 1 ml of the SRBC suspension were gently mixed and submitted to a Ficoll density centrifugation. T cells were enriched in the pellet. SRBC were lysed by adding 0.5-1 ml ammonium chloride (NH₄Cl) and incubation for 3-5 minutes. After three washes with RPMI with 5% FBS, the (E⁺) T cells were resuspended in culture medium.

Isolation of CD4⁺ and CD8⁺ T cells

40 µg/ml α-CD4 or α-CD8 and 6 µg/ml α-CD56 antibodies were added into 20x10⁶/ml (E⁺)T cells and incubated for 30 min on ice. The cells were then washed and resuspended with RPMI1640. Freshly prepared complement was added at a ratio of 1:4 (v/v) followed by incubation at 37°C for 60 min. After removing the dead cells by Ficoll gradient centrifugation, the cells were recovered and checked for surface expression of CD4 and CD8. Cells were then activated by TCR/CD3 stimulation with or without the engagement of FasL. Some CD8⁺ T cells were used to generate cytotoxic cell lines.

Establishment of CD8⁺ T cell lines

Freshly isolated CD8⁺ T cell were resuspended in RPMI1640 medium with 10% (v/v) AB serum and stimulated with irradiated EBV-transformed lymphoblastoid cells for

three days. The cells were then expanded in RPMI1640 medium with 10% (v/v) AB serum supplemented with 10 U/ml rIL-2 and restimulated in the same way every 14 days. After the third stimulation, a chromium release assay was carried out to evaluate the cytolytic potential of the cell lines.

3.2.3. Functional analysis of cells

Chromium-51 (⁵¹Cr) release assay

EBV-transformed lymphoblastoid cells were used as target cells: 1x10⁶ (0.5 ml) target cells were labelled with 50 µCi (1.85 Mbq) ⁵¹Cr at 37°C for 60 min. After 3 washes with medium (RPMI1640 and 10% FBS), the cells were resuspended in 5 ml medium. Two cytotoxic CD8⁺ cell lines (CD8⁺-K and CD8⁺-L) were used as effector cells. The cells were washed and adjusted to 2x10⁶/ml with medium and serial 1:2 dilutions were made. Starting with the lowest E/T ratio (3.125:1, 12,500 cells) and ending with the highest (50:1, 200,000 cells), 100 µl of cell suspension were seeded in triplicate into 96-well U-bottom plates (96U TC plates). For each target, 6 wells were left for spontaneous release (SR) and 3 wells were left for maximal release (MR). 100 µl medium were added to the SR wells and 100 µl of detergent (10% TritonX-100) were added to the MR wells. After the effectors were seeded, 25 µl (4,000) labelled target cells were loaded into each well. The plates were then centrifuged for 3 minute at 1000 rpm and incubated at 37°C for 4 hours. The supernatant was then harvested and the ⁵¹Cr release level was assessed in the γ-counter. The percentage of specific lysis was calculated as:

$$\frac{\text{experimental } ^{51}\text{Cr release} - \text{spontaneous } ^{51}\text{Cr release}}{\text{maximum } ^{51}\text{Cr release} - \text{spontaneous } ^{51}\text{Cr release}} \times 100\%$$

Proliferation assay

To determine effects of FasL-engagement on CD3/TCR-induced proliferation of PBMC or T cell blasts, wells of 96-well flat-bottomed tissue culture plates (96F TC plates) were coated or not for 2 hours at 37°C with 1.0 µg/ml OKT3 or 0.5 ng/ml staphylococcal enterotoxin (SE) superantigens without or with 25 µg/ml FasFc or 20 µg/ml anti-FasL mAb 5G51 or 25 µg/ml IgG Fc control proteins as indicated. In some experiments, 5.0 µg/ml α-CD28 was coated together with OKT3. Pretreated TC plates were washed three times with PBS before different cell subpopulations were

plated at 50,000 per well in 200 μ l culture medium. 10 U/ml rIL-2 was added where indicated. On day 3, cells were "pulsed" with ^3H -thymidine (1 $\mu\text{Ci}/\text{well}$) and cultured for additional 18 hours. Cells were harvested and ^3H -thymidine incorporation was assessed in a β -counter.

3.2.4. Cell transfection and selection

Calcium phosphate precipitation

293T cells were seeded and grown to 60-70% confluency. The calcium phosphate transfection reactions were set up by mixing the same volume of BES (2x) or HBS (2x) with 250mM CaCl_2 containing vector DNA. The CaCl_2 solution was slowly dropped into the agitated BES (2x) or HBS (2x) solution on a vortex at a speed of 800 rpm. The reactions remained at room temperature for 10 minutes then were added dropwise into the culture medium. The cells were cultured and used after 18-24 hours. For different tissue culture dishes or plates (TC dishes or plates), the cell number and the amount of vector DNA and volume of buffer were adjusted according to **Table. 3.2.1.**

Table. 3.2.1. Cell number, vector DNA and buffer volume used in different TC dishes

dish or plate	cell number/ volume of medium	amount of vector (1:2)	volume of buffer (2xBES/2.5 M CaCl_2)
10 cm dish	5-6 $\times 10^5$ /10 ml	5 μg : 1 μg	500 μl /50 μl
20 cm dish	2.5-3 $\times 10^6$ /40 ml	20 μg : 6 μg	2 ml/200 μl
6-well plate	1.2-1.5 $\times 10^5$ /2 ml	1 μg : 0.2 μg	100 μl /10 μl
12-well plate	1.2 $\times 10^5$ /2 ml	1 μg : 0.2 μg	100 μl /10 μl

Electroporation

Cells grown to 0.3-0.5 $\times 10^6$ /ml or 80% confluency were pelleted and washed three times with PBS. Cell density was adjusted according to **Table. 3.2.2.** with electroporation medium. 20 μg vector (1-2 $\mu\text{g}/\text{ml}$) alone or with 6 μg (1-2 $\mu\text{g}/\text{ml}$) second vector and 200 μl of cell suspension were placed in a gene pulser cuvette and mixed. The cells were then pulsed in a Gene Pulser II (RF model). The parameters were fixed at a frequency of 40 kHz, 5 pulses with 1 second individual time. The voltage (Vol.), modification rate (Mod.) and duration time (Dur.) per pulse were adjusted accordingly. **Table 3.2.2.** lists the settings used for different cells in the

experiments. After electroporation, cells were immediately transferred into pre-warmed complete medium and cell clusters were resuspended thoroughly. Cells were cultured for 24-48 hours before they were used for staining, protein purification or selected for stable transfectants.

Table 3.2.2. Different settings for cells pulsed by Gene Pulser II (RF model)

cell type	cell density	Electroporation medium	Culture medium	Settings		
				Vol. (V)	Mod. (%)	Dur. (mSec)
RBL2H3	10x10 ⁶	RPMI	RPMI+10%FBS	300	100	5
HeLa	10x10 ⁶	RPMI	DMEM+10%FBS	240	50	5
Jurkat	20x10 ⁶	RPMI	RPMI+10%FBS	370	100	7
HEK	100x10 ⁶	FreeStyle™	293T expression medium	300	100	5

Selection of stable Jurkat FasL transfectants

4 x10⁶ Jurkat cells (JM301 or J16Rapo) were transfected with 20 µg FasLpEFBOS and 6 µg hygromycin-resistant vector by electroporation. 24 hours post transfection, the dead cells were removed by Ficoll density centrifugation. The living cells were counted, resuspended with culture medium and seeded into 96U TC plates under limiting dilution conditions starting from 10,000 cells per well at the volume of 100 µl. Cells were cultured for another 24 hours before 100 µl culture medium containing 600 µg/ml (2x concentrated) hygromycin B were added. Every 4 days, half of the medium was carefully removed and replaced with fresh medium containing 300 µl/ml hygromycin B. Cells were kept in culture until some cell clusters were visible under an inverse light microscope (around 20 days). Clusters were selected and transferred to 24 well plates for further expansion. The FasL expression was checked by FACS analysis, RT-PCR and western blotting. FasL expressing cells were then subcloned. The J16Rapo FasL stable transfectants were named as JFL while the JM301 FasL stable transfectants were named JMFL.

3.2.5. FACS analysis

Surface antigen staining

50,000-100,000 cells were stained in 96-well V-bottom (96V) TC plates according to a standard FACS staining procedure: Cells were pelleted by centrifugation at 1000 rpm for 4 minutes at 4°C and washed once by FACS wash buffer. For staining, cells were

incubated with FITC- or/and PE-conjugated antibody for 20-30 min on ice. The cells were then washed 3 times before they were fixed with 100 μ l 1% PFA and transferred into a FACS analysis tube. Alternatively, gam-PE was used to detect unlabelled primary antibodies and SA-PE or Avidin-FITC was used to analyze biotinylated antibodies. The samples were analyzed in a flow cytometer (FACScan) with cellquest software. In some cases, the reading value of geometric log mean fluorescence of the stained samples were batched and transferred to windows-excel for further analysis.

DNA staining for cell cycle analysis

A propidium iodide (PI)-based nuclear DNA staining indicated cell cycle phase analysis was used as one of the parameters to measure lymphocyte activation and proliferation: $0.5-1 \times 10^6$ cells were transferred into a 15 ml centrifuge tube, washed, resuspended in wash buffer and fixed by dropping of 1ml of 100% ethanol into the agitated cell resuspension. Cells were fixed at room temperature for 30 minutes or 4°C overnight. Fixed cells were pelleted by short spin (5 minutes) at high speed (3000 rpm) and resuspended with 100 μ l wash buffer plus 4 μ l RNase (1 mg/ml) for 30 minutes followed by adding 100 μ l 50 μ g/ml PI solution. Samples were then analyzed in the flow cytometer.

PI staining of dead cells

Being pelleted and washed once with FACS washing buffer, cells were resuspended with 2.5 μ g/ml PI solution and analyzed immediately in flow cytometer. Propidium iodide (PI) intercalates into double-stranded nucleic acids. It is excluded by viable cells but can penetrate cell membranes of dying or dead cells.

Molecular biology

3.2.6. Reverse transcription-polymerase chain reaction-based cloning

Standard reverse transcription polymerase chain reaction (RT-PCR)-based cloning methods were used for most constructs. cDNA derived from either human Jurkat T cells or re-stimulated T cell PHA blasts served as templates. The primers were designed according to the published sequences with adding flanking restriction sites for unidirectional insertion.

RNA extraction and RT-PCR

1-2x10⁶ cells (restimulated T cell blasts, HUT78 cells) were washed in PBS, pelleted and used for RNA extraction with RNeasy[®] Mini Kit following the manufacturer's instruction. RNA was eluted in ddH₂O and the concentration was determined in a spectrophotometer. 500 ng RNA was used for the reverse transcription reaction. 4 µl of cDNA were used for GAPDH PCR by GeneAmp[®] RNA PCR kit (Applied Biosystems, Darmstadt). For cloning PCR, „proofreading“ (*Pfu*) DNA polymerase was used. The set up of reactions and the PCR programs used are listed in **Table 3.2.3**. The production was checked by loading 10% of individual PCR products on a 1% agarose gel containing 0.5 µg/ml EB, separated by electrophoresis and visualized with ultraviolet (UV) light.

Table 3.2.3. PCR mixes and programs for RT-PCR

Reactions					
RT		Regular PCR		Cloning PCR	
MgCl ₂ (25 mM)	4 µl	MgCl ₂ (25 mM)	3 µl	PCR-buffer (10x)	5 µl
PCR-buffer (10x)	2 µl	PCR-buffer (10x)	5 µl	dNTPs (10 mM each)	1 µl (each)
dNTPs (10 mM each)	1 µl (each)	dNTPs (10 mM each)	1 µl (each)	Primers (10 pmol/µl each)	2.5 µl (each)
RNase Inhibitor (20 U/µl)	1 µl	ddH ₂ O	28.5 µl	Pfu DNA polymearse	0.5 µl
MuLV-RT (50 U/µl)	1µl	AmpliTaq (5 U/µl)	0.5 µl	cDNA	4 µl
Oligo d(T) ₁₆ Primer (50 µM)	1 µl	Primers (10 pmol/µl each)	2.5 µl (each)	ddH ₂ O	31.5 µl
RNA	500 ng	cDNA	4 µl		
Program for RT: 42°C, 30sec; 99°C, 5min; 4°C, ∞					
Programs for PCR					
Step		Regular PCR		Cloning PCR	
Initial denaturation		94°C, 5 min		94°C, 5 min	
Denaturation		94°C, 30 sec		94°C, 50 sec	
Annealing	Cycles	58°C, 30 sec	x25-35	Tm, 50 sec	x35
extension		72°C, 40-60 sec		72°C, 1-2 min/Kb	
Final extension		72°C, 7-10 min		72°C, 7-10 min	
Soak		4°C, ∞		4°C, ∞	

Restriction endonuclease digestion

PCR products were purified and eluted in 30 µl ddH₂O by using QIAquick PCR purification kit. According to the flanking restriction sites included within the respective primers, the restriction endonuclease (RE) reaction were set up by adding 5-10 U RE(s) with appropriate buffer to 30 µl PCR products or 5 µg target cloning vector in 50 µl volume and incubated at 37°C overnight.

Extraction of DNA fragments from agarose gels and ligation

The whole reactions were loaded on a 1% agarose gel. After electrophoresis, the stained DNA fragments were excised from the gel under UV light followed by extraction and purification by using QIAquick Gel Extraction Kit. 2 µl of recovered DNA were checked by electrophoresis. A standard DNA ladder with indicated concentration was used to estimate the amount of DNA. 50-200 ng insert DNA and 50 ng vector DNA were ligated by 1 µl T₄ DNA ligase with T₄ DNA ligase buffer in a volume of 20 µl. The ligation reactions were incubated at 16°C overnight.

TA cloning

In some cases, addition of 3'-overhangs was done post amplification before the PCR products were cloned into a PCR 2.1 TOPO TA Cloning vector. Briefly, after amplification with a *Pfu* polymerase, vials were placed on ice and supplemented with 1 unit of *Taq* polymerase followed by incubation at 72°C for 8-10 minutes. The TOPO cloning reactions were set up by gently mixing 4 µl PCR product, 1 µl salt solution with 1 µl Topo vector and incubated at room temperature for 5-30 minutes.

Transformation

2 µl of each ligation reaction was transformed into "Subcloning Efficiency™ DH5α™ Competent Cells" according to the manufacturer's protocol. In brief, competent cells were thawed on ice and divided into prechilled 1.5 ml centrifuge tubes (50 µl per vial). 2 µl of ligation reaction was pipetted directly into the cells and incubated on ice for 30 minutes. Cells were then "heat shocked" for exactly 25 seconds in a 37°C heatblock followed by 2 minutes incubation on ice. 450 µl prewarmed LB medium was added to each vial and the cells were incubated by shaking horizontally at 300 rpm, 37°C for exactly 1 hour before spread onto LB agar plates containing antibiotics (50 µg/ml ampicillin or 30 µg/ml kanamycin) and cultured in a 37°C incubator for 18-24 hours until the transformed bacteria expressing the resistance gene were visible as colonies. 3-6 colonies were selected and cultured in LB medium with antibiotic at 37°C overnight. Plasmid DNA was extracted with QIAGEN® plasmid Mini Kit and used for further analysis.

Positive colony selection

Positive colonies were selected by checking the restriction endonuclease cleavage sites of the plasmid DNA and proved by sequencing. The Big-dye™ terminal sequencing kit was used for sequencing PCR and the primers used for sequencing were T7 promoter sequencing primer, pGEX 5' primer, pGEX 3' primer and the same primer used for PCR. **Table 3.2.4.** lists the set up of reactions and programs for sequencing PCR. After removing the dye with DyeEx spin Kit, the PCR products were sent for in house sequencing. The data were analyzed with blast software from NCBI.

Table 3.2.4. PCR mix and program for sequencing PCR

Reaction		Program		
DNA	0.4 µg	Denaturation	96°C, 10 sec	25 cycles
Big-Dye terminator	4 µl	Annealing	50°C, 5 sec	
Primer 10 pmol/µl	1 µl	Extension	60°C, 4 min	
ddH ₂ O	up to 20 µl	Soak	4°C, ∞	

3.2.7. Subcloning

Some constructs were obtained by cutting DNA fragments from a previously constructed vector with specific restriction endonucleases which allowed in-frame re-ligation into another opened vector (as summarized in **Table 3.2.5.**). In some cases, a blunt end ligation strategy was used.

Table 3.2.5. Constructs obtained from subcloning

Insert	From	RE sites	Target vector	RE sites	Ligation
FasL	pEYFP C1	EcoRI / BamHI	pEGFP C1	EcoRI / BamHI	cohesive-ended
FasL	pcDNA3.1	EcoRI, 5' fill in	pEFBOS	XbaI	blunt-ended
SH3P12	PCR2.1TOPO	HindIII / EcoRI	PCDNA3.1myc	HindIII / EcoRI	cohesive-ended
BAP2-β	PCR2.1TOPO	BamHI / EcoRI	PCDNA3.1myc	BamHI / EcoRI	cohesive-ended
Nck1 all SH3s mut	pcDNA3/myc	BamHI / EcoRI	PEGX2T	BamHI / EcoRI	cohesive-ended

SH3P12 encoding FLAF2; BAP2-β encoding FLAF3; mut: mutated

5' modifications of insert and vector for blunt-ended ligation

In order to produce blunt-ended insert DNA, the Klenow fragment of DNA polymerase I was used to fill in the 5' overhang of digested DNA. After inactivating the RE reaction at 72°C for 15 minutes, 20 U Klenow (8 U/µl) and 1 µl of 1 mM dNTPs were added into the reactions and incubated for 15 min at room temperature. Meanwhile, in order to prevent self ligation, alkaline phosphatase (AP) was used to remove the 5' phosphate

group from blunt-end opened vectors by twice heating the reactions to 56°C for 10 minutes followed by supplementing with 5.5 µl AP buffer and 1 µl (140 U/µl) AP and incubation at 37°C for 30 minutes. The modified insert and vector reactions were then loaded on 1% agarose gel separately. After electrophoresis, the respective DNA fragments were extracted from the gel and processed for ligation.

Biochemistry

3.2.8. Purification of FasFc fusion protein

The FasFc fusion protein was produced from transiently transfected HEK 293 cells and purified by affinity chromatography on a Protein A column. 72 hours after transfection, culture supernatant was collected, filtered and the pH was adjusted to pH 7.0. The medium was then passed over a protein A sepharose CL-4B column which was balanced with binding buffer (start buffer) followed by extensive washes with start buffer again. The bound protein was eluted from the column to collection tubes in a fraction collector. The collection module was set to 30 drops per fraction. 50 µl of neutralizing buffer was added into each collection tubes. The protein concentration in fractions was determined by Coomassie[®] Protein Assay Reagent in comparison to an albumin standard and read in a Smart-Spec[™] 3000 spectrophotometer at the wavelength of 595 nm. The fractions which contained most protein were then pooled, concentrated by Centricon[®]-30 concentrator (30,000 MWCO), and dialyzed in Slide-A Lyzer[®] dialysis cassette (10,000 MWCO) against PBS. The fusion protein was separated by SDS-PAGE on a 10% gel and stained in gel with coomassie blue solution. The bioactivity was tested by inhibition of Fas-mediated lysis on Jurkat cells or AICD of T cell clones. After usage, the protein A sepharose CL-4B column was cleaned by 5 beds of elution buffer followed by at least 20 beds start buffer containing 0.01% NaN₃, closed and stored at 4°C.

3.2.9. GST fusion protein expression and purification

GST fusion proteins were derived by induced expression with IPTG from transformed *E.coli* (DH5α) followed by affinity binding to glutathione beads as follows:

For small scale GST-fusion protein expression, bacteria (DH5α) were cultured in 3 ml medium (LB medium with 50 µg/ml Ampicillin) in a horizontally shaking incubator at 300 rpm, 37°C overnight. The next day, 500 µl cell resuspension were 1:10 diluted into

fresh medium and cultured for 2 hours before IPTG was added to a final concentration of 1.0 mM. Cells were allowed to grow for an additional 5 hours to produce protein before they were pelleted and washed once in PBS. Upon resuspension in 900 μ l PBS, bacteria were transferred into a 1.5 ml centrifuge tube. Cells were kept on ice throughout the procedure and were lysed by two cycles of sonication for 5 seconds each followed by adding 100 μ l TritonX-100 (1% final concentration). The cell lysates remained on ice for 20 minutes and were then centrifuged at 140,000 rpm, 4°C for 10 minutes. The fusion protein in the supernatant was isolated by binding to glutathione sepharose 4B beads as follows: 60 μ l 50% glutathione sepharose 4B beads (in PBS) were incubated with cell lysates for 30 minutes at 4°C on a rotator. After quick spin centrifugation, beads were washed extensively with PBS for at least three times. The beads-bound fusion protein were ready to use.

For large scale GST-fusion protein expression, 100 ml LB-Amp medium were used for the initial culture. The cells were 1:10 diluted into 300 ml fresh medium for 2 hours before adding IPTG for 5 hours. Afterwards the cells were pelleted, washed and lysed by sonication in 27 ml PBS, 3x20 seconds followed by addition of 3 ml 10% Triton X-100. After centrifugation, 1 ml of 50% glutathione sepharose 4B beads (in PBS) was used to precipitate the fusion protein during 20 minutes of rotation at room temperature. After several washes, the protein concentration was determined and the purity was visualized by electrophoresis. In some cases, the proteins were further eluted by three cycles of incubation with glutathione elution buffer for 5 minutes each at room temperature on a rotator. The proteins were collected, concentrated, dialysed against PBS and stored at -80°C.

3.2.10. Protein “pull down” assays

For protein “pull down” assays with GST fusion protein, lysates from $10\text{-}20 \times 10^6$ cells were used. The cells were pelleted, washed with PBS and lysed in 1 ml of 1% NP40 buffer with protease and phosphatase inhibitors followed by 10 times homogenization with a dounce-homogenizier. Lysates remained on ice for 10 minutes before centrifugation at 4°C and 14000 rpm for 10 minutes. Supernatants were then transferred into fresh tubes and incubated for 2 hours rotating at 4°C with 20-50 μ g of indicated GST fusion protein. 50 μ l of a 50% slurry of glutathione sepharose 4B beads were added directly to the samples. The beads were then pelleted, washed thrice in

cold PBS, boiled in sample buffer containing β -ME and separated by SDS-PAGE followed by western blotting.

3.2.11. Immunoprecipitation

For co-immunoprecipitation, 3×10^6 293T cells were collected and lysed in 1 ml 1% NP40 buffer 24 hours after transfection. Lysates remained on ice for 10 minutes before centrifugation at 4°C and 14000 rpm for 10 minutes. Supernatants were divided equally and incubated for 2 hours rotating at 4°C with 2-5 μ g of the respective antibody and 50 μ l of a 50% slurry of Protein A sepharose CL4B beads. The beads were then pelleted, washed thrice in cold lysis buffer, boiled in sample buffer containing β -ME and separated by SDS-PAGE followed by western blotting.

3.2.12. Cell stimulation and anti-phosphotyrosine western blotting

To analyze potential effects of FasL engagement on TCR/CD3-induced tyrosine phosphorylation, cells were pre-incubated with or without FasFc (50 μ g/ml) crosslinked with 10 μ g/ml anti-human IgG Fc or 20 μ g/ml anti-FasL mAb 5G51 crosslinked with 5 μ g/ml rabbit anti-mouse IgG. Cells were then incubated at 37°C for 30-120 minutes in the presence or absence of the indicated reagents before aliquots of $1.5-2 \times 10^6$ cells were exposed to OKT3 at 10 μ g/ml for the indicated time periods. Stimulation was stopped by adding 1 ml ice-cold PBS, quick spin centrifugation, aspiration of the PBS/antibody supernatant and immediate lysis in 30 μ l of 1% NP40 lysis buffer with protease and phosphatase inhibitors. Lysates remained on ice for 15-30 minutes before centrifugation at 4°C and 14000 rpm for 7 minutes. Supernatants were then transferred into fresh tubes, boiled in an equal of sample buffer containing β -ME and were separated by SDS-PAGE followed by western blotting procedure.

3.2.13. SDS-PAGE and Western blot

The cleaned glass plates were assembled and filled in with standard running gel followed by stacking gel. The gel apparatus were assembled and the gels were run either at 60 voltage overnight or at 200 voltage within 6 hours with cooling. The gels were transferred right after the electrophoresis. The transfer sandwich was assembled from cathode to anode with sponge, 2 pieces of Whatman 3MM-paper, gel, nitrocellulose, 2 pieces of Whatman 3MM-paper, sponge in a plastic cassette. The cassette was placed into the transfer tank and the protein transfer was performed at

0.8 A, 4°C for 2 hours or 0.15 A overnight. The efficiency and quality of transfer was monitored by staining the membrane with Ponceau S solution. After the washes with TBST to remove the staining from proteins, the blots were blocked with 5% BSA blocking solution for 1 hour and incubated with primary antibody diluted in TBST for 1 hour followed by HRP-linked secondary antibodies diluted in TBST for 45-60 minutes at room temperature. Between each step, the blots were washed thrice with TBST for 10 minutes. After rinsing in water, ECL developing solutions were prepared and added to the blot for one minute. Hyperfilm™ ECL films were used for visualizing emitted chemiluminescence.

3.2.14. *In vitro* kinase assay

The full length FasL cytosolic region (FasLcyto), the N-terminal part (FasLcyto1) and the membrane-proximal portion (FasLcyto2) expressed as GST fusion proteins, kept on glutathione sepharose beads (**Fig. 3.2.1**) were used as substrates for *in vitro* casein kinase assay: 50 µg fusion protein combined to beads were used for each reaction. After the beads had been

washed extensively in kinase buffer and dried by aspirating all buffer with a 27G needle, the kinase reactions were carried out by incubating the dry beads with 30 µl kinase buffer in the absence or presents of 100 U or 500 U recombinant casein kinase1 together with 10 µCi [³²P]ATP for 20 minutes at room temperature.

The reaction was stopped by

adding 60 µl 2× sample buffer containing β-ME and heating to 100°C for 5 minutes. Samples were separated by SDS-PAGE and the gel was stained by coomassie blue and dried in a gel dryer. The autoradiography was performed by using Hyperfilm™ MP films.

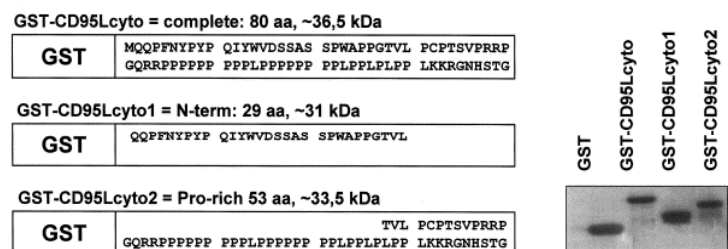


Fig.3.2.1. FasL cytosolic GST fusion protein constructs.

FasLcyto contains the complete cytoplasmic tail of FasL, consisting of 80 aa (36.5 kDa); FasLcyto1 contains the N-terminal region of 29 aa (33.5 kDa) and FasLcyto2 contains the membrane proximal proline-rich stretch with 53 aa (31 kDa). Importantly, FasLcyto and FasLcyto1 contain the putative CK1 motif SSASS.

Immunostaining and confocal microscopy

3.2.15. Coverslips and cell preparation

Cleaning and pretreatment of the coverslips

Coverslips were cleaned in 37.5% HCl for 15 min, washed in ddH_2O followed by 70% ethanol and sterilized by dry heating at 180°C for 2 hours.

Pretreatment of the coverslips

Coverslips were coated with 50-100 $\mu\text{g/ml}$ poly-L-lysine for 30 min at room temperature. Afterwards, the liquid was removed and the coverslips were washed with PBS. In some experiments, 10 $\mu\text{g/ml}$ OKT3 or 0.5 ng/ml SEA diluted in PBS were loaded on poly-L-lysine pretreated coverslips at 37°C for 2 hours.

Cell preparation

For adherent cells, $1.2\text{-}1.5 \times 10^5$ cells were grown on coverslips in 12 well plates for 24-28 hours before they were used for transfection or co-culture experiments.

For cells in suspension, $1\text{-}1.5 \times 10^6$ cells were washed and resuspended in 300 μl PBS and loaded on poly-L-lysine pretreated coverslips at 4°C for 15 minutes. Cell adhesion was controlled by light microscopy. Non-adherent cells were removed carefully and the samples were ready for fixation.

Stimulation of the cells

$1\text{-}1.5 \times 10^6$ cells were cultured on pretreated coverslips in 300 μl of medium without FBS for the indicated time intervals. Stimulation was stopped by removing the non-adherent cells carefully, washing the sample once with PBS followed by fixation.

In experiments where cells were stimulated by soluble agents, the cells were cultured in wells containing pretreated coverslips and stimulated by adding the stimuli directly to the culture medium to a final concentration of 10 ng/ml TPA and 500 ng/ml ionomycin. To determine kinetics of the stimulations, the experiments were designed to allow simultaneous fixation and treatment of all samples. To this end, cells were quickly fixed by -20°C methanol for 5 minutes.

Pretreatment of the cells

Cells were cultured in medium supplemented with respective inhibitors or dyes for the indicated time periods (LysoTracker Red DND-99, 100 nM, 1 hour; Latrunculin A, 5 nM, 30 minutes; Cytochalasin D, 10 μ M, 30 minutes) before they were washed, resuspended in PBS and loaded on coverslips.

Co-culture of the T cells and B cells

T cells and target B cells were mixed at a ratio of 2:1 and cultured for 20 minutes before they were carefully moved onto poly-L-lysine pretreated coverslips for 15 min at 4°C. After removing non-adherent cells, the samples were washed once with PBS and processed for fixation.

3.2.16. Fixation

Cells were fixed by -20°C methanol for 5 minutes or alternatively, by a pH-shift/formaldehyde fixation method. To this end, cells were washed once with PBS, fixed with 3% PFA in PEM buffer for 5 min followed by 3% PFA in borate buffer for 10 minutes and permeabilized in 1% Triton-X100 for 15 min. After rinsing 3 times with PBS, the samples were treated twice with freshly dissolved 1 mg/ml borohydride (NaBH₄) for 10 minutes each to reduce the unreacted aldehydes followed by 3 rinses with PBS. The samples were then ready for staining.

3.2.17. Staining

The samples were blocked with 0.2% BSA in PBST for one hour followed by incubation with appropriate primary and fluorescent-conjugated secondary antibodies or reagents. The incubation periods were 1 hour at room temperature or overnight at 4°C for the primary antibodies and 50 minutes at room temperature for the secondary reagents. Samples were washed 3 times in PBS between each step. In double stained samples, one antibody and one colour-tagged vector were used while in triple-stained samples, two different species of primary antibodies and one colour-tagged vector were used. After being mounted with anti-fade mounting medium and sealed by nail polish, the stained samples were processed for analysis and kept at 4°C in dark.

3.2.18. Laser scan confocal microscopy

The stained samples were analysed under the laser scanning microscope LSM510 with software. The emission and excitation wavelengths used for different dyes or vectors are listed in **Table 3.2.6**. Laser 488, 543 and 633 were set for two- or three-fluorescence imaging as shown in **Fig.3.2.2**. (adapted from Bio-Rad fluorescence database).

Table 3.2.6. Excitation (Ex) and emission (Em) wavelengths (nm) for different dyes or vectors

Fluorochrome	Ex(max)	Em (max)
Alexa 488	492	520
Alexa 546	557	572
CY5	649	666
DsRed	556	583
EGFP	498	516
EYFP	520	532
Rhodamine	550	573
Lysotracker Red DND-99	577	590

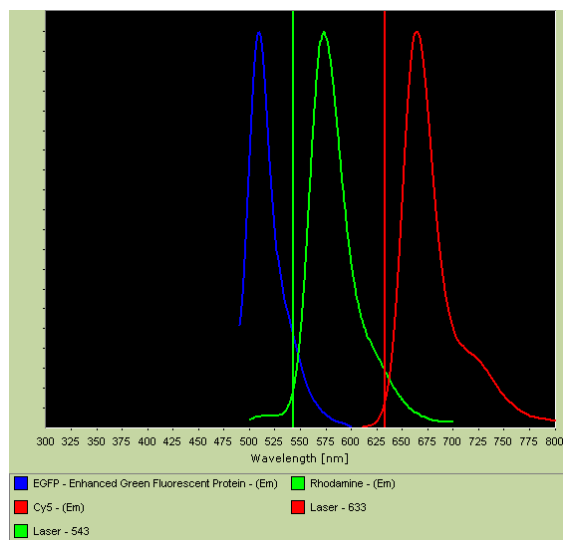


Fig. 3.2.2. The distribution of Em wavelengths excited from different lasers. The curves from the left to right indicate EGFP-(Em), Rhodamine-(Em), CY5-(Em) and the lines from the left to the right indicate Laser-543 and Laser-633.

3.2.19. Observation of living cells and video recording

To visualize the contact of $\gamma\delta$ T cells (EP3) and tumor cells. 50,000 MeWo cells were grown on Lab-TekII chambered coverslips for 24 hours. 1×10^6 EP3 cells were cultured in medium containing 50 nM Lysotracker Red DND-99 for 1 hour followed by 2 times washes with medium. Right before the EP3 cells were loaded to the MeWo cells, 200 nM BrHPP was added. Medium alone with 200 nM BrHPP was used as control. The chamber was then plated on a temperature-controlled specimen stage of the microscope and the culture medium of MeWo cells was replaced by either the 1 ml Lysotracker Red loaded EP3 cell resuspension or the control medium. Sequential confocal images were acquired every 1 minute up to 2 hours with the start point the MeWo cells were focused. Laser 546 was used to monitor the lysosomal compartment stained with lysotracker Red in EP3 cells and a normal transmission light was used to show the cell morphology changes. After 2 hours, the cells in the control chamber were observed for comparison.

4. Results

4.1. Reverse signal transduction of FasL in human T cells

Over the past few years, it became obvious that several members of the TNF superfamily exert a bi-directional signaling capacity (see for a review¹³⁷). However, in most cases the underlying biochemical mechanisms remained unclear. For FasL, the most convincing data stem from experiments done with Fas (*lpr*, *lpr*^{cg}) or FasL (*gld*) mutant mice. Cells from those mice are in principle resistant to Fas-FasL induced cell death and develop lymphoaccumulation and splenomegaly and autoimmune diseases^{63,64}. Utilizing FasL or Fas defect mutant mice, several groups demonstrated that the expression of functional FasL is required for "normal" activation of mature CD4⁺ or antigen-specific CD8⁺ T cells⁶⁸⁻⁷¹. Besides, FasL-to-TCR-crosstalk seems to be involved in positive selection of thymocytes depending on the antigen affinity during the selection process⁷². For human cells, FasL signaling has not been convincingly demonstrated. Most effects of an intervention into Fas/FasL system were claimed to involve Fas rather than FasL signal transduction¹³⁸. One aim of the present study was to demonstrate an influence of FasL stimulation on the outcome of TCR/CD3-triggered activation or effector function.

4.1.1. Generation and functionality of a FasFc fusion protein

In order to specifically engage FasL, we constructed a FasFc fusion protein. The construct was designed to encode the extracellular domain of human Fas (aa 1-173) and the Fc portion of human IgG1 (Fig. 4.1.1A). The protein was purified from supernatant of HEK 293 transfectants by affinity chromatography. On 10% gels, the fusion protein migrated at around 60 kDa. The purified FasFc was tested by analyzing the inhibitory effect on activation-induced cell death (AICD) in a staphylococcal enterotoxin superantigen A (SEA)-reactive T cell clone. To this end, clone cells were incubated with SEA or TPA/ionomycin in the presence or absence of FasFc (25 µg/ml) or anti-FasL mAb 5G51 (20 µg/ml). As shown in Fig. 4.1.1B, AICD induced by SEA and TPA/ionomycin could be blocked in part by FasFc as well as the anti-FasL antibody 5G51.

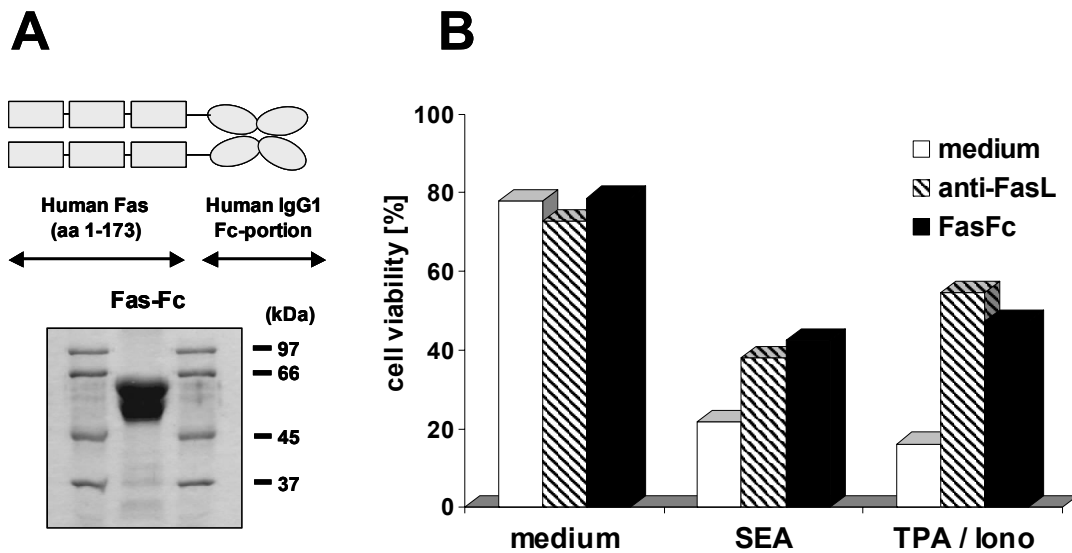


Fig. 4.1.1. FasFc fusion protein and anti-FasL mAb 5G51 block AICD of CD4⁺ clone cells.

(A) Generation and purification of FasFc: the vector for FasFc was designed that at the protein level the extracellular domain of human Fas (aa 1-173) was fused to the Fc portion of human IgG1. The chimeric protein migrates at 60 kDa in denaturing SDS-PAGE. (B) Inhibition of AICD: CD4⁺ clone cells were cultured in medium alone or in the presence of staphylococcal enterotoxin superantigen A (SEA, 0.5 ng/ml) or TPA/ionomycin (10 and 500 ng/ml, respectively) in the absence or presence of 20 µg/ml anti-FasL mAb 5G51 or 50 µg/ml FasFc. After 16 hours, cells were harvested and stained with propidium iodide (PI) followed by FACS analysis. The cell viability was determined.

4.1.2. Crosslinked but not soluble FasL inhibits proliferation of PBMC

Since the bi-directional modulation of signaling pathways often requires crosslinking of the receptors involved, the following experiments were designed to mimic crosslinking of the TCR/CD3 complex and/or FasL. To this end, wells of 96-well flat-bottom tissue culture plates (96F TC plates) were pre-coated with OKT3 mAb or staphylococcal enterotoxin (SE) superantigen alone or together with FasFc fusion protein. Under conditions where we used low concentrations of the respective TCR/CD3 stimulus, the presence of plate-bound FasFc fusion protein had a quite dramatic effect. As shown in Fig. 4.1.2A and B, OKT3- (A) or superantigen- (B) induced stimulation of proliferation of freshly isolated PBMC from all tested donors was inhibited by at least 64% (A, donor 1) and at most 92% (A, donor 3). In contrast, when soluble FasFc fusion protein was added to the medium of cells that were stimulated by plate-bound TCR/CD3 agonists, only a very mild inhibition of thymidine uptake was detectable (Fig. 4.1.2C, 5.3% for OKT3 and 15% for superantigen). It is important to note that the Fas but not the Fc part of the fusion protein displayed the inhibitory function. As shown in Fig. 4.1.3A, the Fc fragment of human IgG had only little or no effect on the CD3- or

superantigen-induced proliferation of PBMC whereas the FasFc fusion protein reduced the thymidine uptake by 92% in the case of OKT3 and by 77% in the case of superantigen.

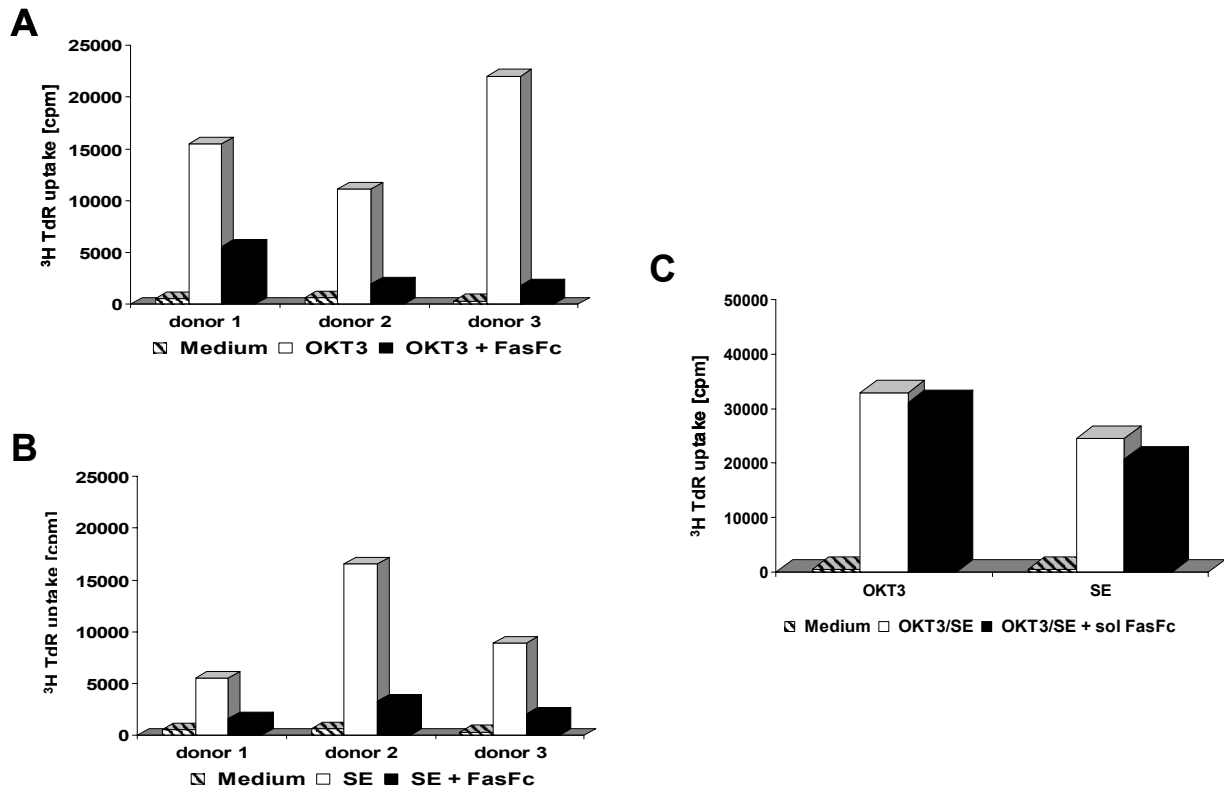


Fig. 4.1.2. Crosslinked but not soluble FasL inhibits proliferation of PBMC. PBMC from 3 different donors were cultured for 3 days in 96F TC plates coated with 1 μ g/ml anti-CD3 mAb OKT3 (A,C) or 0.5 ng/ml staphylococcal enterotoxin (SE) superantigen (B,C). FasFc (25 μ g/ml) was either also coated on the plates (A, B) or added as a soluble factor to the culture medium (C). Proliferation was determined by 3 H-thymidine incorporation. Data are represented as mean values of triplicate wells.

4.1.3. Crosslinked FasL inhibits proliferation of T cell blasts in the absence of exogenously added rIL-2

We also observed an inhibitory effect of FasL crosslinking on the proliferation of T cell blasts in the absence of exogenously added IL-2. Although T cell blasts at that stage showed only a limited increase in TCR/CD3-induced proliferation (probably due to the lack of growth factor), the reduction in the presence of plate-bound FasFc but not in the presence of the Fc control fragment was quite obvious (Fig. 4.1.3B).

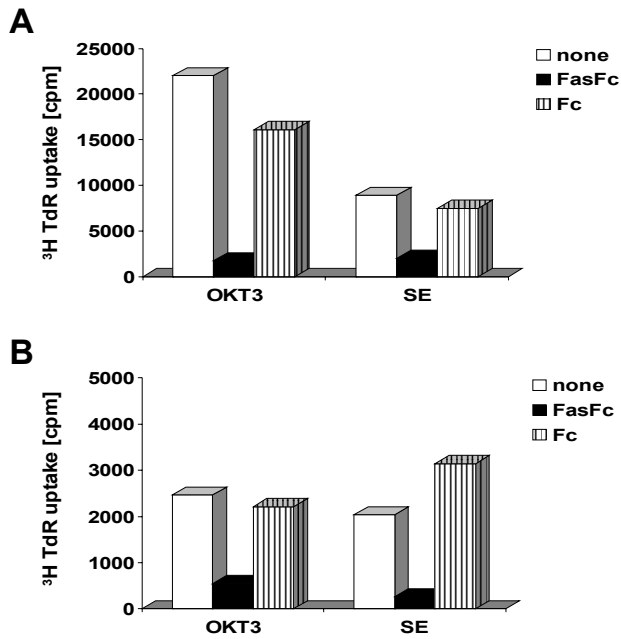
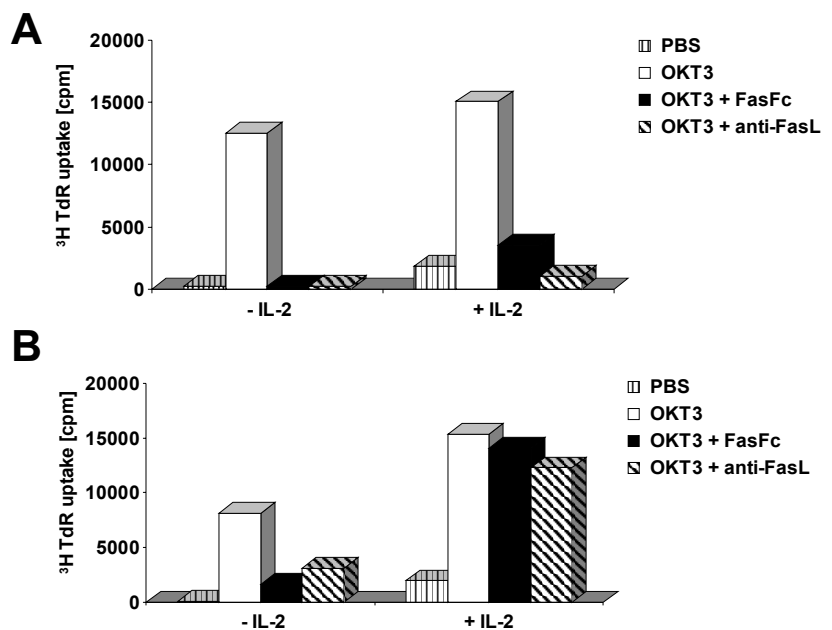


Fig. 4.1.3. FasL signaling inhibits proliferation of PBMC and T cell blasts. PBMC (A) or T cell blasts (B) were cultured for 3 days in wells coated with 1 μ g/ml anti-CD3 mAb OKT3 or 0.5 ng/ml staphylococcal enterotoxin (SE) superantigen with or without 25 μ g/ml FasFc or human IgGFc control protein. Proliferation was determined by 3 H-thymidine incorporation. Data represent mean values of triplicate cultures.

To further analyze a possible involvement of IL-2 and the activation state in the FasL-sensitivity of T cell populations, we added exogenous growth factor. Note that the inhibition could also be achieved when plate-bound anti-FasL antibody instead of FasFc was used to crosslink FasL (Fig. 4.1.4). Interestingly, as demonstrated in Fig. 4.1.4, there was a clear bias in the IL-2 effect between freshly isolated PBMC (A) and T cell blasts (B). Whereas in PBMC, addition of exogenous recombinant IL-2 (rIL-2) had only little effect on the FasFc- or anti-FasL-dependent reduction of proliferation, in T cell blasts the inhibitory effect of both reagents was completely overcome by adding rIL-2.

Fig. 4.1.4. rIL-2 counteracts FasL effects in T cell blasts but not in PBMC. PBMC (A) or T cell blasts (B) were cultured for 3 days in culture plates coated with 1.0 μ g/ml anti-CD3 mAb OKT3 without or with 25 μ g/ml FasFc or 20 μ g/ml anti-FasL mAb 5G51 in the absence or presence of 10 U/ml rIL-2. Data for 3 H-thymidine uptake are given as mean value of triplicate cultures.



4.1.4. FasL-engagement inhibits proliferation of freshly isolated human peripheral T cells

Next we examined effects of FasL-engagement on different freshly isolated T cell populations. T cells were purified by E-rosette formation with sheep red blood cells (E^+). $CD4^+$ or $CD8^+$ subsets were further enriched by negative selection using complement mediated lysis. The purity of $CD4^+$ or $CD8^+$ T cells was more than 90% (Fig. 4.1.5).

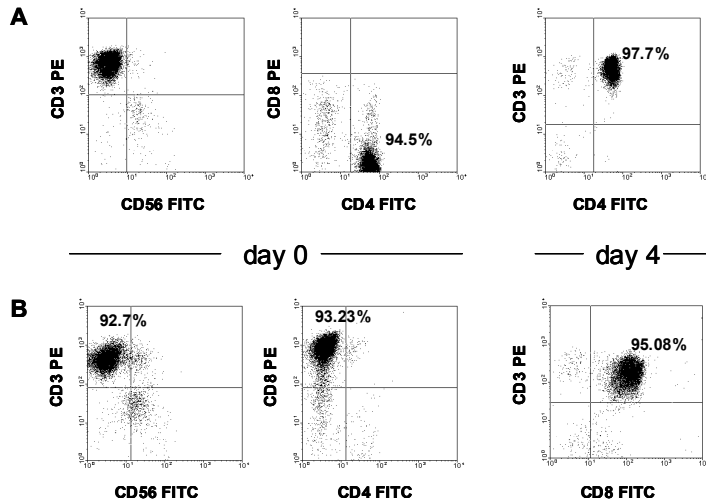
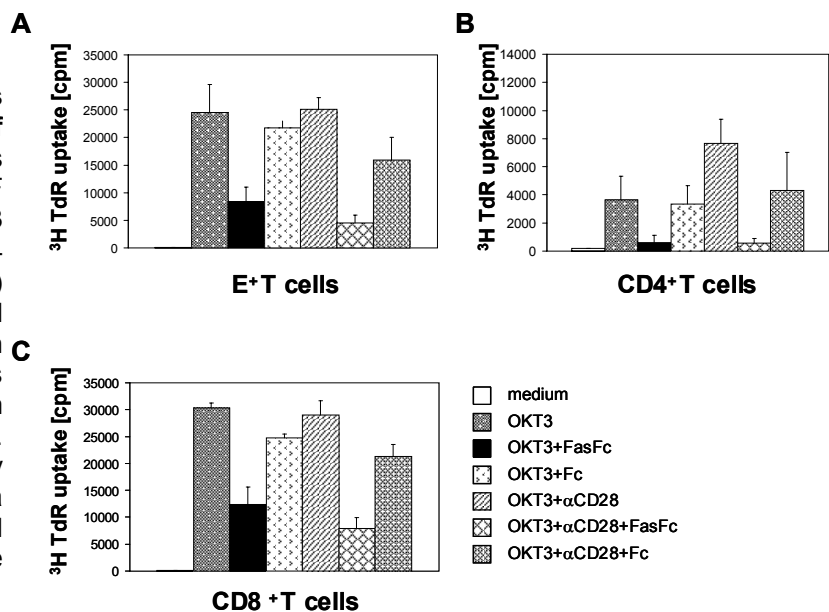


Fig. 4.1.5. Purity of isolated T cells. Isolated T cell subpopulations (A. $CD4^+$ and B. $CD8^+$ T cells) were double-stained with FITC- or PE-conjugated antibodies to CD56 and CD3 or CD4 and CD8 right after the purification (left panel) or to CD3 and CD4 or CD8 after 4 days of culture (right panel).

In all experiments, we consistently found that anti-CD3 or anti-CD3 and anti-CD28 triggered proliferation of E^+ , $CD4^+$ and $CD8^+$ T cells was substantially inhibited in the presence of plate-bound FasFc compared to the control groups. This inhibitory effect suggested that crosslinked FasL can deliver a strong negative signal to the T cells (Fig. 4.1.6).

4.1.6. FasL signaling inhibits TCR/CD3 driven proliferation of freshly isolated T cells.

Cells were stimulated for 3 days in 96F TC plates coated with anti-CD3 mAb OKT3 (1 $\mu\text{g}/\text{ml}$) or OKT3+ α -CD28 (5 $\mu\text{g}/\text{ml}$). FasFc (25 $\mu\text{g}/\text{ml}$) or the same amount of Fc control protein was coated together with the stimuli where indicated. Cells were cultured in PRMI medium with 10% (v/v) AB serum. Proliferation was determined by ^3H -thymidine incorporation. Data represent mean values and standard deviations from triplicate wells.



We also observed differences in morphology of the T cells stimulated under different conditions. As expected, during the 4 days of culture, the cells kept in medium remained small and round while the stimulation led to enlargement and formation of proliferation clusters. Clearly, most of the cells treated with FasFc also remained small and round. Importantly, we did not detect an increase in the number of dead cells in the presence of FasFc. The differences were most obvious on day two. While the cells in absence of FasFc started to proliferate, the FasFc treated cells remained "silenced". Only on day three, some FasFc-treated cells started to proliferate but to a much lesser degree compared to the other groups. The flow cytometric analyses confirmed our observation (Fig. 4.1.7). It should be stressed that the inhibitory effect of FasL engagement on proliferation was observed in both CD4⁺ and CD8⁺ subpopulations.

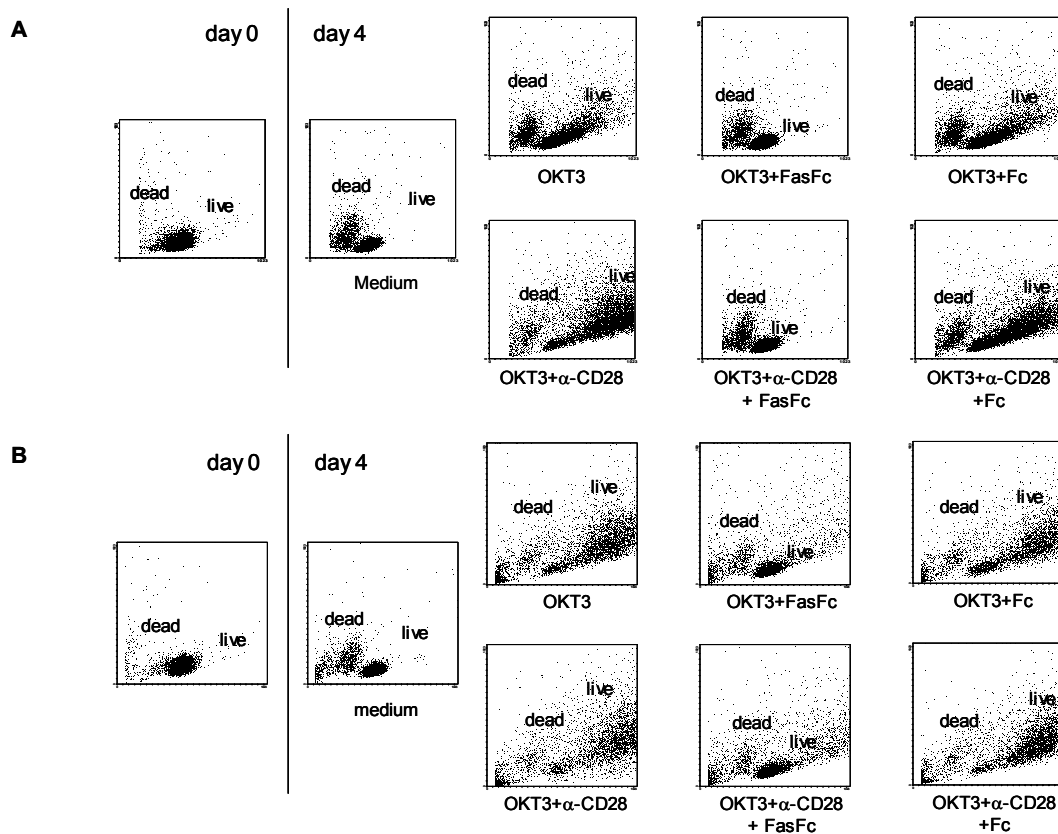


Fig. 4.1.7. FasL-engagement inhibits TCR/CD3-induced T cell activation. CD4⁺ (A) or CD8⁺ (B) T cell population were enriched as described. Cells were stimulated for 4 days in 24 well TC plates coated with anti-CD3 mAb OKT3 (1 µg/ml) or OKT3+α-CD28 (5 µg/ml) in the presence or absence of FasFc (25 µg/ml) or the same amount of IgGFc control protein. Cells were cultured in PRMI medium with 10% (v/v) AB serum. Activation was monitored on the basis of cell size (forward scatter) and granularity (side scatter) determined by FACS analysis. Cells were analyzed on day 0 (left panel) and after 4 days (right panel) of culture.

We also analyzed the expression of the two activation markers CD69 (known as activation inducer molecule, very early activation antigen, MLR-3 and Leu-23) and CD25 (IL-2 receptor α chain) on cells of the individual groups after 4 days of stimulation. As expected, both antigens were heavily induced on both CD4⁺ and CD8⁺ T cell subsets upon stimulation with anti-CD3 and anti-CD28 antibodies. Moreover, all cells cultured in the presence of plate-bound FasFc showed no or only slightly increased expression of both surface antigen (Fig. 4.1.8).

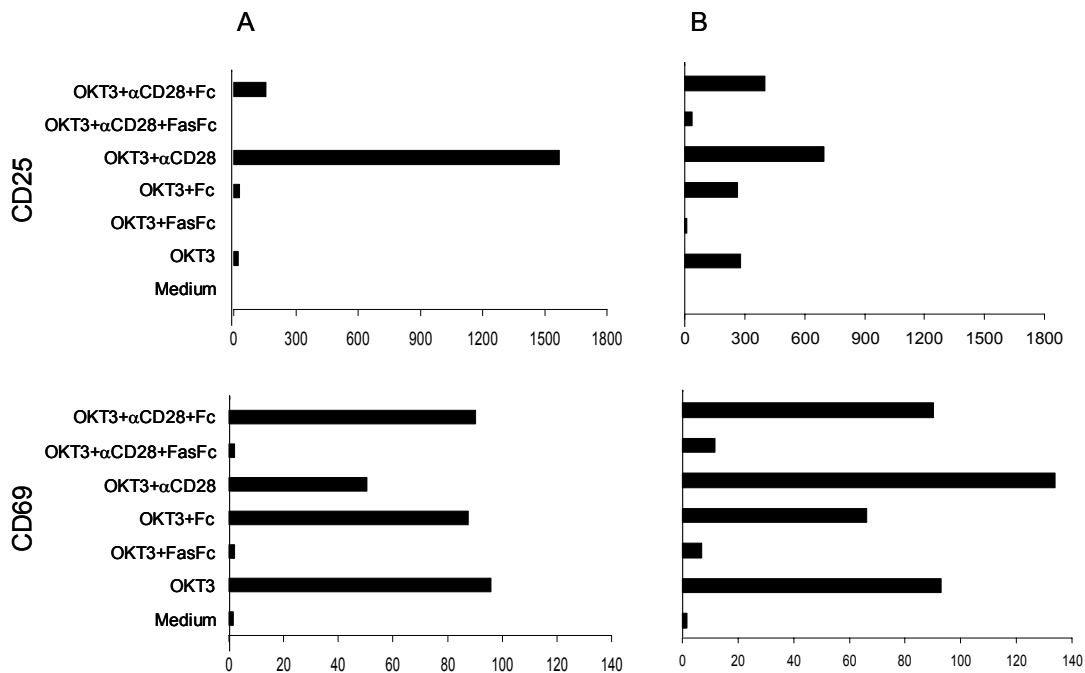
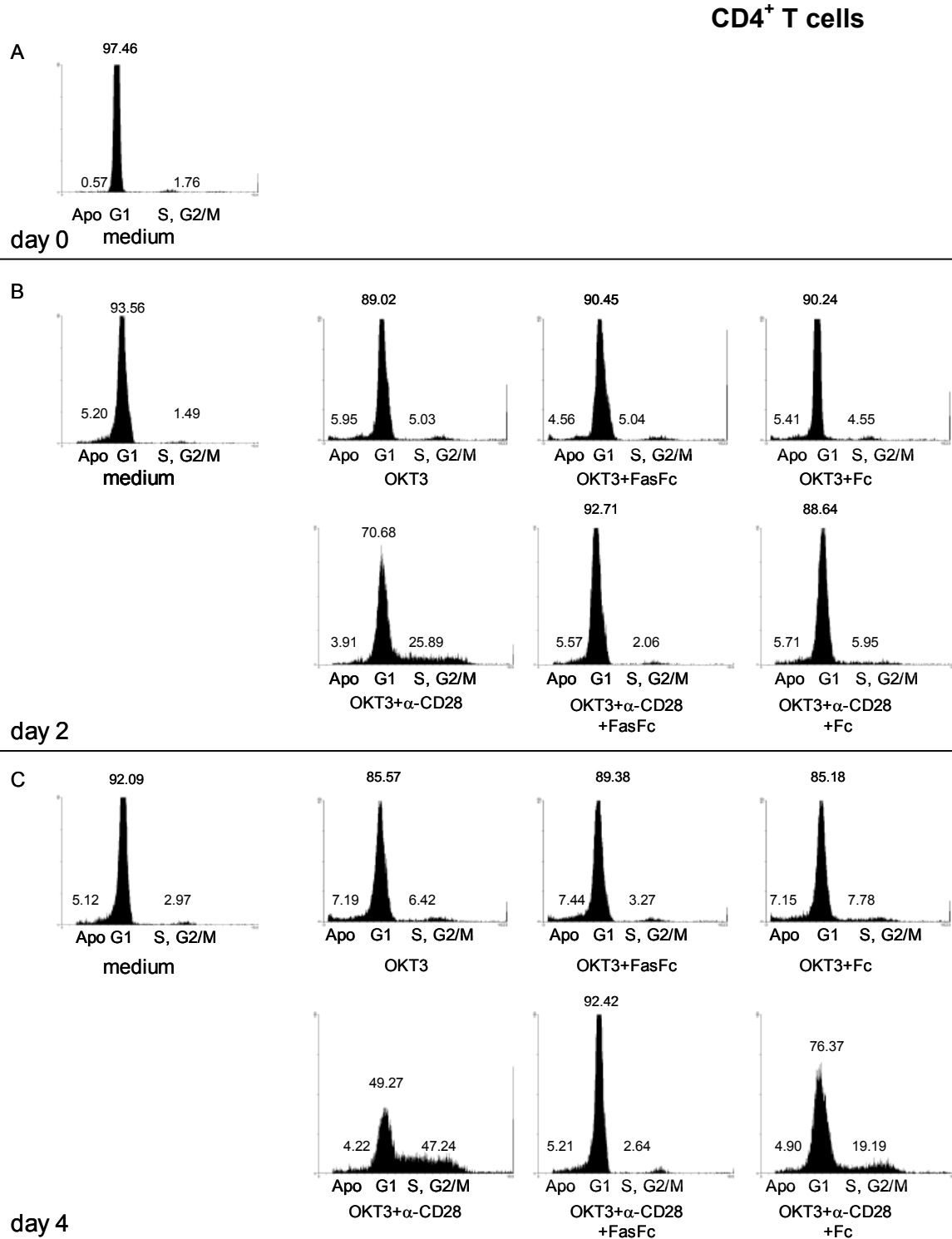


Fig. 4.1.8. Inhibited surface expression of CD25 and CD69 of activated T cells crosslinked with FasL. T cells (A. CD4⁺ or B. CD8⁺ T cells) were cultured in wells coated as described in Fig. 4.1.7. for 4 days. Surface expression of CD25 (upper panel) and CD69 (lower panel) was assessed by staining with PE- conjugated α -CD25 or α -CD69 followed by FACS analysis. The graphs show the geometric log mean fluorescence intensity.

4.1.5. FasL-engagement blocks cell-cycle progression of freshly isolated human peripheral T cells

Cell-cycle analyses were also performed in parallel. The results supported the observations on the morphological changes of the cells. 2 days after stimulation, a fraction of cells started to enter into G₂/S phase. On day 4, the number of cells in G₂/S phase was further increased and only some apoptotic cells could be detected. As expected, co-stimulation by OKT3 and anti-CD28 lead to enhanced cell-cycle progression as compared to stimulation by OKT3 alone. Also activation of CD4⁺ T cells seemed to depend more on the co-stimulatory signal through CD28. Clearly, FasL-

engagement kept the cells resting at G_0/G_1 and inhibited G_2/S entry. Importantly, we did not observe a significant increase in apoptotic cells during the 4 days culture. Thus, FasL-engagement resulted in growth arrest but not apoptosis of freshly isolated T cells. (Fig. 4.1.9).



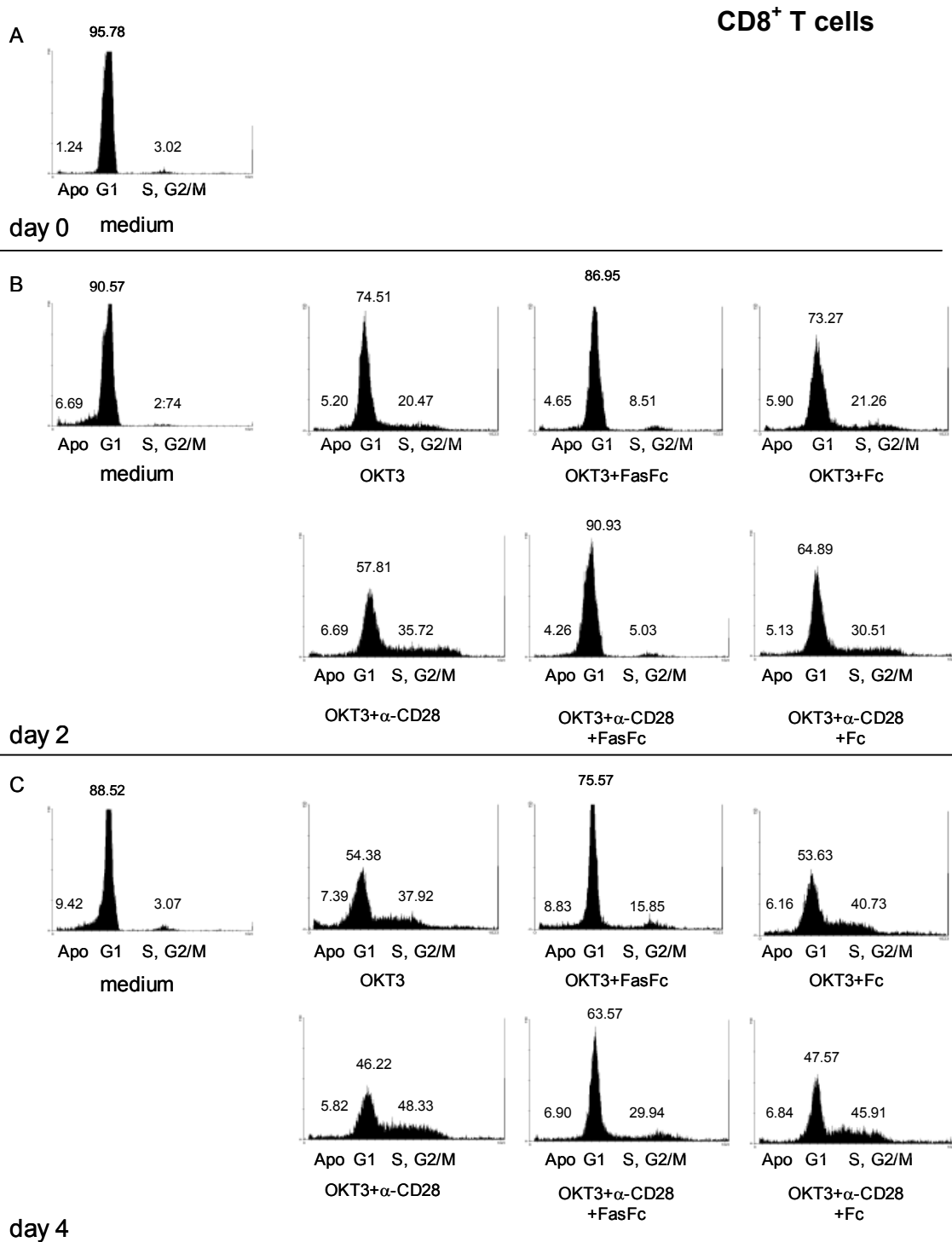


Fig. 4.1.9. FasL-engagement results in cell-cycle arrest. Cell-cycle progression of T cell subpopulations was analyzed upon isolation (A) and after 2 days (B) or 4 days (C) in culture. The cells were then collected from individual wells, fixed and permeabilized and stained with 50 μ g/ml propidium iodide for DNA content analysis by flow cytometry. The percentages of apoptotic (apo, <2n DNA), G₀/G₁ (G₁, 2n DNA), and S, G₂/M (>2n DNA) cells are indicated.

4.1.6. Exogenous IL-2 does not counteract FasL-induced inhibition of T cells

As described before in Fig. 4.1.8, the stimulated cells treated with plate-bound FasFc showed no or slightly increased expression of CD25 after 4 days stimulation. To check whether the inhibition through FasL signal might be due to a reduced production of IL-2, we added additional exogenous rIL-2 into culture medium. Clearly, the exogenous IL-2 was not able to restore the proliferation ability of freshly isolated T cells (Fig. 4.1.10). When compared to effect of FasL-ligation in the absence of rIL-2 (shown in Fig. 4.1.6), we did not observe a major effect of the growth factor.

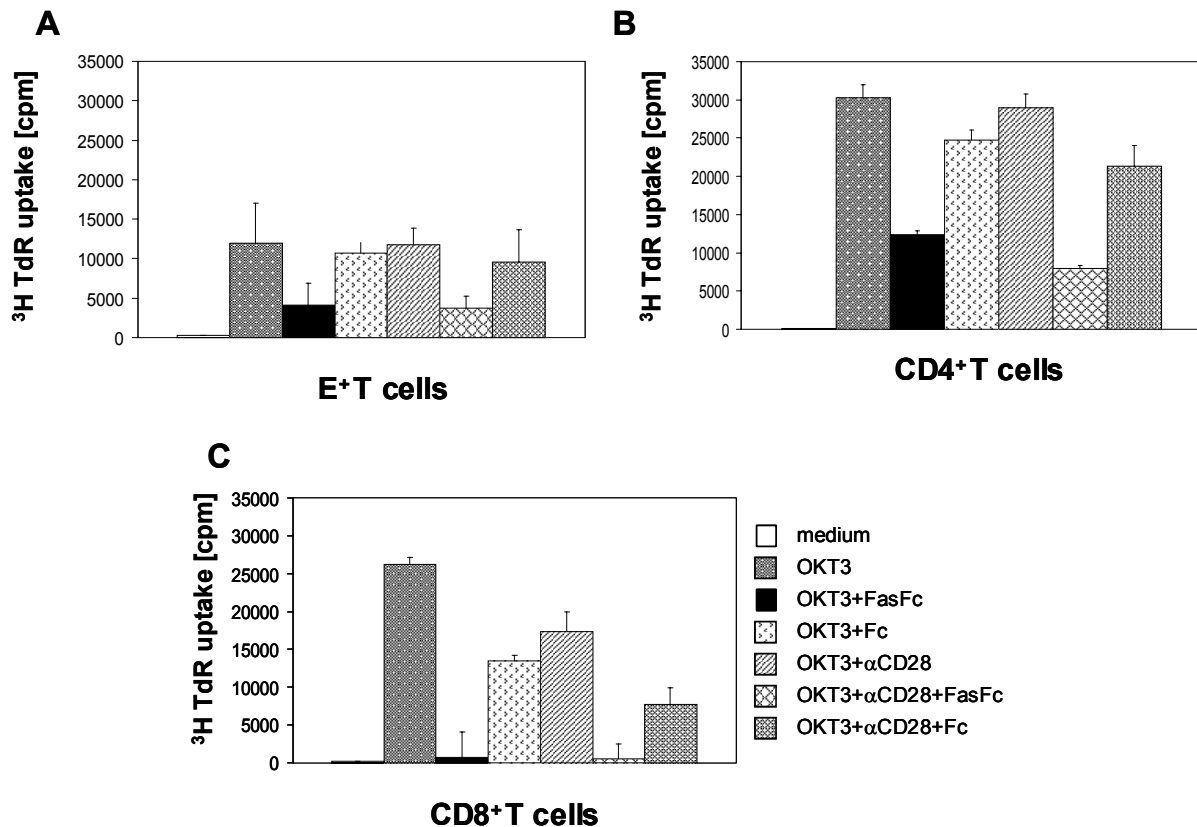


Fig. 4.1.10. IL-2 does not counteract FasL effects in T cells. T cells (A. CD8⁺, B. CD4⁺ or C. E⁺ T cells) were stimulated as described in Fig. 4.1.6. for 3 days in 96F TC plates. Cells were cultured in PRMI and 10% (v/v) AB serum with exogenous added 10 U/ml rIL-2. Proliferation was determined by ³H-thymidine incorporation. Data represent mean values and standard deviations from triplicate wells.

4.1.7. Enhanced proliferation upon FasL-engagement in T cell clones

Then we analyzed the effects of FasL engagement on established T cell clones and lines. In contrast to freshly isolated T cells, engagement of FasL by plate-bound FasFc in T cell clones resulted in an increased thymidine uptake in response to TCR/CD3 stimulation (either OKT3 or OKT3 and anti-CD28). Notably, cells maintained in the medium also showed a higher degree of ^3H TdR uptake than stimulated cells. When comparing cells that had been restimulated for 7 or 28 days prior to the assay. The former one (7 days) showed a stronger inhibition of proliferation (Fig. 4.1.11). Note that the cells were kept in IL-2 containing medium, therefore the medium control showed a high degree of ^3H TdR uptake. Upon restimulation, the reduction of proliferation was probably due to the induction of AICD, which then might be blocked by FasL-engagement.

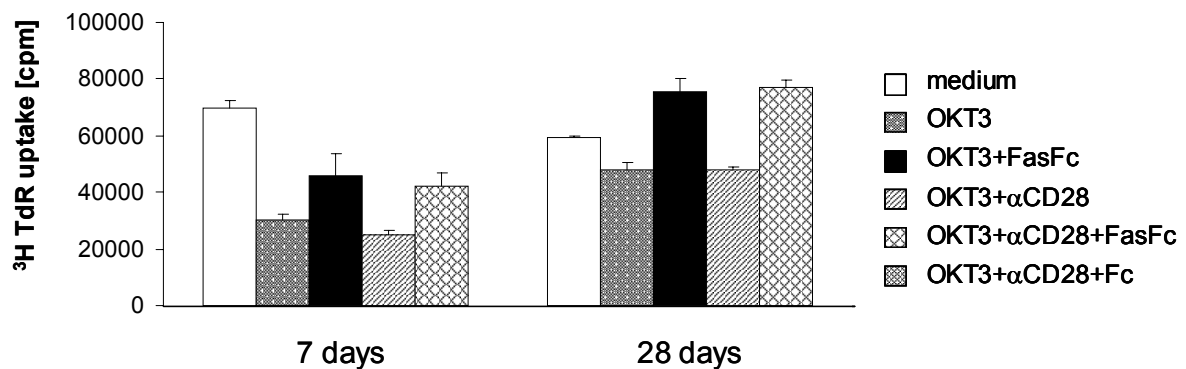


Fig. 4.1.11. FasL signaling enhances TCR/CD3 driven proliferation of T cell clones. Clone cells that had been restimulated 7 days (left panel) or 28 days (right panel) were further stimulated for 3 days with the stimuli where indicated. Proliferation was determined by ^3H -thymidine incorporation with the data presents as mean values and standard deviations of triplicate culture after 3 days.

4.1.8. FasL-engagement blocks cell-cycle progression of T cell clones

Cell-cycle analyses were performed before and after 4 days of stimulation of clone cells which had been last restimulated 25 days before. As shown in Fig. 4.1.12, cells cultured in medium without exogenous added IL-2 showed a high rate of apoptotic DNA. The stimulation with OKT3 or OKT3 and anti-CD28 resulted in enhanced S/G₂M progression accompanied by increased apoptosis. There was no difference where the cells were co-stimulated with OKT3 and anti-CD28 or only with OKT3. FasL-engagement did not lead to enhanced proliferation or accumulated apoptosis compared to the stimulated cells or the un-stimulated cells. Most of the cells were kept

at the G₀/G₁ phase and obviously inhibited from S/G₂M entry. Thus, FasL-engagement resulted in growth arrest but not apoptosis in T cell clones.

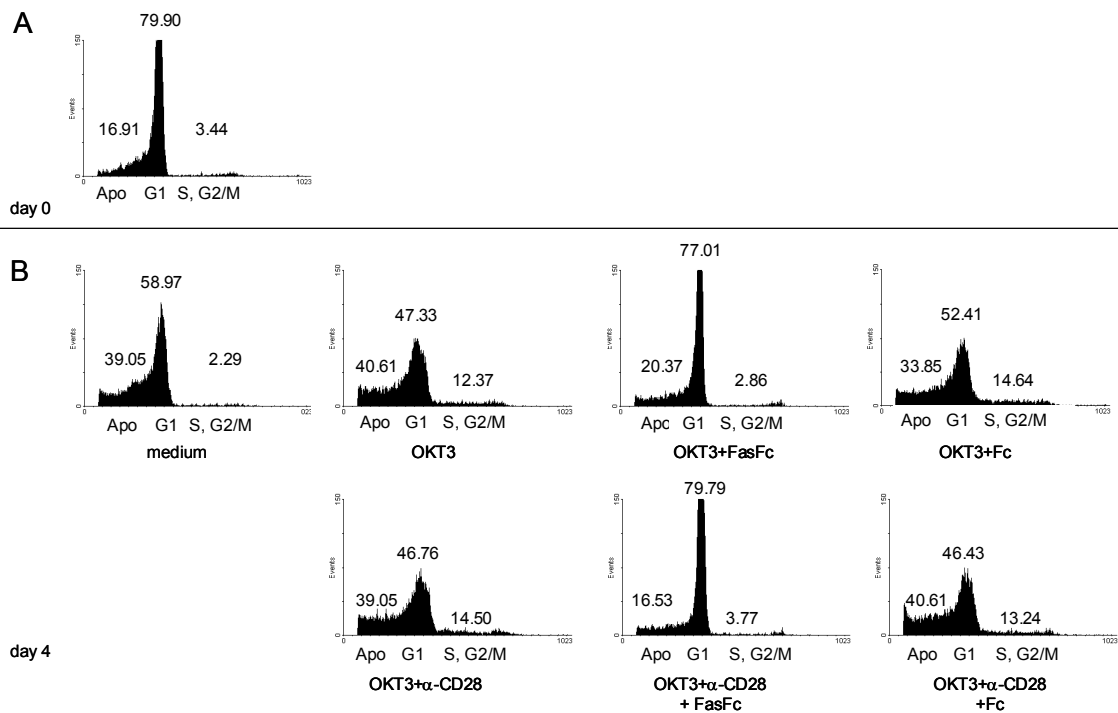


Fig. 4.1.12. FasL-engagement results in cell-cycle arrest of cultured T cell clones. Clone cells were stimulated as described in Fig. 4.1.7. Cell-cycle progression was analyzed before (A) and after 4 days (B) culture by staining the fixed cells with 50 μ g/ml propidium iodide and analyzing the DNA content by flow cytometry. The percentages of apoptotic (apo, <2n DNA), G₀/G₁ (G₁, 2n DNA), and S, G₂/M (>2n DNA) cells are indicated.

4.1.9. Inhibition of TCR/CD3-induced tyrosine phosphorylation by FasL-engagement

Having demonstrated that FasL-engagement alters TCR/CD3-mediated activation, we tried to find whether this was also reflected in biochemical alterations of signaling events due to FasL ligation. Tyrosine phosphorylation mediated by non-receptor PTKs is required to initiate TCR/CD3-dependent activation. We therefore performed phosphotyrosine western blots using T cell blasts or T cell clones. We extensively crosslinked the FasFc with anti-human IgG (Fc-specific) mAb and anti-FasL mAb 5G51 with rabbit anti-mouse antibody for 30 min to 1 hour prior to stimulating the cells with OKT3 for the indicated 2 or 5 minutes. We consistently observed a mild reduction of overall tyrosine phosphorylation in all the tested cells. The most obvious blockage

was observed in PHA blasts as shown in Fig. 4.1.13A. The protein loading was checked by Ponceau S staining of the blots. According to the standard molecular weight, we estimated that proteins at 60, 70-76, 95-100, 120-130 and 145 kDa showed altered tyrosine phosphorylation (Fig. 4.1.13). Regardless of the identity of the individual proteins, the data presented so far indicated the physical and biochemical crosstalk between FasL and the TCR/CD3 complex.

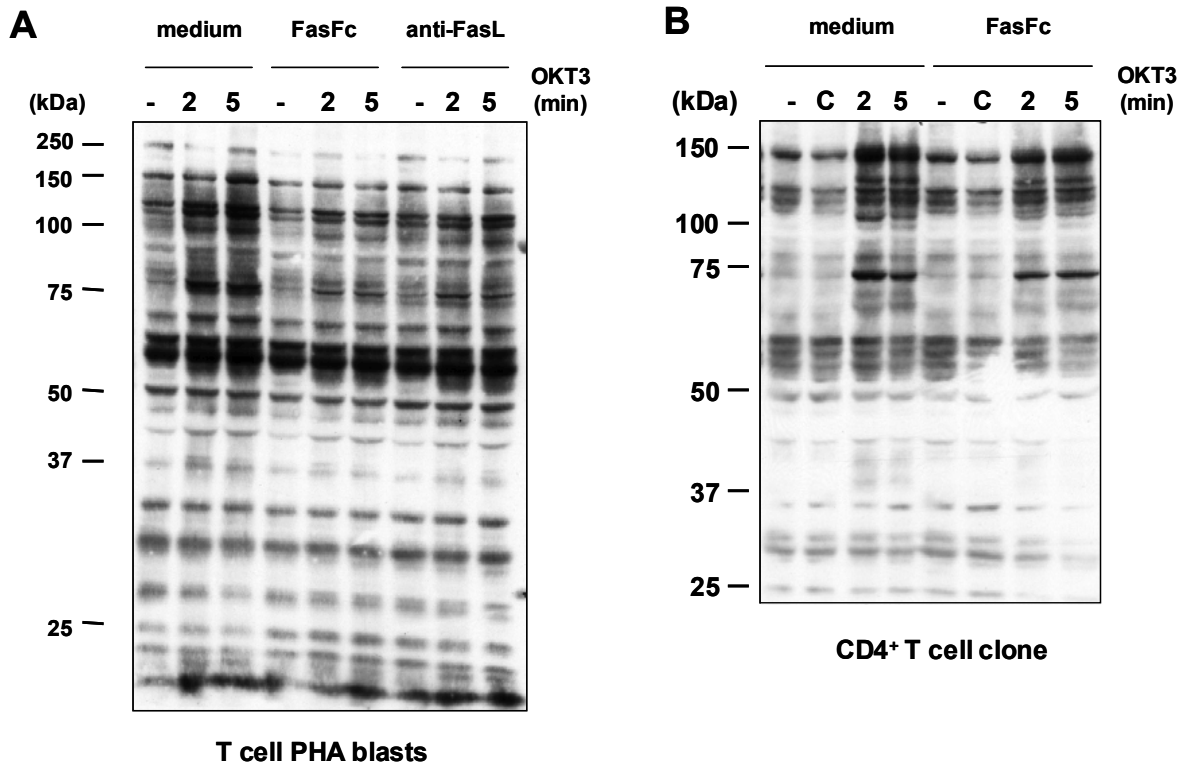


Fig. 4.1.13. FasL crosslinking inhibits TCR-induced tyrosine phosphorylation. T cell blasts (A) and CD4⁺ Clone cells (B) were incubated for 1 hour in the absence or presence of 50 μ g/ml FasFc crosslinked with 10 μ g/ml anti-human IgG (Fc-specific), or 20 μ g/ml anti-FasL mAb 5G51 crosslinked with 5 μ g/ml rabbit anti-mouse IgG. Aliquots of $1.5-2 \times 10^6$ cells were then exposed to 10 μ g/ml OKT3 mAb for the indicated time periods and lysed in 1% NP40 lysis buffer. Proteins were separated by SDS-PAGE and blotted to nitrocellulose. Blots were immunoprobed with the anti-pTyr mAb 4G10. (-) indicates unstimulated control and (C) indicates rabbit anti-mouse antibody control.

4.1.10. *In vitro* phosphorylation of a casein kinase 1 motif present in the FasL cytoplasmic tail

As one of the structural characteristics, the cytoplasmic tail of FasL contains a putative casein kinase 1 (CK1) motif (SSASS). It has been shown that recombinant CK1 is able to phosphorylate transmembrane tumor necrosis factor- α (mTNF α) in murine

macrophages¹⁰⁸. Since casein kinase motifs are present in at least the six TNF family members associated with retrograde signaling, the authors predicted that CK1-dependent mechanism might explain the reverse signaling capacity of those TNF family members. To analyze whether CK1 may also be involved in the reverse signaling of FasL, we performed an *in vitro* kinase assay in which we added exogenous CK1 to GST fusion proteins that contain different parts of the cytoplasmic tail of FasL (Fig. 4.1.14A). In fact, we observed that the fragments containing the putative CK1 substrate motif (FasLcyto1 and FasLcyto) were more heavily phosphorylated than the GST control and the FasLcyto2 (Fig. 4.1.14B). The finding that CK1 can phosphorylate the cytoplasmic tail of FasL might help to get further insights into the potential signaling capacity of this motif in the future.

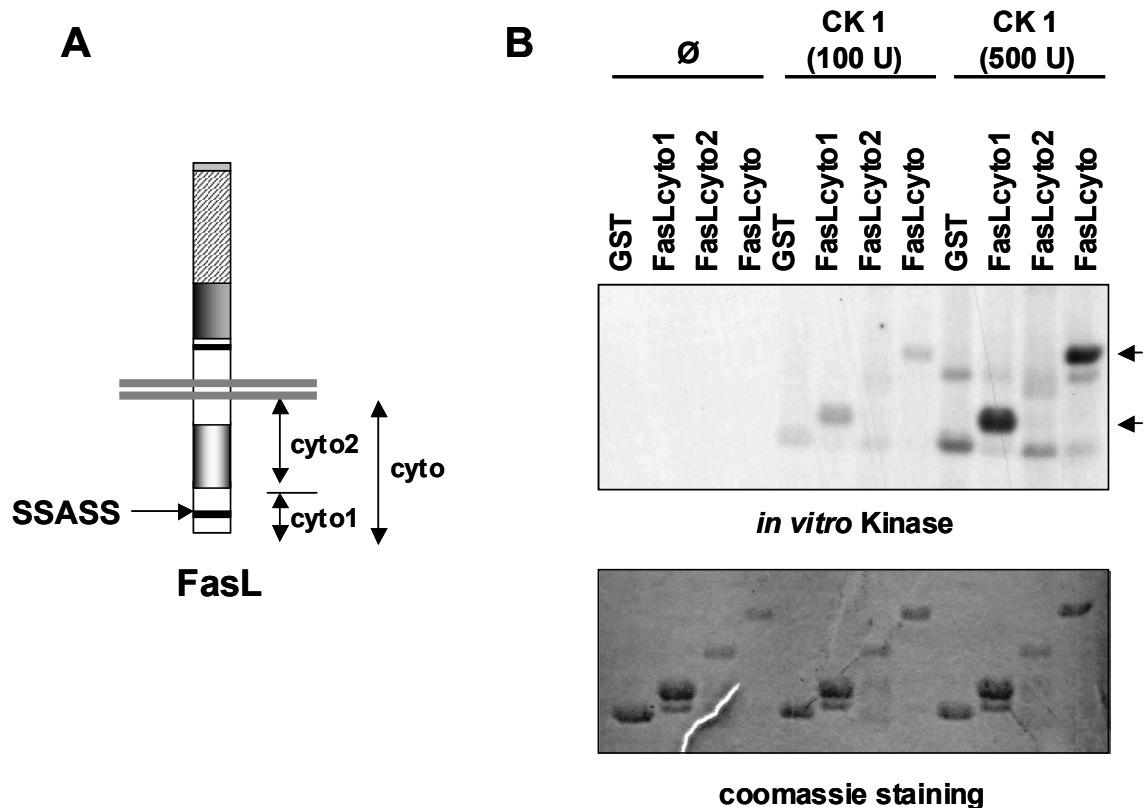


Fig. 4.1.14. Recombinant casein kinase 1 specifically phosphorylates CK1 motif of FasL *In vitro*. A. Three different GST-FasLcyto fusion protein constructs were used in our experiments: FasLcyto contains the complete cytoplasmic tail of FasL, consisting of 80 aa (36.5 kDa); FasLcyto1 contains the N-terminal region of 29 aa (33.5 kDa) and FasLcyto2 contains the membrane proximal proline-rich stretch with 53 aa (31 kDa). Importantly, FasLcyto and FasLcyto1 contain the putative CK1 motif SSASS. B. The *in vitro* kinase assay was performed by adding exogenous CK1 to the indicated GST fusion proteins on beads. Coomassie staining of the loaded proteins is shown in the lower panel, the autoradiograph of incorporated radiolabelled ATP in the upper panel.

4.2. Defining FasL interacting proteins

Hematopoietic and non-hematopoietic cells differ in the composition of the lysosomal compartment. Only in specialized hematopoietic cells (e.g. T cells, NK cells, mast cells and macrophages), so-called secretory lysosomes are found²¹. It was suggested that FasL is located into these secretory lysosomes by virtue of protein-protein interaction

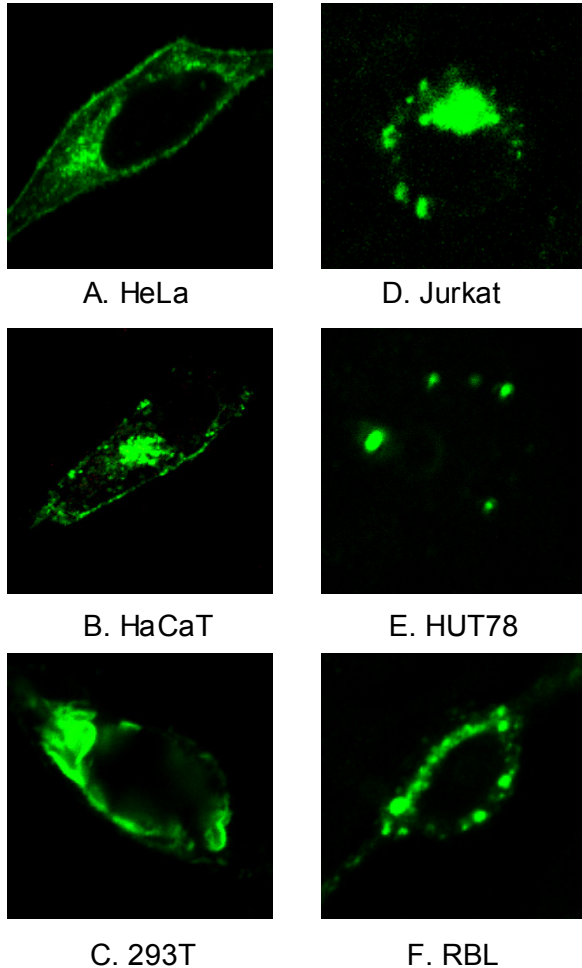


Fig. 4.2.1. Expression of FasL in different cells. FasL-GFP was transiently expressed in the non-hematopoietic cell lines A. HeLa, B. HaCaT and C. 293T or hematopoietic cells D. Jurkat, E. HUT78 and F. RBL. 24 hours after transfection, cells were fixed and analysed by confocal microscopy.

mediated via its proline-rich cytoplasmic region^{17,86}. Thus, in our studies we aimed at identifying molecules that regulate FasL localization to the secretory lysosomes. We initially started to search for suitable cell lines by analyzing the FasL localization upon transfection. Each cell line was transfected with a GFP-tagged human FasL construct. Under these conditions, in non-hematopoietic cell lines (HeLa, HaCaT and 293T), FasL-GFP was mainly expressed at the plasma membrane. In contrast, transfection of hematopoietic cell lines (Jurkat, HUT78 and RBL2H3) resulted in a distribution of FasL-GFP to intracellular granules as shown in Fig. 4.2.1. These results suggest that different sorting motifs or proteins may exist that regulates FasL lysosomal or surface expression. The proline-rich domain (PRD) in the intracellular tail of FasL is likely to contain such sorting motifs.

Identification of FasL interacting proteins that bind to this docking site would enable us to investigate the molecular mechanism of differential protein trafficking in hematopoietic and non-hematopoietic cells. In previous work of this group, various parts of the intracellular region of FasL expressed as GST fusion proteins (see Fig. 3.2.1) were used to precipitate FasL binding proteins from T cell lysate¹¹³. The

precipitates were separated by two-dimensional gel electrophoresis and sequence information was obtained by MALDI-TOF-based peptide finger-print analyses. With PACSIN2 (= protein kinase C and casein kinase substrate in neurons 2) and FBP17 (= formin binding protein 17), two structurally related proteins were identified that are likely to be involved in protein trafficking and cytoskeletal organization¹¹³. These two proteins belong to a larger family of structurally related polypeptides characterized by a similar modular composition of so-called FCH (Fes/CIP4 homology) and SH3 domains. We named it “FCH/SH3 protein family”. Besides PACSIN2 and FBP17, the PACSIN isoforms PACSIN1 and PACSIN3, CD2BP1/PEST PIP (= CD2 cytoplasmic tail-binding protein1 or proline-serine-threonine phosphatase interacting protein), CIP4 (= cdc42 interacting protein 4), the RhoGAP C1 (= Rho-GTPase-Activation hematopoietic protein C1), the hypothetical protein KIAA0456 (which has a comparable domain structure with Rho GAP C1) and the hypothetical FLJ00007 protein (which contains two SH3 domains) belong to this family (Fig. 4.2.2). Since all known proteins of this family are involved in cytoskeletal reorganization and lysosomal transport in different cellular systems, we wondered whether they could bind to FasL and whether the association and co-expression together with FasL would alter the subcellular localization of FasL.

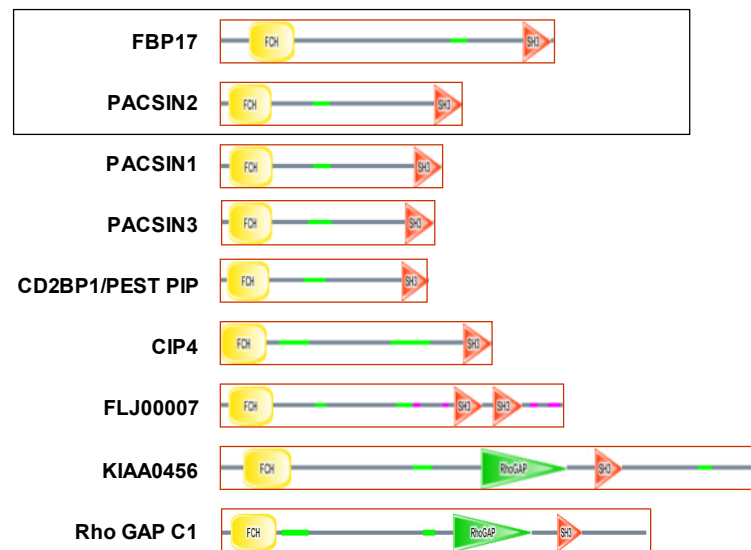


Fig. 4.2.2. The modular composition of “FCH/SH3-family”. FBP17 and PACSIN2 belong to a family of structurally related proteins which share an overall composition with an N-terminal FCH (Fes/CIP4 homology) domain, a central coiled-coil region and a C-terminal SH3 domain (except FLJ00007 which contains two SH3 domains).

4.2.1. The interaction of FasL with FCH/SH3 proteins is mediated by SH3 domains

As reported earlier, we could clearly demonstrate the interaction of FasL with SH3 domains of PACSIN2 and FBP17¹¹³. This was verified when we used fusion proteins containing full length PACSIN2 wild-type (wt) or mutants (P478L). As shown in Fig. 4.2.3, a single point mutation (P478L) within the PACSIN2 SH3 domain completely abrogated FasL binding.

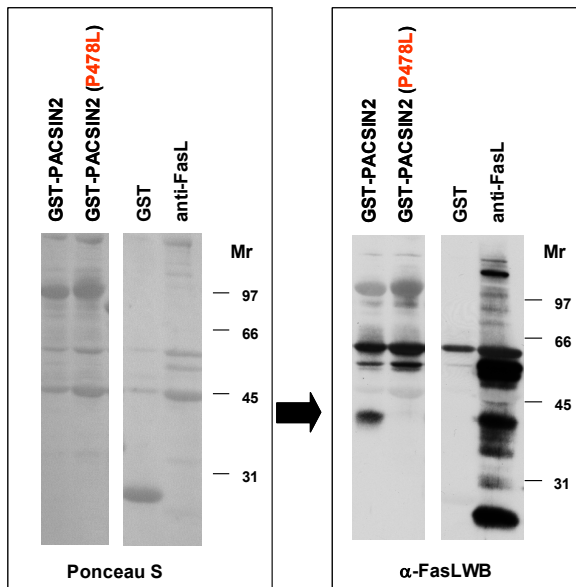
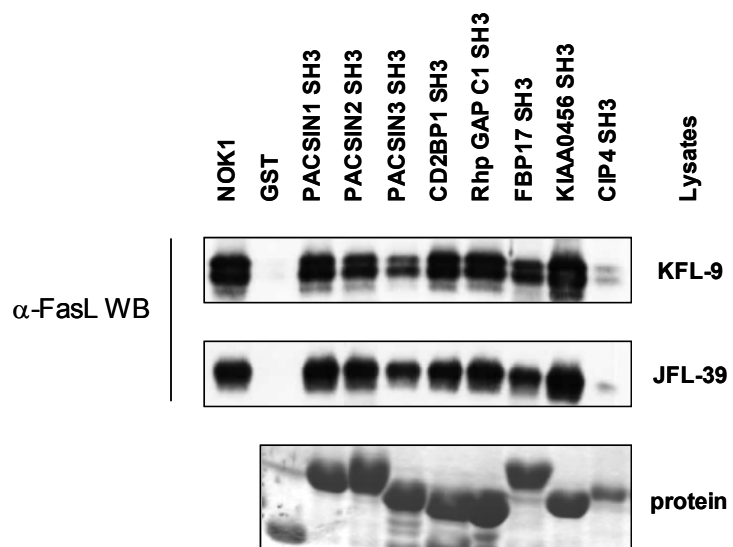


Fig. 4.2.3. FasL interacts with PACSIN2 via SH3 domain. GST fusion proteins containing full length PACSIN2 wt or P478L were used to precipitate FasL from lysates of human T cell PHA blasts stimulated with TPA and ionomycin for five hours. For each precipitation, 90×10^6 T cell blasts were used in 1 ml lysate buffer. Ponceau S staining (left panel) and anti-FasL immunoblotting (right panel). Precipitates with anti-FasL mAb NOK1 of the same lysate served as a positive, GST as a negative control.

In fact, as shown in Fig. 4.2.4, isolated SH3 domains of most if not all FCH/SH3 family member precipitated FasL from stable transfectants (KFL-9 or JFL-39). In this particular exploit, we demonstrated the binding of SH3 domains of eight different members of the FCH/SH3 family to FasL. With the exception of CIP4, all proteins expressed *in vitro* bind with a similar affinity. Note that from KFL cells, SH3 domains consistently precipitated FasL as a double band and from JFL as a signal band.

Fig. 4.2.4. FasL interacts with the SH3 domain of FCH/SH3 proteins. 25 μ g of indicated GST-SH3 domain fusion proteins on glutathione beads were incubated with lysates prepared from 20×10^6 KFL-9 or JFL-39 cells. Coomassie staining (lowest panel) and anti-FasL immunoblotting (upper and middle panel). Precipitates with anti-FasL mAb NOK1 and GST served as positive and negative controls.



4.2.2. FasL coprecipitates with FCH/SH3 proteins

Having shown that the SH3 domains of FCH/SH3 proteins interact with FasL in *in vitro* “pull down” assays, we tried to get *in vivo* evidence for the interaction. To this end, vectors encoding myc-tagged full length FCH/SH3 proteins (including FBP17, PACSINs, CD2BP1 and CIP4 Δ CC that lacks part of coiled-coil region) were transfected individually or together with a FasL expression vector (pI217s or FasLpEFBOS) into 293T cells. We also expressed FBP17 lacking the SH3 domain (FBP17-SH3) and PACSIN2 with a point-mutation in the SH3 domain (PACSIN2P478L) to assess the role of SH3 domains in the interaction with FasL. It should be mentioned that all the constructs used in the experiments are of human origin except the PACSIN2 and PACSIN2P478L proteins which were of murine origin. Sequence analysis reveals that murine PACSIN2 shares 87% homology with the human protein and that the SH3 domain (amino acid 535-485) is in fact identical (Fig. 4.2.5).



Fig. 4.2.5. Sequence alignment for murine and human PACSIN2. Data were batched from GeneBank database and analyzed with “BLAST” software from NCBI. Asterisks indicate identical amino acids in the FCH and SH3 domains.

Cell lysates were used 24 hours post transfection for co-immunoprecipitation analyses. The interactions of FasL with myc-tagged FCH/SH3 proteins were detected in two ways: either anti-FasL mAb was used for precipitation to detect the co-associated proteins with anti-myc immunoblotting or anti-myc mAb was used for IP followed by

anti-FasL western blot. Protein expression was analyzed by stripping the blots and re-probing them with the same antibodies used for precipitation, or alternatively by probing the cell lysates with anti-FasL and anti-myc antibodies. As shown in Fig. 4.2.6, anti-myc immunoprecipitation followed by FasL staining of the western blot revealed the interaction of FasL with all the full length proteins tested. Importantly, FasL was only co-precipitated in the presence of intact SH3 domains. On the other hand, when FasL was precipitated from double transfectants, only PACSIN2 was detected as co-precipitated myc-tagged material.

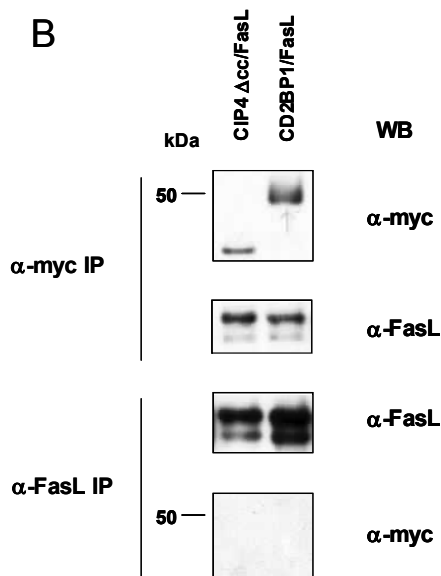
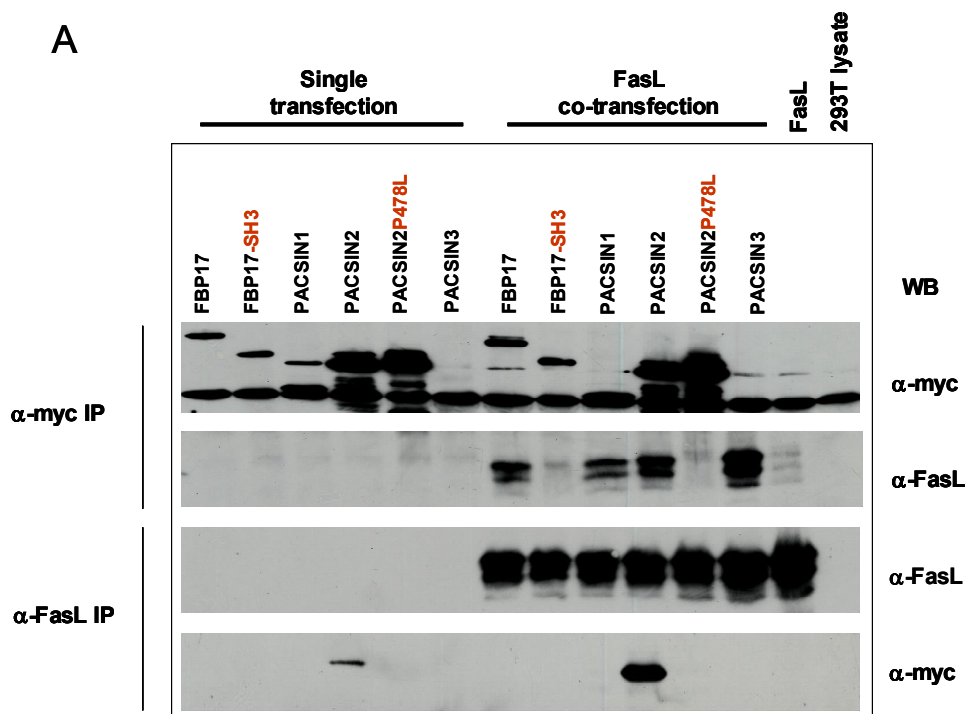


Fig. 4.2.6. FasL co-precipitates with FCH/SH3 proteins. Wild-type or mutated FCH/SH3 proteins were transiently transfected into 293T cells as myc-tagged fusion proteins alone or co-transfected with FasL by the calcium phosphate method. NP40 lysates were made 24 hours after transfection. The lysates were split into two aliquots for parallel immunoprecipitation (IP) with anti-CD95L or anti-myc mAb as indicated. Proteins were transferred to nitrocellulose and analyzed with anti-CD95L and anti-myc antibodies (A, B obtained from two different experiments).

4.2.3. FasL co-localizes with FCH/SH3 proteins

Next, we analyzed the intracellular distribution of FCH/SH3 proteins in 293T transfectants and their interactions with FasL. As shown in Fig. 4.2.7, When FCH/SH3 proteins were expressed in 293T cells, the PACSINs appeared mostly cytosolic. FBP17 seemed to be expressed in the cytosol as well in compartment underneath the

cell membrane. CD2BP1 and CIP4 Δ CC were also localized in different distribution in the cytosolic to intracellular structures.

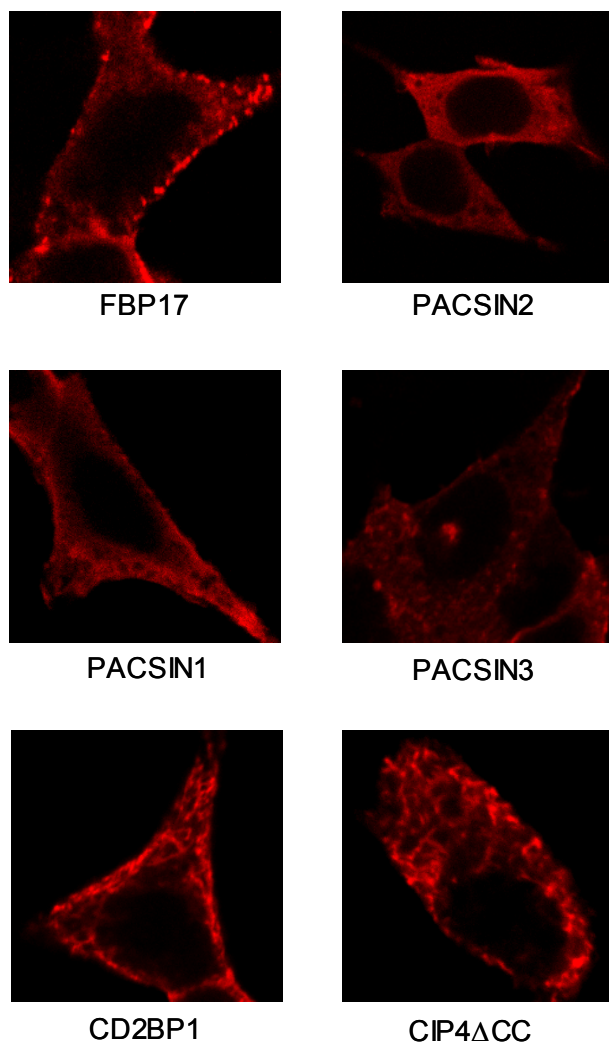


Fig. 4.2.7. Intracellular distribution of FCH/SH3 proteins Individual myc-tagged FCH/SH3 proteins were expressed in 293T cells. 24 hours after transfection, cells were fixed, permeabilized and stained with anti-myc mAb and Alexa Fluor 546 conjugated goat anti-mouse secondary antibody (gam/Alexa Fluor 546). The images were analyzed with a Zeiss laser scanning microscope (Zeiss LSM 510).

As shown in Fig. 4.2.8, when co-expressed, FasL co-localizes with the respective FCH/SH3 protein. Importantly, we did not detect co-localization of FasL with mutated PACSIN2, indicating once again that the interaction was mediated by the SH3 domain. As shown before in Fig. 4.2.1, FasL was mainly expressed at the cell membrane in 293T transfectants. In contrast, we noticed that the presence of FCH/SH3 proteins seemed to influence the subcellular localization of FasL from the membrane into intracellular vesicles, possibly lysosomes. Therefore, FCH/SH3 proteins might regulate FasL lysosomal targeting and surface expression.

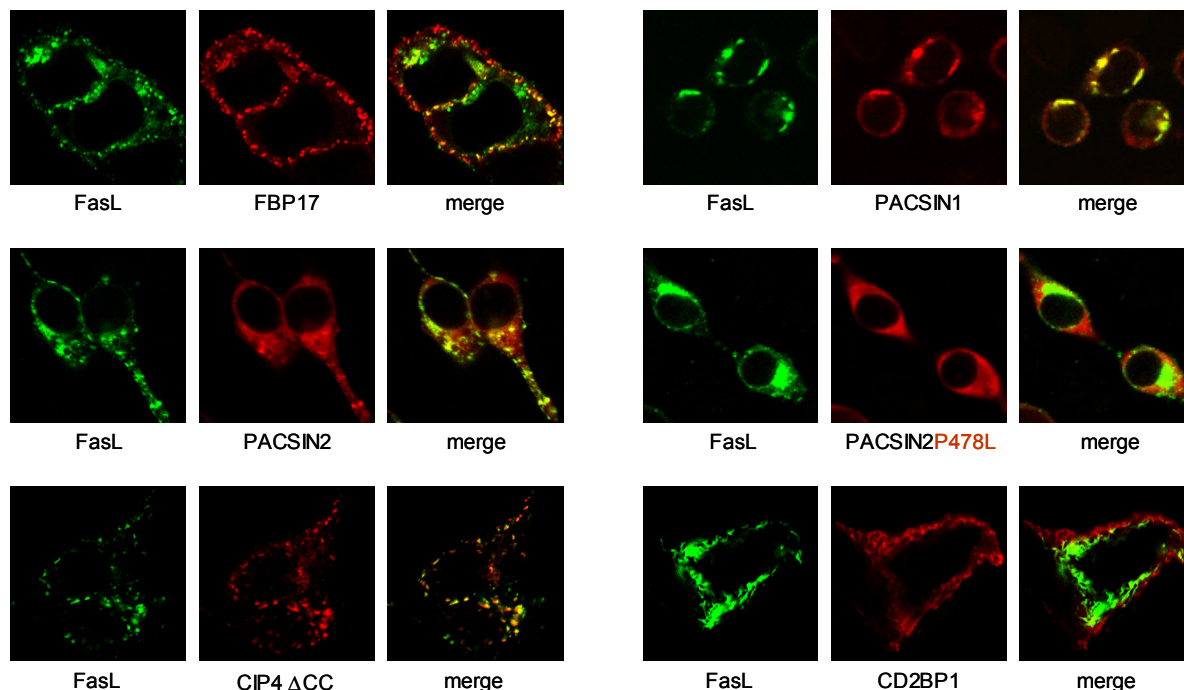


Fig. 4.2.8. The interaction of FCH/SH3 proteins with FasL. FasL-GFP was transiently expressed together with the individual FCH/SH3 proteins in 293T cells. 24 hours after transfection, cells were fixed, permeabilized and stained with α -myc mAb and gam/Alexa Fluor 546. The individual images were analyzed by Zeiss LSM 510 and merged to demonstrate the co-localization of FasL and the indicated proteins.

4.2.4. FCH/SH3 proteins co-localize with FasL in the lysosomal compartment

So far, we identified the SH3 domain-mediated interaction of FCH/SH3 protein with FasL. Intracellular staining also indicated that members of this protein family might be involved in regulating FasL intracellular trafficking and lysosomal targeting. To confirm this assumption, besides 293T cells, we assessed the effect of some FCH/SH3 proteins on the distribution of FasL in either the non-hematopoietic cell line HeLa or the hematopoietic cell line RBL2H3. Myc-tagged FCH/SH3 proteins and FasL-GFP were expressed and their subcellular distribution in relation to lysosomes was examined by laser scanning microscopy.

Fig. 4.2.9 demonstrates that in HeLa cells, the presence of FBP17 (A), PACSIN2 (B, left panel), CIP4 Δ CC (C), CD2BP1 (D) directed the surface expression of FasL to intracellular compartments. A large amount of the protein was co-localized with the lysosomal and late endosomal marker Cathepsin D (CTSD) or another lysosomal marker lamp1 (lysosome associated membrane protein 1). As expected, PACSIN2P478L did not co-localize with FasL or CTSD (B, right panel).

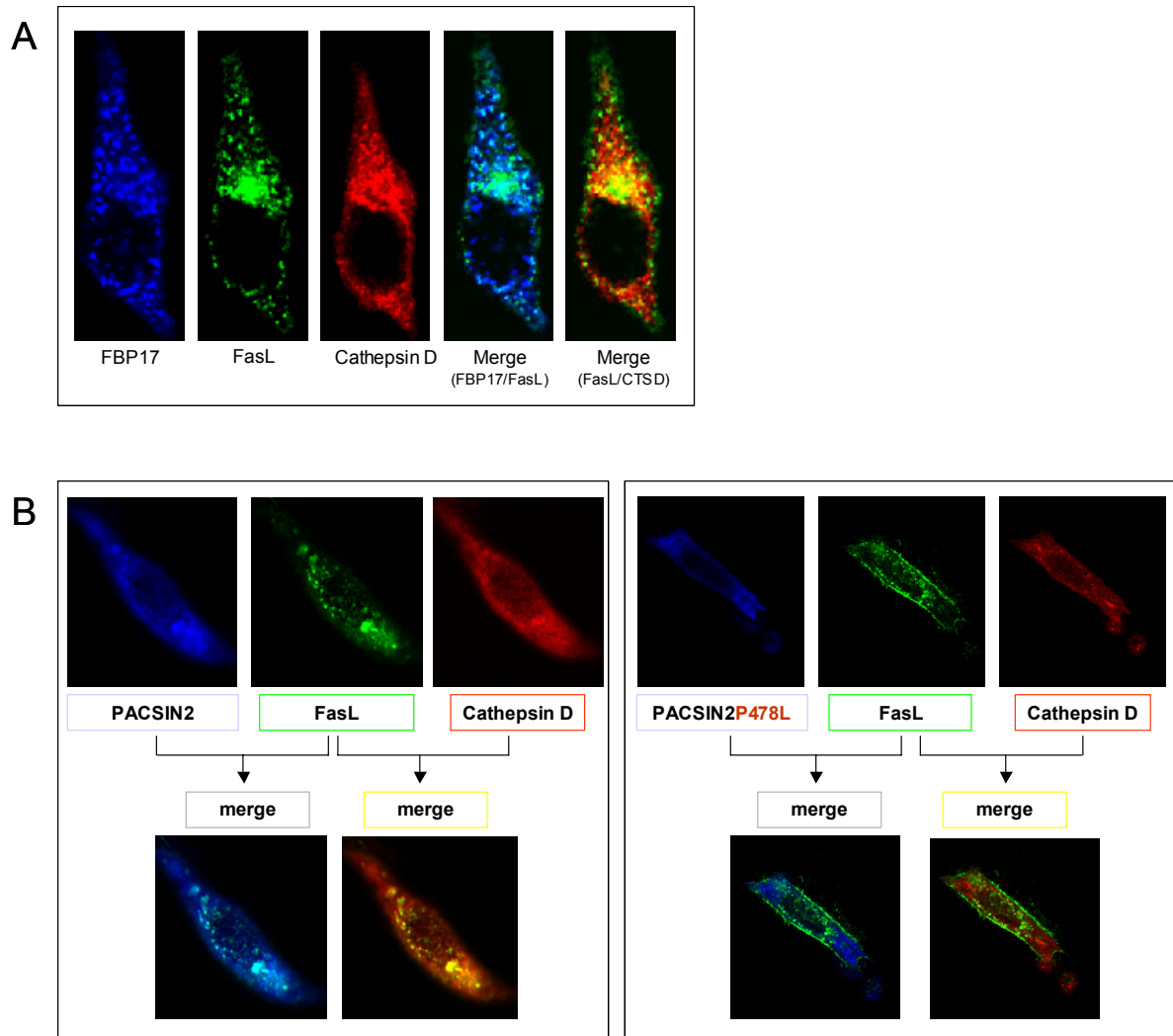


Fig. 4.2.9. FCH/SH3 proteins co-localize with FasL in the lysosomal compartment in HeLa cells.

Myc-tagged FCH/SH3 proteins and FasL-GFP were co-expressed in HeLa cells by electroporation. 24 hours after transfection, cells were fixed by 3% PFA and stained with indicated antibodies to visualize the myc-tagged proteins and the lysosomal compartment. All samples were stained with secondary antibodies as controls. Samples were analysed by Zeiss LSM 510 with the laser 633, 546 and 488. The merged images show the co-localization of indicated proteins.

A. Co-localization of FBP17 with FasL and Cathepsin D (CTSD). Cells were transfected with FBP17 and FasLEGFP and stained with α -myc mAb and α -Cathepsin D (CTSD) pAb followed by CY5 conjugated donkey anti-mouse and donkey anti-rabbit rhodamine conjugated antisera.

B. SH3 domain-mediated co-localization of PACSIN2, FasL and Cathepsin D. Wild-type myc-tagged PACSIN2 (left panel) or PACSIN2P478L (right panel) constructs were used for transfection with FasLEGFP and stained as described in A.

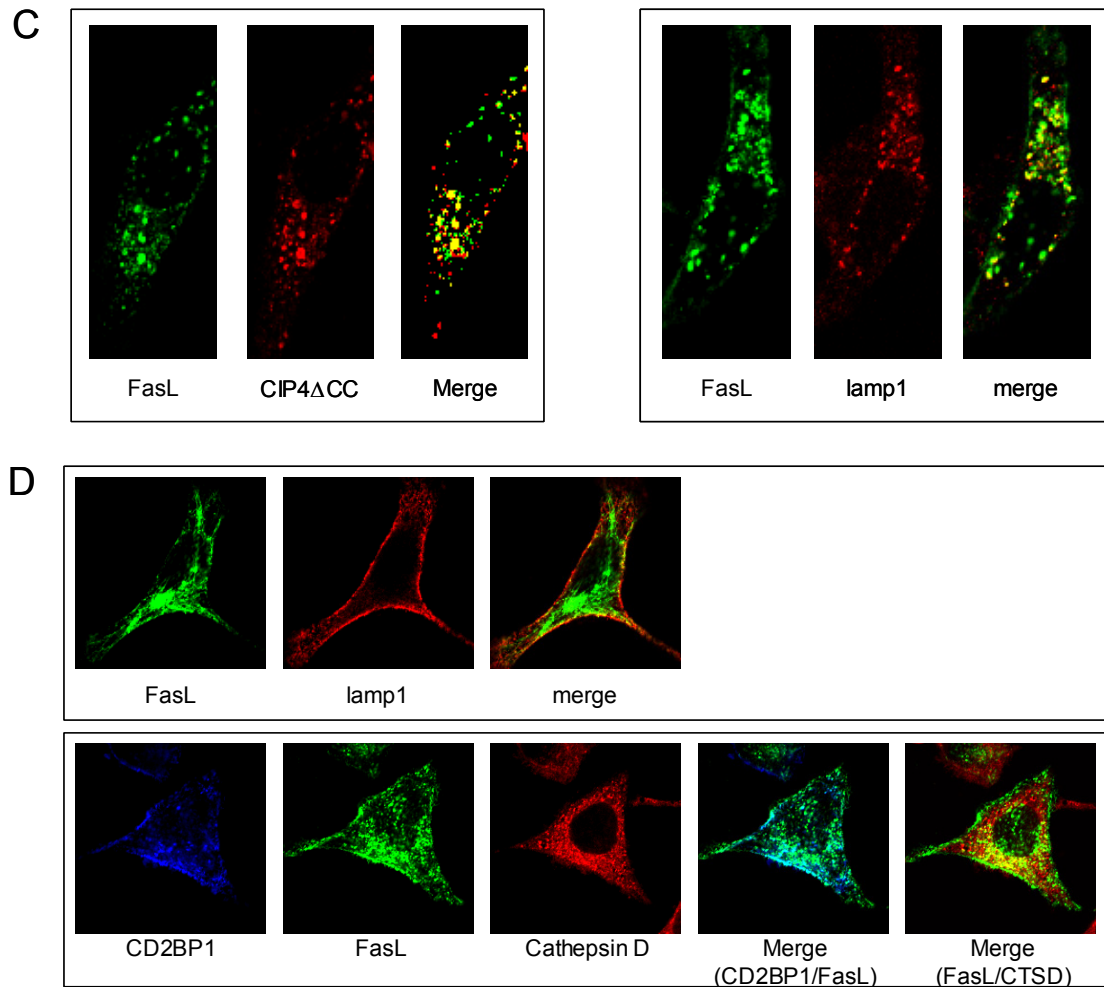


Fig. 4.2.9. FCH/SH3 proteins co-localize with FasL in the lysosomal compartment in HeLa cells.

C. Co-localization of CIP4 Δ CC and FasL with lamp1. CIP4 Δ CC and FasLEGFP were expressed and immunostaining was carried out by using either α -myc (left panel) or α -lamp1 (right panel) mAb. Gam/Alexa Fluor 546 was used as secondary antibody in both cases.

D. CD2BP1 co-localizes FasL with Cathepsin D and lamp1. HeLa cells co-transfected with CD2BP1 and FasLEGFP were stained with either α -lamp1 mAb as described in C (upper panel) or α -myc mAb together with α -Cathepsin D (CTSD) pAb as described in A (lower panel).

Fig. 4.2.10. shows that in RBL2H3 cells, although FBP17 (A, left panel) and PACSIN2 (B, left panel) co-localized with FasL, the distribution of FasL was restricted to the intracellular areas. Expression of FasL was detected in enlarged granules surrounding the lysosomal compartment stained with Cathepsin D. Again, the SH3 domain mutants did not show the co-localization with FasL (A, right panel for FBP17-SH3 and B. right panel for PACSIN2 P478L). Interestingly, as indicated in Fig. 4.2.10C, CD2BP1 co-localized with FasL in membrane protrusions of RBL2H3 cells indicating a potential influence on rearrangement of the cytoskeleton.

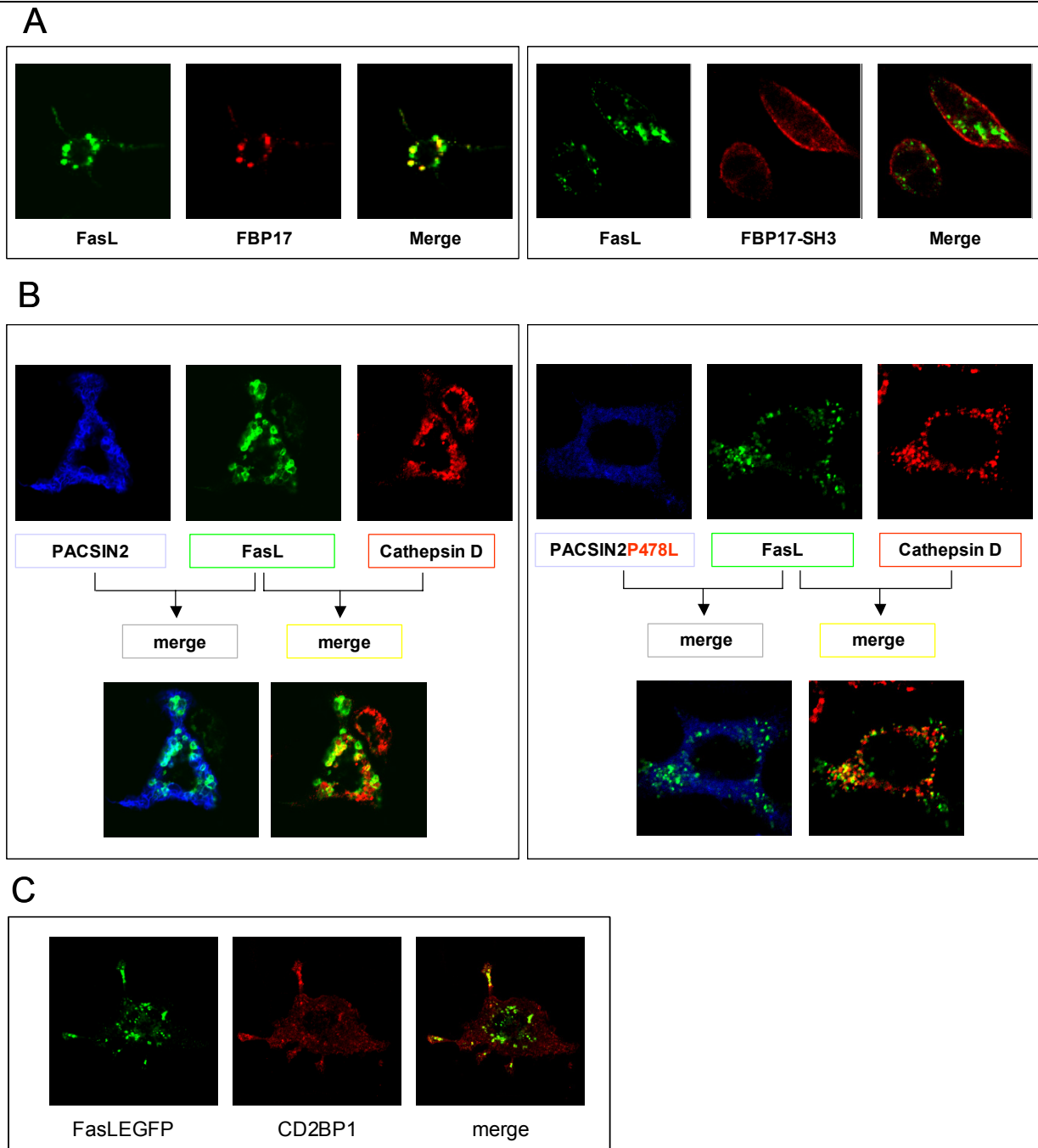


Fig. 4.2.10. FCH/SH3 proteins co-localize with FasL in the lysosomal compartment in RBL2H3 cells. Myc-tagged FCH/SH3 proteins and FasL-GFP were co-expressed in RBL2H3 cells by electroporation. 24 hours post transfection, cells were stained and analyzed as described in Fig. 4.2.9.

A. Cells were transfected with FBP17 (left panel) or FBP17-SH3 (right panel) and FasLEGFP and stained with α -myc mAb followed by gam/Alexa Fluor 546.

B. Wide type Myc-tagged PACSIN2 (left panel) or PACSIN2P478L (right panel) constructs were used for co-transfection and stained with α -myc mAb and α -Cathepsin D (CTSD) pAb followed by CY5 conjugated donkey anti-mouse and donkey anti-rabbit rhodamine conjugated antisera.

C. Co-transfection of CD2BP1 with FasLEGFP and staining with α -myc mAb followed by gam/Alexa Fluor 546.

4.3. FasL interacts with Nck1: linking FasL and the cytoskeleton to the TCR/CD3 complex?

Cytotoxicity exerted by T lymphocytes and NK cells is in part mediated by FasL and potentially other members of the TNF family. Upon receptor-induced fusion of intracellular secretory lysosomes with the plasma membrane, FasL reaches the cell surface and may trigger target cell apoptosis to help the action of perforin and granzymes. From earlier studies we knew that Nck1 can bind to FasL *in vitro* by virtue of two of its three SH3 domains¹¹². Nck1 is a classical adaptor protein that consists of one SH2 and three SH3 domains (Fig. 4.3.1). It is one of the molecules involved in cytoskeletal rearrangement and formation of the immunological synapse¹³². Therefore we asked the question whether Nck1 might be involved in the regulation of FasL transport and expression to the immunological synapse.

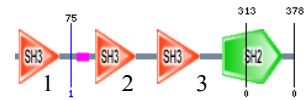


Fig. 4.3.1. The modular composition of Nck1. It contains three N-terminal SH3 domains and one C-terminal SH2 domain. The 2nd and 3rd SH3 domains were shown to bind to FasL.

4.3.1. Degranulation and surface expression of FasL in T cells

Degranulation of FasL in T cell blasts

We examined changes in expression of FasL in different T cell populations in the course of activation. T cell blasts were stimulated with TPA/ionomycin for five minutes up to three hours. The cells were stained with the anti-FasL antibody NOK1 and examined by laser scanning microscopy. As shown in Fig. 4.3.2, in un-stimulated cells FasL was localized in well defined intracellular granules. Under these conditions, no FasL appeared to be detectable on the cell surface. After 30 minutes of stimulation, FasL appeared to be detectable on the cell surface. After 105 minutes, FasL was detectable at the plasma membrane and after 165 minutes, FasL appeared to be almost completely transported to the surface since hardly any FasL remained inside the cell.

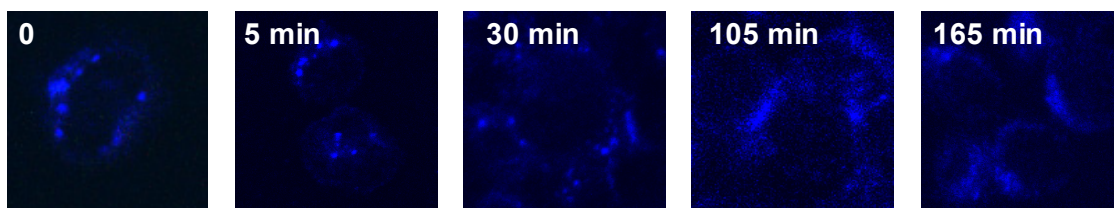


Fig. 4.3.2 Degranulation of FasL in re-activated T cell blasts. T cell blasts were stimulated with 10 ng/ml TPA and 500 ng/ml ionomycin for indicated time intervals and fixed at -20 °C with methanol for 5 minutes. Cells were labelled with the anti-FasL antibody NOK1 and CY5-conjugated goat anti-mouse antisera and examined by Zeiss LSM 510.

Surface expression of FasL in T cell clones

Cloned T cell populations were also tested for changes of FasL expression. To this end, we stimulated clone cells with TPA/ionomycin for different time intervals and examined the surface expression of FasL by flow cytometry. As shown in Fig. 4.3.3, in both CD4⁺ and CD8⁺ T cells, two peaks of FasL expression were detected during three hours of stimulation. The first peak developed after approximately 10 minutes. Following downregulation with a minimum at around 60 minutes, another increase of FasL expression after 2 hours was observed.

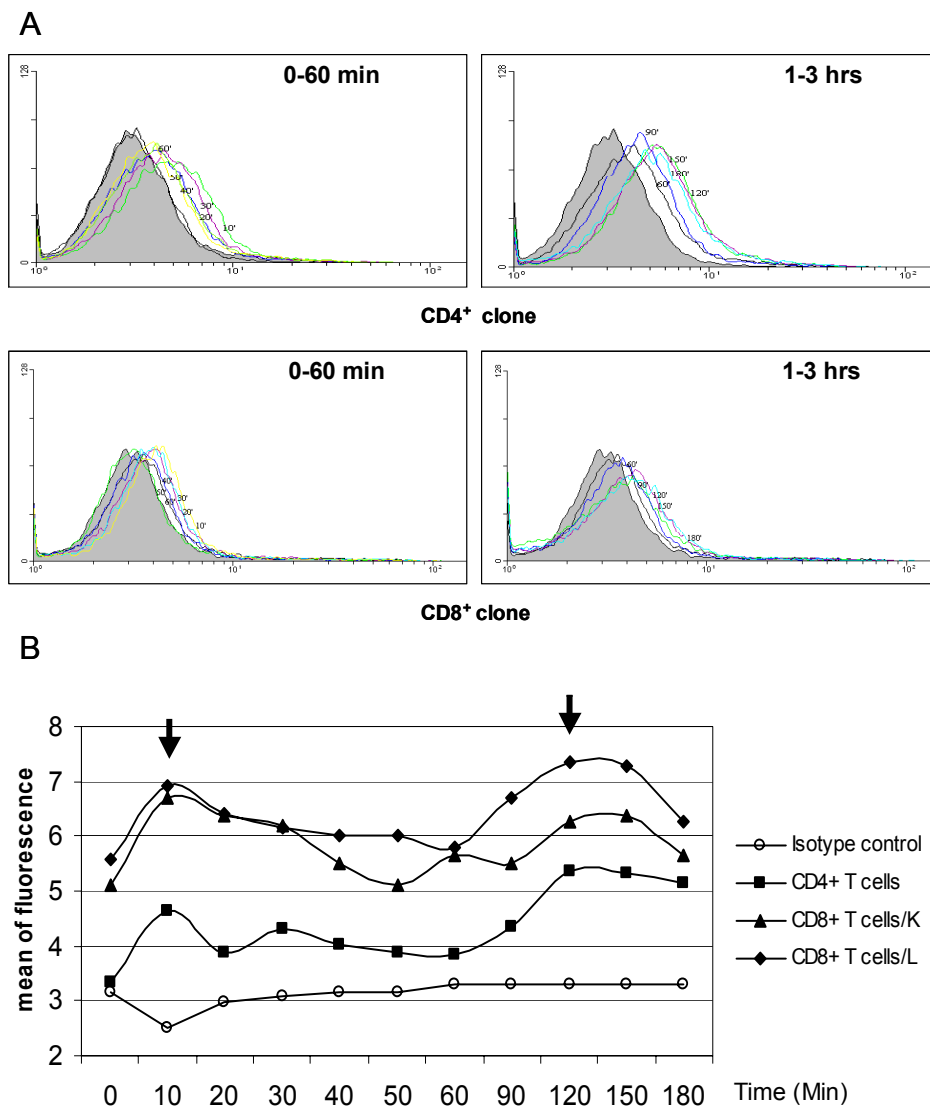


Fig. 4.3.3. Surface expression of FasL in T cell clones. Different clone cells were stimulated with TPA and ionomycin for indicated time intervals. Surface expression of FasL was assessed by staining with anti-FasL mAb 5G51 and gam/PE followed by FACS analysis. PE-conjugated IgG₁ was used as isotype control. A. The histograms show the fluorescence intensity of FasL in comparison to isotype control (filled histograms). B. The graphs indicate the mean fluorescence intensity at different time points.

Lysosomal localization of FasL in T cells

To characterize the intracellular localization of FasL in T cells, we double-stained FasL and Cathepsin D in Jurkat cells constitutively expressing FasL (JFL). As shown in Fig. 4.3.4, there was a substantial overlap between FasL and Cathepsin D. Interestingly, in addition to the granules containing both molecules, some vesicles lacking FasL were visible as well structures with FasL only.

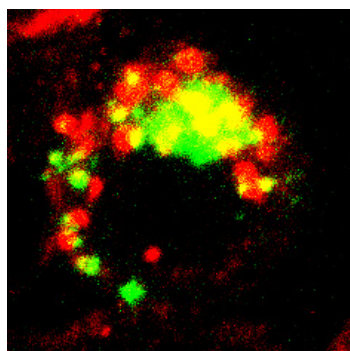


Fig. 4.3.4. Co-localization of FasL with the lysosomal marker Cathepsin D in T cells. FasL stable transfectants of Jurkat cells (JFL) were stained with anti-FasL mAb NOK1 and anti-Cathepsin D pAb followed by Alexa fluor 488-conjugated goat anti-mouse (gam/Alexa fluor 488) and rhodamine-linked donkey anti-rabbit antibodies. The image was analyzed by Zeiss LSM 510 and showed the FasL (green), Cathepsin D (red) and the co-localization (yellow).

Trafficking of FasL in superantigen-activated T cell clones

Besides using TPA/ionomycin to induce an intracellular Ca^{2+} flux and trigger T cell degranulation, we also stimulated superantigen-reactive T cell clones with SEA to analyze the transport of FasL. In this case, cells were stimulated by coverslip-bound SEA for 1 hour and the expression of FasL and Cathepsin D was detected by staining with antibodies. As shown in Fig. 4.3.5, in stimulated clone cells, both FasL and Cathepsin D were moved towards a protruding cell pole (A). In some cells, FasL was expressed on the cell surface and separated from Cathepsin D (B).

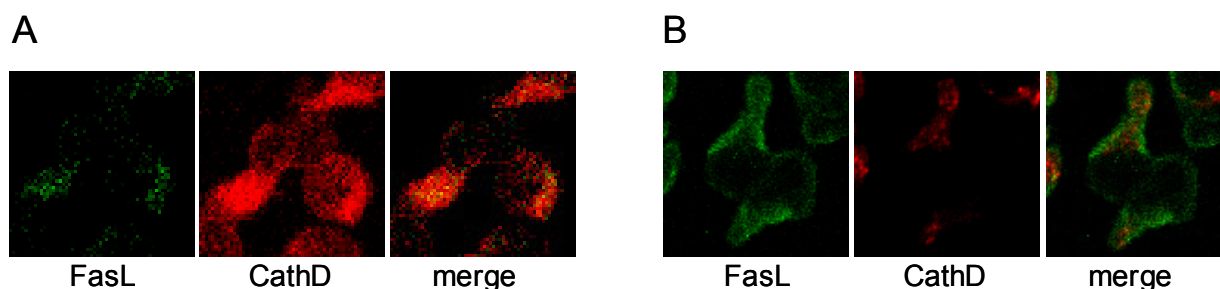


Fig. 4.3.5. Transport of FasL in SEA-activated clone cells. Cells of the $CD4^+$ clone were stimulated on coverslips with SEA for 1 hour before fixation and staining for FasL and Cathepsin D (CTSD). The images to the right represent overlays to indicate co-localization of the two proteins. A and B were two typical images chosen from one experiment.

Trafficking of lysosomes in cytotoxic T cells stimulated by target cells

We also investigated the trafficking of lysosomes in T cells stimulated by target cells *in vivo*. $\gamma\delta$ T cells (clone EP3) were pre-stained with LysoTracker Red DND-99 to visualize lysosomes and given to melanoma-derived fibroblasts (MeWo) in the presence of phosphoantigen BrHPP. The cells were analyzed by laser scanning microscopy and sequential images were acquired. According to the images shown in Fig. 4.3.6, EP3 cells were "attracted" by the MeWo cells within 10 minutes. Upon contact, the lysosomes of EP3 cells were targeted towards the contact area and released. This caused the MeWo cells to become round and detach from the coverslip. The MeWo cells died after approximately 80 minutes.

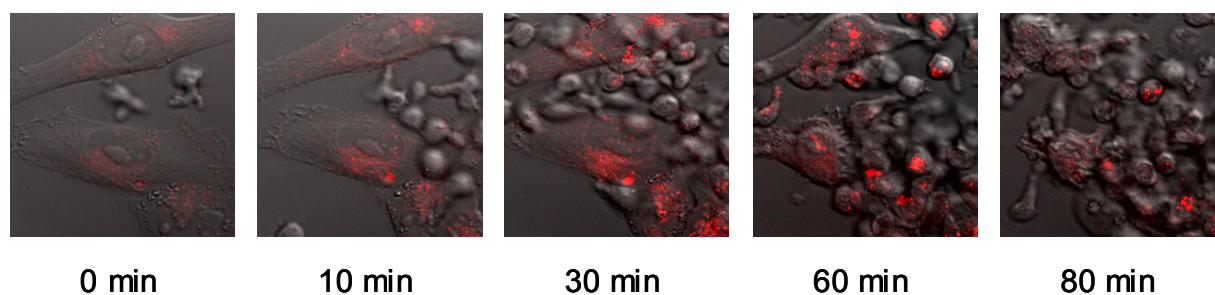


Fig. 4.3.6. Release of lysosomal content during targeting of tumor cells by $\gamma\delta$ T effectors. MeWo cells were grown on Lab-TekII chambered coverslips for 24 hours. 1×10^6 EP3 cells pre-stained with 50 nM LysoTracker Red DND-99 were loaded in the presence of 20 nM BrHPP. Cells were examined by confocal microscopy and sequential images were acquired every minute up to 2 hours. Laser 546 was used to monitor the lysosomal compartment stained with LysoTracker Red and a light transmission was used to show the cell morphology changes.

4.3.2. Interaction of FasL with Nck1

Clearly, lysosomes containing cytotoxic material were moved to the contact area of T cells and target cells. The next question to address was which molecules might be directing FasL and the lysosomes to the forming cytotoxic synapse. Looking back to the interactions that had been identified earlier¹¹², one candidate was Nck1. In the meantime Nck1 had been described as an adaptor that links the TCR and the cytoskeleton to move molecules to the immunological synapse¹³². Therefore, the idea was that Nck1 might also be involved in the movement of secretory lysosomes to the cytotoxic synapse.

To characterize the interaction of FasL and Nck1, we used the same strategies described for the interaction of FasL and FCH/SH3 family proteins: "pull down", co-

precipitation and co-localization assays. According to the structure of Nck1 (Fig. 4.3.1), a series of GST-, Myc- or GFP- tagged constructs encoding different domains of Nck1, either wild-type or point mutated, were used in the experiments.

"Pull down"

Earlier results from this group indicated that the 2nd and 3rd SH3 domain of Nck1 might interact with FasL¹¹². In this experiment, besides the separated SH3 or SH2 domains, we also used fusion proteins containing the combination of the three SH3 domains or full length protein. In case of "mutants", either one of the separated domain or all the three SH3 domains were mutated. Both KFL-9 or JFL cell lysates were used for "pull down" assays. As shown in Fig. 4.3.7, besides the 2nd and 3rd SH3 domain of Nck, the combined three SH3 domains and the complete protein also interact with FasL. A single SH3 mutation resulted in milder interaction. Only when all three SH3 domains were mutated, the binding was abolished.

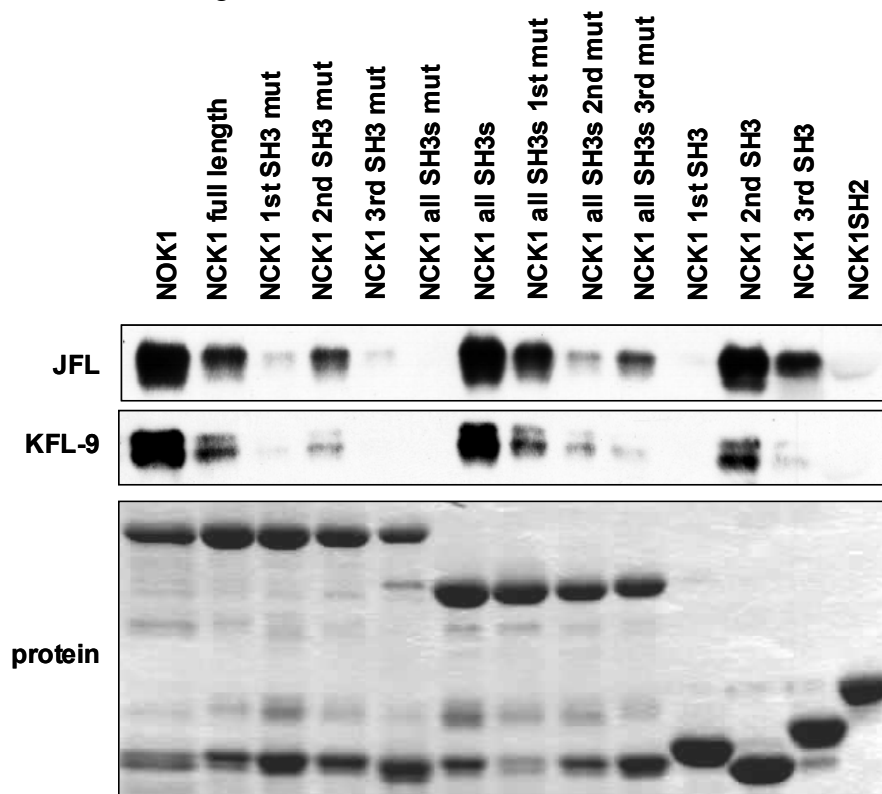


Fig. 4.3.7. FasL interacts with two out of three SH3 domains of Nck1. 40 μ g of indicated GST-SH3 domain fusion proteins on glutathione sepharose beads were incubated with lysates prepared from 20×10^6 KFL-9 or JFL cells. The proteins were separated by SDS-PAGE followed by anti-FasL western blotting. Precipitates with anti-FasL mAb NOK1 of the same lysate served as a positive control. Ponceau S staining (lowest panel) and anti-CD95L immunoblotting (upper and middle panels).

Co-precipitation

Vectors encoding wild-type, SH2 mutated and all the SH3s mutated myc-tagged Nck1 were transfected together with a FasL expression vector into 293T cells. Cell lysates (24 hours post transfection) were subjected to anti-FasL or anti-myc immunoprecipitation. As shown in Fig. 4.3.8, Anti-myc immunoprecipitation followed by FasL staining revealed co-precipitated FasL in the presence of wild-type and SH2 mutants of Nck1 but not when the SH3s were mutated. The use of anti-FasL mAb for precipitation revealed similar results: only the wild-type and SH2 mutated but not the SH3s mutated myc-tagged Nck1 was detected as co-precipitated protein.

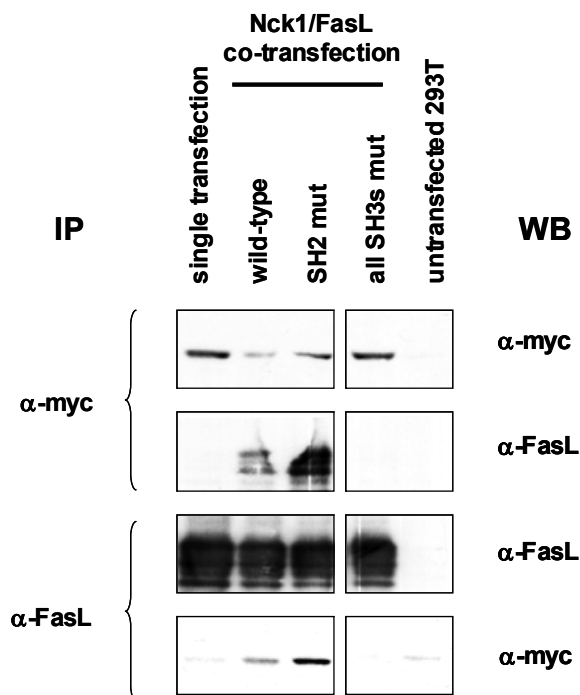


Fig. 4.3.8. FasL co-precipitates with Nck1. Myc-tagged proteins were transiently co-expressed with FasL in 293T cells. Cell lysates prepared 24 hours after transfection were split into two aliquots for parallel immunoprecipitation (IP) with α -FasL mAb NOK1 or α -myc mAb 9C11. Proteins were transferred to nitrocellulose followed by western blotting (WB). α -myc IP followed by α -FasL WB revealed co-precipitated FasL and α -FasL IP followed by α -myc staining revealed co-precipitated myc-tagged proteins. To monitor protein expression, the blots were stripped and stained with α -myc (for α -myc IP) and α -FasL (for α -FasL IP).

Co-localization

Wild-type or mutated GFP-tagged Nck1 were co-expressed with FasL in either 293T or RBL2H3 cells. 24 hours after transfection, the cells were fixed and the co-localization was analyzed by staining with anti-FasL antibody NOK1. As shown in Fig. 4.3.9A, FasL colocalizes with wild-type or SH2 point mutated (R308K) Nck1 but not with the mutants carrying a point mutation in any of the three SH3 domains (W38K, W143K or W229K). Like shown for FCH/SH3 proteins, we also noticed that the presence of Nck1 changed the intracellular distribution of FasL from the membrane into intracellular,

lysosome-like vesicles. Notably, in RBL2H3 cells, Nck1 co-localized with FasL but the interaction did not alter the intracellular localization of FasL.

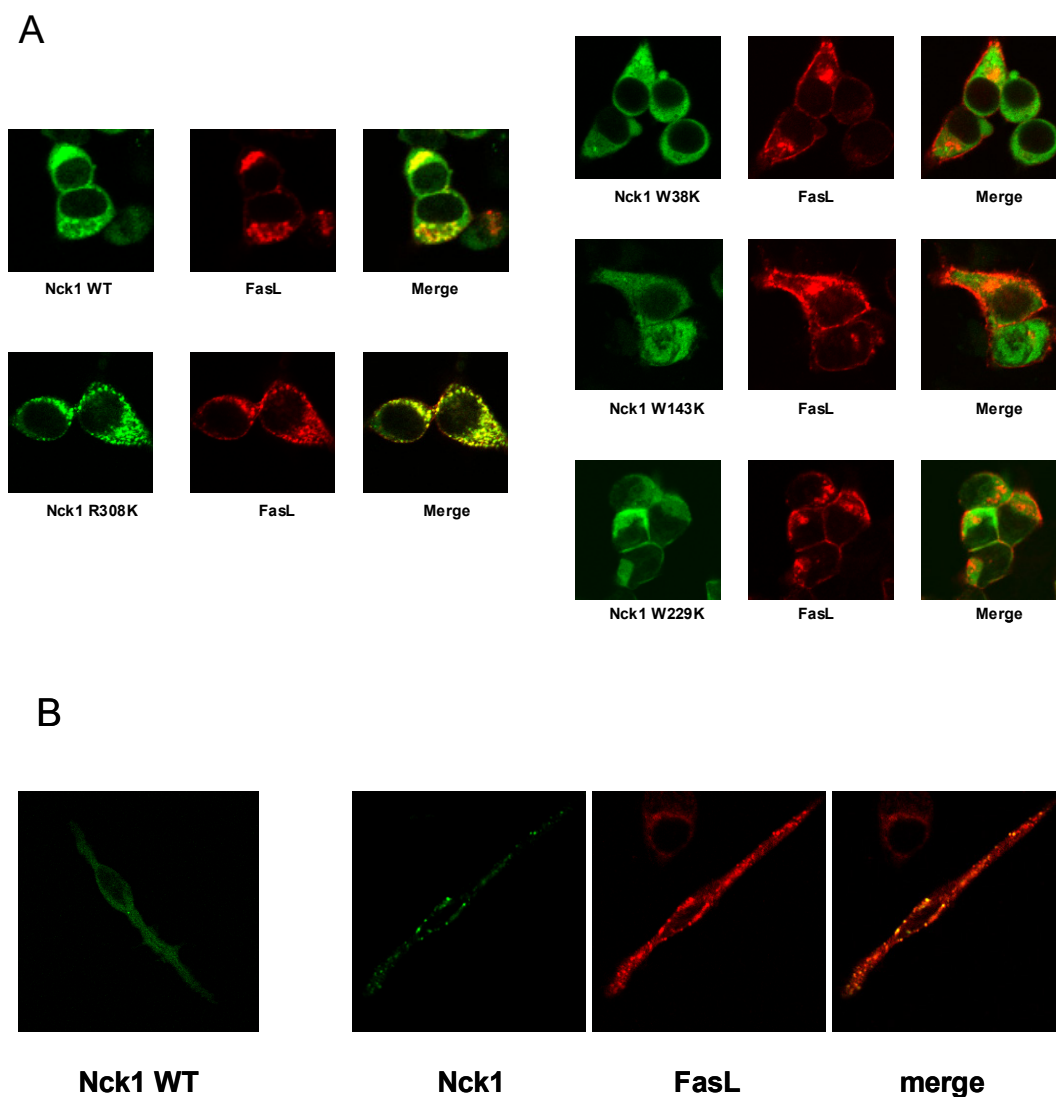


Fig. 4.3.9. Intracellular distribution of FCH/SH3 proteins and the interaction with FasL. A. Wild-type (WT) or mutated Nck1 were co-expressed with FasL in 293T cells. 24 hours after transfection, cells were fixed, permeabilized and stained with α -FasL mAb NOK1 and gam/Alexa fluor 546. The samples were analyzed confocal microscopy. B. Co-localization of Nck1 with FasL in RBL2H3 transfectants.

4.3.3. Co-localization of FasL with Nck1 in activated cytotoxic T cells

Having shown that Nck1 co-localizes with FasL when overexpressed, we tried to detect the interaction of the two proteins in mature human T cells. Firstly, we checked the subcellular distribution of Nck1 by staining with anti-Nck1 antibody. As shown in Fig. 4.3.10A, Nck1 is expressed as a cytosolic protein and does not localize in

intracellular vesicles in T cells. Upon activation with superantigen sensitive CD8⁺ T cell clones; both Nck1 and FasL co-localized with Cathepsin D in pseudopodia-like protrusions. (Fig. 4.3.10B).

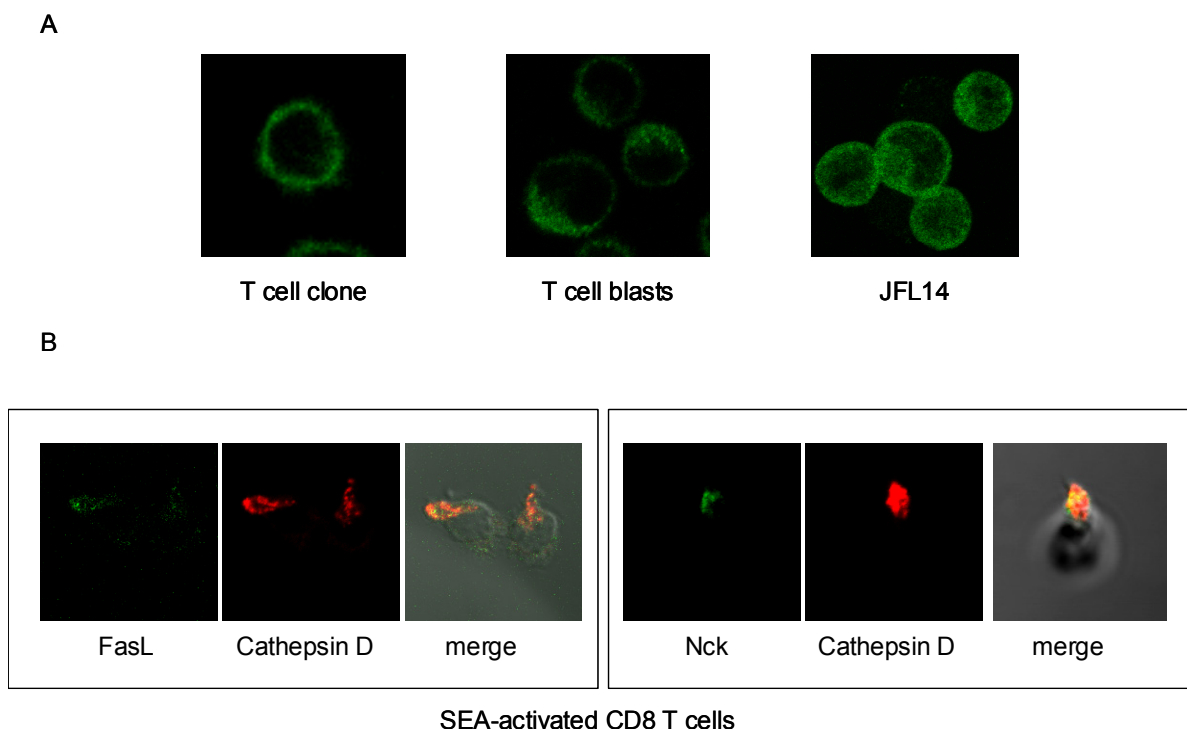


Fig. 4.3.10. Intracellular distribution of Nck1 and the interaction with FasL. A. Intracellular distribution of Nck1 was analyzed by immunostaining with anti-Nck1 mAb and gam/Alex fluor 488 in indicated T cells. B. SEA superantigen sensitive CD8⁺ T cell clones were stimulated on coverslips with 0.5 ng/ml SEA for 1 hour before they were fixed and stained for FasL and Cathepsin D (left panel) or stained for Nck1 and Cathepsin D (right panel). The images were merged to show the co-localization and normal transmission light was used to show the protrusion forming in activated cells.

4.3.4. Co-localization of Nck-1, FasL and Cathepsin D in the contact region between cytotoxic CD8⁺ T and target cells

As mentioned, TCR-triggered recruitment of Nck1 to CD3 ϵ is essential for T cell receptor signaling and synapse formation¹³². From our results, the capacity of Nck1 binding to FasL in activated T cells raises the hypothesis that Nck1 couples the actin cytoskeleton to FasL within the T cell/target cell contact region during T cell activation. To address this, we next generated cytotoxic CD8⁺ T cell lines (cytotoxicity were confirmed by chromium release assay as shown in Fig. 4.3.11A) and used these cells for T cell/target B cell conjugate assay. The induction of synapse formation was examined by evaluation of the actin distribution by phalloidin staining. As shown in Fig. 4.3.11B, actin accumulation could be observed at the T cell/target B cell contact site. Pretreatment of T cells with latrunculin A or cytochalasin D (Fig. 4.3.12A) to block actin

polymerization resulted in abrogated synapse formation (Fig. 4.3.12B). Importantly, as shown in Fig. 4.3.13, both Nck1 and FasL were located at the T cell/target B cell contact site.

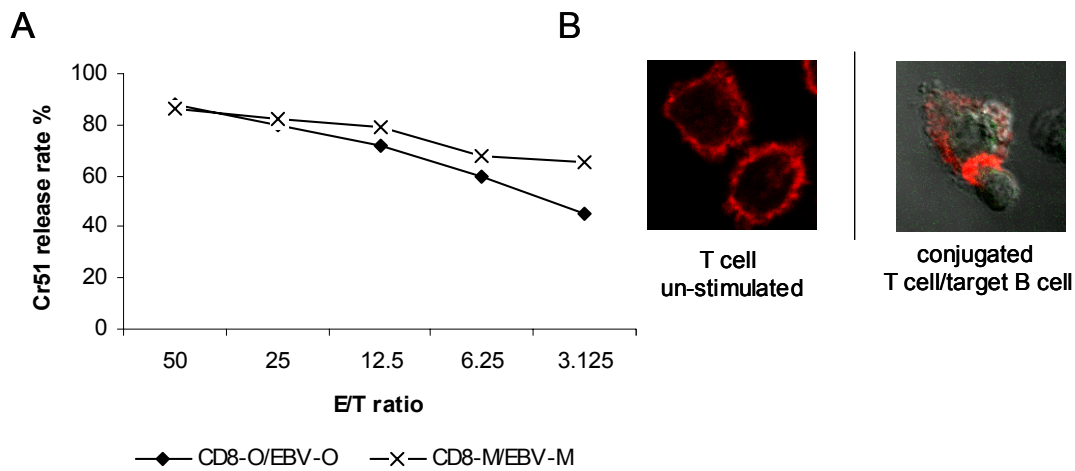


Fig. 4.3.11. Cytotoxicity of CD8⁺ T cell lines and the synapse formation in T cell/target B cell interface. A. CD8⁺ lines (CD8-O and CD8-M) were used as effector cells against EBV transformed B cells (EBV-O, EBV-M) in a chromium-51 (⁵¹Cr) release assay. Data present the percentage of specific lysis at different effector/target cell ratios (E/T ratio). B. T cells were either unstimulated (left panel) or incubated with target B cells (right panel), fixed, permeabilized, and stained for actin by using rhodamine conjugated phalloidin. Normal transmission light was used to show cell shapes.

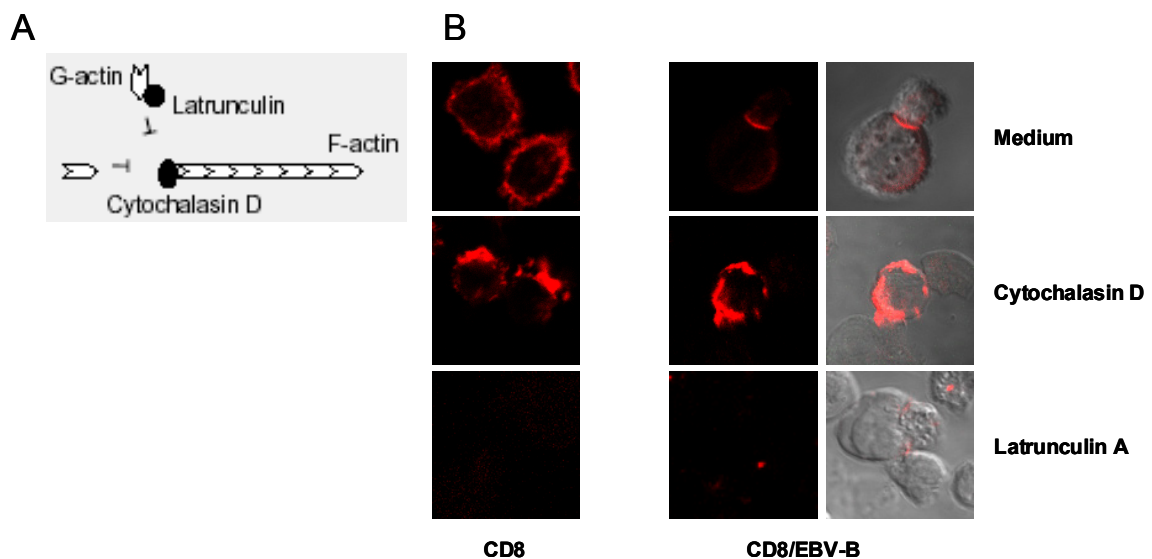


Fig. 4.3.12. Actin cytoskeleton-dependent synapse formation in T cell/target B cell interface. A. Actin polymerization can be blocked either by latrunculin A, which sequesters monomeric G-actin in a 1:1 molar ratio and prevents its addition to growing filaments, or by cytochalasin D, which caps the barbed end of filaments, thereby precluding addition of new G-actin monomers. B. CD8⁺ T cells were preincubated with 5 nM latrunculin A or 10 μ M cytochalasin D for 30 minutes before the conjugation assays was carried out. Rhodamine-phalloidin was used to stain the actin filaments as described in Fig. 4.3.11B.

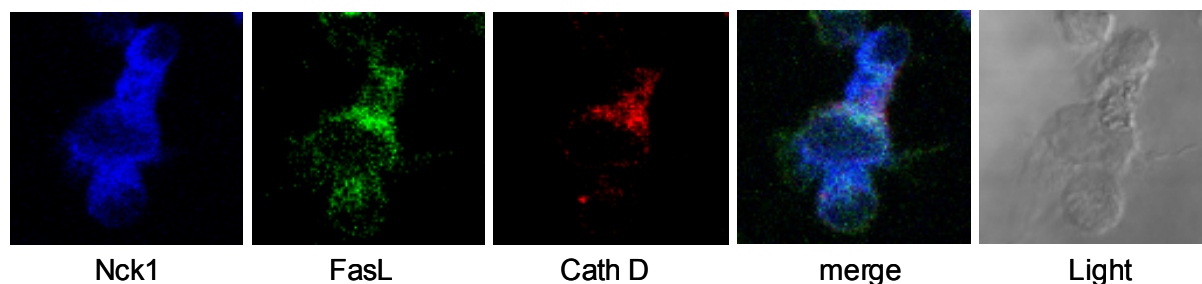


Fig. 4.3.13. Co-localization of Nck1 and FasL in the contact zone of T cells and target B cells. T cells and B cells were mixed at the ratio of 2:1 and co-cultured for 20 minutes. After conjugation, cells were fixed, permeabilized and stained for Nck1, FasL and Cathepsin D by biotinylated anti-FasL mAb NOK1 with streptavidin-FITC, anti-Nck1 mAb with CY5-goat anti-mouse and anti-Cathepsin D with rhodamine-donkey anti-rabbit antibodies. Samples were examined by Zeiss LSM 510. The "merged" image shows the overlay of three proteins and the normal transmission light was used to show T cell: target B cell interface.

4.4. Other FasL interacting proteins and the potential role in the regulation of FasL expression

In 1996, Hachiya and coworkers deposited several protein fragments in the NCBI database that were found to interact with FasL in a yeast two-hybrid screen. Although these "Fas-ligand associated factors" (FLAF1-3 - AAB93495, AAB93496, AAB93497) contained either a WW domain (FLAF1) or one or more SH3 domains (FLAF2,3) no further results were published except a note that FLAFs might regulate FasL stability. Sequence comparison with novel entries in the databases reveals that FLAF-1 forms part of the formin binding protein 11 (FBP11, also called the huntingtin-interacting protein HYP A), FLAF2 is part of the c-Cbl-associated protein SH3P12 = "sorbin and SH3 domain containing 1", and FLAF3 represents a portion of the BAI1-associated protein 2 (BAP2)-beta (Fig. 4.4.1). We therefore studied the interaction between FLAFs and FasL. First of all, we used GST-fusion proteins containing WW domain of FLAF1, 1st or 3rd SH3 domain of FLAF2 and SH3 domain of FLAF3 for *in vitro* "pull down" assays. As expected, all proteins could precipitate FasL from KFL-9 cell lysates (Fig. 4.4.2A). We also constructed myc-tagged expression vectors encoding full length SH3P12/FLAF2 and BAP2 β /FLAF3 and transfected them together with FasL into 293T cells. Co-immunoprecipitation (Fig. 4.4.2B) or intracellular staining (Fig. 4.4.2C) confirmed the protein-protein interaction. Interestingly, the interaction of FLAF2 and FLAF3 with FasL did not result in translocation of FasL into intracellular vesicles but rather enhances the surface expression of FasL.

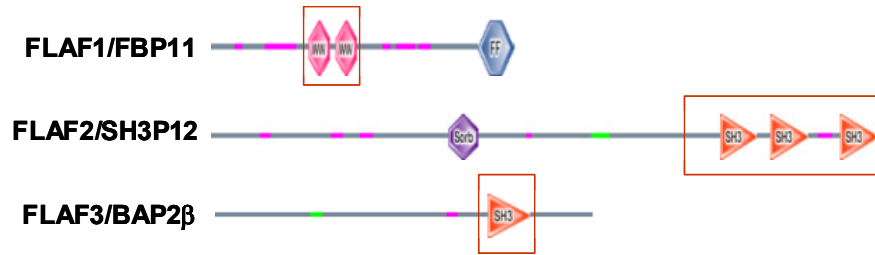


Fig. 4.4.1. Fas ligand associated factors (FLAFs). The modular composition of FLAFs were indicated in frames. Sequence comparison with novel entries in the databases reveals that FLAF1 forms part of the formin binding protein 11 (FBP11, also called the huntingtin-interacting protein HYPA) which contains 3 WW domain, FLAF2 is part of the c-Cbl-associated protein SH3P12 = "sorbin and SH3 domain containing 1" which contains three SH3 domains, and FLAF3 represents a portion of the BAI1-associated protein 2 (BAP2)-β and contains one SH3 domain.

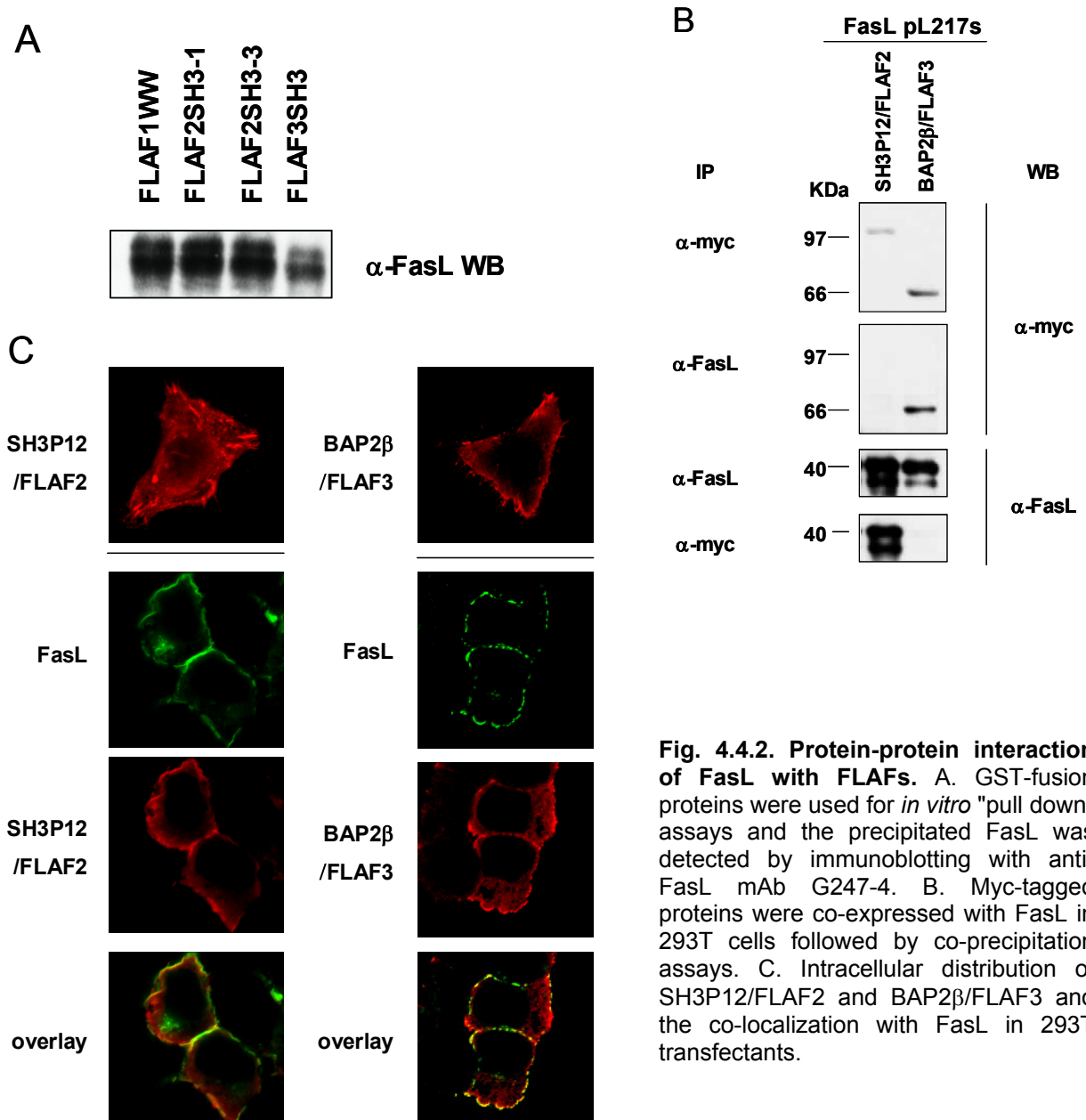


Fig. 4.4.2. Protein-protein interaction of FasL with FLAFs. A. GST-fusion proteins were used for *in vitro* "pull down" assays and the precipitated FasL was detected by immunoblotting with anti-FasL mAb G247-4. B. Myc-tagged proteins were co-expressed with FasL in 293T cells followed by co-precipitation assays. C. Intracellular distribution of SH3P12/FLAF2 and BAP2β/FLAF3 and the co-localization with FasL in 293T transfectants.

5. Discussion

5.1. Reverse signal transduction of FasL in T cells

As stated in the introduction, FasL reverse signaling so far has been exclusively demonstrated in the context of murine T cell populations. Thus, Suzuki, Fink and colleagues reported that expression of functional FasL and its engagement is required to induce maximal proliferation and cytotoxic effector function of CD8⁺ T cells^{68,69,71}. In contrast, for CD4⁺ cells, cell-cycle arrest followed by elevated levels of apoptosis was observed when cells were activated by TCR- and FasL-stimulation⁷⁰. Thus, it seemed that FasL-engagement would exert positive and negative signals depending on the T cell subpopulation under investigation. In our experiments, we mostly observed a negative regulation of TCR or TCR/CD28-induced T cell activation in response to FasL-ligation. Thus, in unseparated (E⁺) as well as in purified CD4⁺ and CD8⁺ T cells, FasL-engagement resulted in a marked decrease of proliferation associated with a reduced expression of activation markers and an arrest in cell-cycle progression. However, we also observed a "stimulatory" effect of FasFc fusion protein or anti-FasL antibody crosslinking on the proliferation of pre-activated T cell populations. Under these conditions, we suggest that FasL ligation might have resulted in decreased sensitivity towards activation-induced cell death associated with increased survival and thymidine incorporation in the presence of IL-2 as a growth factor. We assume that the reported differences or "dual function" of FasL in different T cell populations are rather due to the state of activation than to the phenotype of the given T cell population.

Interestingly, for more than 15 donors tested, we observed a major reduction of proliferation of freshly isolated PBMC or T cells in the presence of FasFc. Clearly, FasL crosslinking was absolutely required to exert this inhibitory effect. This result is compatible with the reported observations for murine CD4⁺ T cells⁷⁰. However, whereas Desbarats and colleagues could overcome the inhibitory effect of FasL by adding recombinant IL-2, we (and Suzuki et al.⁶⁹) did not see a major difference in the presence or absence of IL-2 on primary cells. Only in T cell blasts, we observed a restoration of proliferative capacity in the presence of exogenously added growth factor. We did not see any major effect of IL-2 on unseparated (E⁺) T cells, nor on purified CD4⁺ or CD8⁺ T cells. Further, in this context it did not matter whether the cells were stimulated with anti-CD3 alone or in combination with anti-CD28. In all cases,

proliferation was significantly reduced by FasL-crosslinking with FasFc or anti-Fas mAb.

As further parameters for the analysis of FasL-effects, we determined changes in cell morphology, expression of classical activation markers (CD25 and CD69), and cell-cycle progression. Once again, we compared purified CD4⁺ or CD8⁺ T cells in order to consider the suggested dual function of FasL on different T cell subsets. As for the proliferation, for all other tested parameters, we detected almost the same outcome of FasL-ligation on the TCR/CD28-driven activation of CD4⁺ or CD8⁺ T cells. FasFc consistently blocked activation of all primary T cells. To quantify the morphological changes, we used FACS analyses looking at activation-dependent changes in cell size and granularity. Overall, the morphological changes associated with cellular activation were dramatically reduced in the presence of FasFc as compared to cells stimulated in the absence of FasFc or in the presence of the Fc control. Thus, while we observed a major increase in cell size and granularity upon activation with anti-CD3 and even more with co-stimulation, FasFc-treated cells remained almost equal in size compared to the medium control. Only a few cells obviously became activated and seemed to start to proliferate. In case of the tested activation markers CD25 (IL-2 receptor α -chain) and CD69 (very early activation, VEA), ligation of CD3 and co-stimulation induced the expected strong increase of expression of both antigens with CD25 expression on CD4⁺ cells being more dependent on co-stimulation. Clearly, CD25 and CD69-induction were almost completely abrogated in the presence of FasFc but not Fc control protein. In agreement with the data published for murine CD4⁺ cells, we also observed a strong and almost complete block of cell-cycle progression in the presence of FasFc. However, in our hands, the cell cycle blockade was not associated with a major increase in cell death (or hypodiploid nuclei as a measure for apoptosis) during the observation time of up to four days. Also, CD4⁺ and CD8⁺ cells showed an almost superimposable reactivity towards FasL ligation. Thus, in contrast to the co-stimulatory effect on murine cytotoxic T cells that had been suggested by others, we detected a blockage of cell-cycle progression also in CD8⁺ cells. In fact, Suzuki and Fink had not analyzed resting CD8 cells in detail^{68,69}. It should be mentioned, however, that their data pointing to an elevated proliferation and effector function and suggesting a differential role of FasL engagement on CD4⁺ and CD8⁺ cells were obtained with pre-stimulated populations.

In essence, the present work is the first to demonstrate that FasL-engagement is capable of altering signal transduction in human T cells. Since it has been suggested that Fas-engagement also influences T cell activation¹³⁹, it seems still unclear whether the observed effects of the FasFc fusion protein are due to a blockade of a potentially stimulatory Fas signal, due to the induction of an inhibitory signal through FasL or due to a FasL-induced inhibition of the TCR-signal as suggested in Figure 5.1. At the moment, the first possibility cannot be ruled out completely and may account for some aspects of the observed effects.

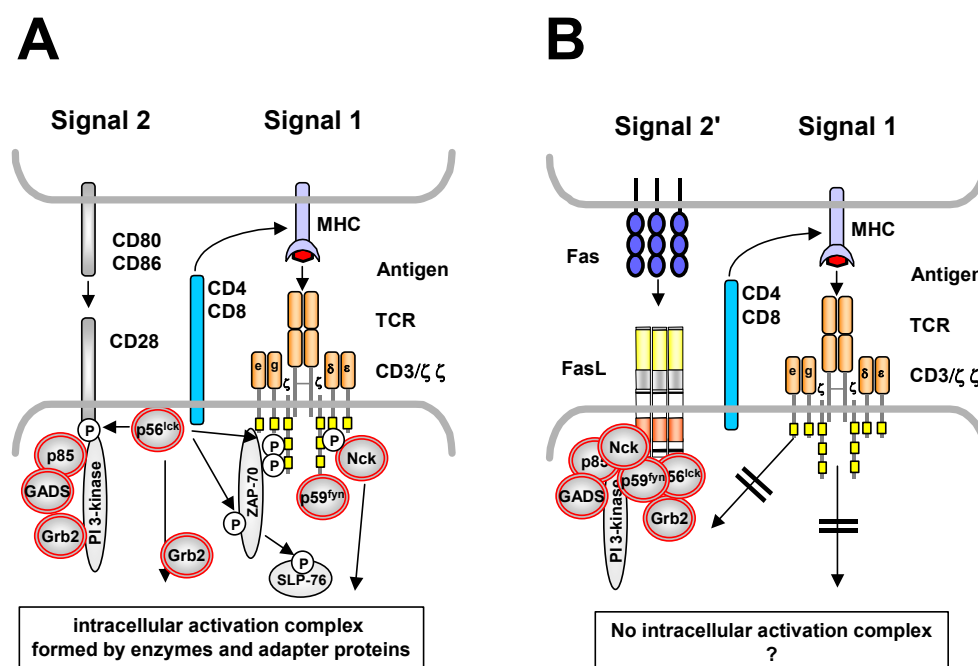


Fig. 5.1. Model for the "negative" costimulatory function of FasL.

A. "Normal" induction of TCR/CD28-signals in the course of antigen-driven T cell activation.

B. FasL-dependent block of TCR signaling: by virtue of assembling with a number of cytosolic SH3 domain proteins required for TCR-dependent activation, FasL could alter the TCR/CD3 stimulus in several different ways. In such a scenario, FasL may serve as a inhibitory molecule that directly interferes with signal 1 given by the TCR or with signal 2 given by classical costimulatory molecules such as CD28. As suggested from the data presented here, FasL could also alter the capacity of the TCR/CD3-associated enzymes and adapters to establish a complete activation complex.

However, the following analyses of signaling events associated with ligation of FasL but not Fas strongly suggest that we are monitoring FasL reverse signaling rather than blocking Fas signaling. In this regard the analysis of protein tyrosine phosphorylation is the most striking effect observed *in vitro*. In T cell blasts and T cell clones (although with a lower amplitude), we clearly saw a decrease in overall tyrosine phosphorylation

in response to CD3-stimulation when cells had been pretreated with crosslinked FasFc or anti-FasL mAb. To our knowledge, Fas-ligation is not necessarily associated with changes in tyrosine phosphorylation. Thus, even under these conditions, treatment with FasFc reflects most probably a direct effect on FasL and not a block of FasL-binding to Fas. We also know now that FasFc interacts with FasL expressed on transfectants since we can use it together with an anti human IgG-Fc antibody for detection of FasL expression by flow cytometry (Marcus Lettau, Diploma Thesis). Thus, at the moment, our favourite model would be that FasL (binding to all kind of SH3 domain containing signaling proteins important for building up the activation complex) would simply prevent the induction of TCR-responses by blocking essential protein-protein interactions (Fig. 5.1.B).

Another indication for the direct reverse signaling capacity of FasL is the observation that purified fusion proteins containing the putative CK1 substrate motif (SSAASS) are more heavily phosphorylated by exogenously added CK1 *in vitro* than fusion proteins lacking this motif. In this context it seems relevant that several members of the TNF superfamily that have been implicated in reverse signaling in different cellular systems¹³⁷ containing similar motifs that point to an involvement of casein kinase type serine threonine kinases in the retrograde signal transduction through these TNF ligands. As mentioned before, for TNF it has been shown that mutation of this casein kinase motif alters its capacity for reverse signal transduction¹⁰⁸. Although still preliminary, the observations made in the course of the present thesis suggest that besides a crosstalk between receptors such as the TCR/CD3 complex and FasL, the molecule may also be linked to yet another, so far unknown signaling machinery. Furthermore, the unique "double serine" feature of the CK1 substrate motif in FasL indicates a regulation of FasL signaling by additional - yet unknown - kinases and phosphatases.

Taken together, the data presented here clearly indicate that FasL might act as an inhibitory receptor to prevent T cell activation. This could be of biological importance for instance in the context of a primary *in vivo* T cell activation. Thus, recent studies performed by monitoring the fate of T cells *in vivo* indicated that although T cells enter the area where they meet the antigen presenting dendritic cells rapidly, it needs around eight to twelve hours until the T cells become activated by close contact with

their specific APC¹⁴⁰. Since dendritic cells were reported to express Fas¹⁴¹, a ligation of FasL on T cells scanning the lymphoid tissue for their antigen could prevent premature activation. However, in this scenario FasL expression would be prerequisite for the silencer function. This leaves us with the open question whether *in vivo* and *in vitro* a minimal expression of FasL is sufficient to exert the reverse signal. In fact, so far we failed to detect substantial surface expression of FasL at the onset of the incubation in the presence of FasFc. Nevertheless the level of FasL expression on resting cells and during TCR-driven activation need further investigation, probably using amplification systems developed for the detection of proteins expressed at low level.

5.2. Defining FasL interacting proteins: the FCH/SH3 family

To address the question which molecules regulate reverse signal transduction and other function of FasL, this laboratory had started to identify FasL interacting proteins several years back^{112,113}. Most of the identified interactors are characterized by containing a SH3 or WW domain likely to mediate the FasL interaction by binding to the proline-rich domain located in the membrane proximal cytosolic portion of FasL. Since it had been noted in the meantime that FasL is stored in specialized lysosomal vesicles, we started with a focus on proteins like FBP17 and PACSIN that had been implicated in vesicular transport or actin dynamics in other systems. As described earlier, FBP17 and PACSIN2 were identified as FasL interactors by Ghadimi et al.¹¹³. They belong to a larger family of proteins with a similar domain structure, therefore termed FCH/SH3 family. Besides PACSIN2 and FBP17, the PACSIN2 isoforms PACSIN1 and PACSIN3, CD2BP1, CIP4, RhoGAP C1 and two hypothetical proteins (FLJ00007 and KIAA0456) belong to this family. Most if not all these proteins are involved in the regulation of actin dynamics, cytoskeletal reorganization and intracellular trafficking in different cellular systems. For example, PACSIN2 has been implicated in lysosomal transport by interacting with several proteins (e.g. dynamin) at the lysosomal basis (M. Plomann, personal communication). Interestingly, all tested SH3 domains of the FCH/SH3 proteins were capable of interacting with FasL in *in vitro* "pull-down" assays. Importantly, also the tested full length proteins bound to FasL. Of course, the interaction site was confirmed to be SH3 domain of the respective interaction partner. In case of FBP17 and PACSIN2, deletion (FBP17) or mutation

(PACSIN2) of the SH3 domains completely blocked the association with FasL in "pull down" experiments. Importantly, when overexpressed together with FasL, FBP17 and all the PACSIN isoforms as well as CD2BP1 and CIP4 co-precipitated FasL from cellular lysates.

A major task of the present work was to analyze how the intracellular localization of FasL maybe altered only co-expressed with FasL-interacting proteins. As has been reported, hematopoietic and non-hematopoietic cells differ in the lysosomal compartment. This is also reflected at the level of FasL expression. In non-hematopoietic cells (including HeLa, HACAT and 293T) FasL is obviously sorted directly to the cell surface whereas in hematopoietic cells (Jurkat, HUT78 and RBL), FasL localizes to granular vesicular structures.

When FCH/SH3 proteins were expressed in 293T cells, the PACSINs appeared mostly cytosolic. FBP17 seemed to be expressed in the cytosol as well as in compartments close to the membrane. Similarly, CD2BP1 and CIP4 Δ CC were also localized in different distribution in cytosolic to intracellular structures. Co-expression with FasL changed the localization of FasL dramatically leading the molecule from the membrane to the lysosomal compartment. Only in the case of the PACSIN2 mutant which did not co-localize with FasL, the recruitment to the lysosomes was not obvious. Importantly, the lysosomal localization was confirmed by partial co-localization with Cathepsin D as a marker for lysosomes/endosomes. The most striking effects were seen in HeLa cells: FasL co-expression with PACSIN2 lead both molecules to lysosomes whereas expression with PACSIN2 carrying the point mutation in the SH3 domain completely abrogated co-localization and resulted in an almost complete surface association of FasL. Of note, we did never observe a 100% overlap of lysosomal, FasL and FCH/SH3 protein staining. In RBL cells, we also observed colocalization. In most cases, when wild-type DNA was transfected, we observed an increase in size of the granular structures. Clearly, this was not seen when SH3 domain lacking (FBP17) or mutated (PACSIN2) proteins were co-expressed. To us this indicated that in cells of the hematopoietic lineage in which FasL is "automatically" located into the lysosomal compartment also in single transfectants, the additional presence of "sorting proteins" somehow leads to a further accumulation of the respective proteins in or around the vesicles.

The suggested function of FBP17 and PACSINs in different systems has been described in the introduction. There is still some controversy as to whether the three isoforms of PACSIN are also functionally expressed in neuronal versus other cells. However, we were able to amplify the SH3 domain and full-length proteins from T cell lines (HUT78) or T cell blasts. The expression of CD2BP1 and CIP4 is restricted to hematopoietic cells^{124,142}. CD2BP1 is a 415 amino acid long cytosolic adaptor protein expressed in T cells that has been proposed to be important in regulating T cell activation by modulation of CD2 activity^{143,144}. In these cells, CD2BP1 regulates cytoskeletal organization¹⁴² and also seems to be involved in the formation of the immunological synapse¹⁴⁵. As recently described, in this context, CD2BP1 acts downstream of CD2/CD2AP to link CD2 engagement to the Wiskott-Aldrich syndrome protein (WASP)-evoked actin polymerisation required for synapse formation and T cell activation¹⁴⁵. CD2BP1 is also named PSTPIP1 (proline, serine, threonine phosphatase interacting protein) based on its interaction with a PEST family protein tyrosine phosphatase¹⁴⁶. PTP PEST in turn is expressed in hematopoietic tissues and has been reported to negatively regulate lymphocyte activation¹⁴². The interaction of CD2BP1 with (murine) PTP PEST has been described to be mediated by the coiled-coil domain of CD2BP1¹⁴⁷. In man, mutations in CD2BP1 have been shown to disrupt the binding to PTP PEST and made responsible for the PAPA syndrome, an auto-inflammatory disorder¹⁴⁸. Our data showed that CD2BP1 might also be involved in the lysosomal targeting or transport of FasL. Importantly, CD2BP1 has been found as an interactor for murine FasL in a yeast-two-hybrid screen by our collaborators Wiebke Baum and Martin Zörnig (Frankfurt). However, more works is needed to establish the role of CD2BP1 in lysosomal targeting or even transport to the immunological synapse.

The cdc42-interacting protein4 (CIP4) was first described as an interactor of a constitutively active mutant of cdc42¹²⁴. Besides interacting with cdc42, CIP4 also mediates the recruitment of WASP to microtubules¹²⁵. It interacts with Src kinase Lyn to phosphorylates WASP in a process regulated by cdc42¹⁴⁹ and with huntingtin¹⁵⁰, an adaptor protein involved in neurodegenerative Huntington's disease.

Besides the SH3 domain, FCH/SH3 proteins also contain so-called FCH domains (=Fes/CIP4 homology). The FCH domain was first described as a region of homology

between the Fps/Fes/Fer protein tyrosine kinases (PTK) and the Cdc42-interacting protein, CIP4¹²⁴. Blast analyses within protein databases reveal the presence of FCH domains in numerous proteins, which fall into three classes: Fer and Fps/Fes protein kinases, adapter-like proteins, and RhoGTPase activating proteins. The FCH/SH3 family proteins that we analyzed are adapter-like or RhoGTPase activating proteins. FCH domains are mostly implicated in the regulation of the cytoskeleton. For example, the FCH domain of CIP4 was reported to bind to microtubules¹²⁵. More recently, the FCH domain in Fes was reported to play an important role in microtubule dynamics including microtubule nucleation and bundling¹²⁶. In the context of FasL, co-expression indicates that the protein-protein interaction is sufficient for lysosomal targeting. Thus, it is possible that the FCH domains of these proteins are also involved in lysosomal targeting or cytoskeleton-dependent vesicular transport.

Taken together, we are convinced that the FCH/SH3 proteins identified as interactors are capable of changing the subcellular distribution of FasL (Fig. 5.2.). However, further work is necessary to evaluate the role of the individual members of the family in T cells and NK cells.

5.3. FasL interacts with Nck1: linking the cytoskeleton and the TCR/CD3 complex?

In cytotoxic T cells (and NK cells), FasL is expressed and synthesized upon primary stimulation and then directed to and stored in specialized secretory lysosomes/granules^{21,22}. As mentioned, in activated cytotoxic T cells, FasL is a transmembrane compound of these secretory granules or lysosomes which (in man) also contain granzymes A, B, H, K and M, pore-forming perforin-monomers and granzymes¹⁵¹. Upon interaction with a target cell, the lipid bilayer of the secretory lysosomes fuses with the plasma membrane, thereby releasing the soluble lysosomal components and presenting mFasL on the cell surface^{22,23}. This trigger of target cell apoptosis has been referred to as the “kiss of death”¹⁵². This cytoskeletal association may also play a role in FasL transport to the cell membrane. Like various other protein that were identified as FasL interactors, two adaptor proteins that bound to FasL via SH3 domains attracted our attention in the context of vesicular transport or cytoskeletal movement. The interaction of FasL with Grb2 has been verified by various assays before^{112,113}. In the present work, we thus focused on Nck1 and followed its

fate when co-expressed with FasL or in an *in vivo* stimulation when cytotoxic T cells meet their cognate target cells. Nck1 is an adapter protein of 377 amino acids that is built of one c-terminal SH2 and three SH3 domains. It was shown to constitutively associate with the active $\gamma 2$ isoform of casein kinase 1 (CK1- $\gamma 2$)¹³³ and therefore could be involved in recruitment of the kinase into proximity of FasL as a putative substrate. The second function of Nck1 is the regulation of cytoskeletal assembly through interaction with the Wiskott-Aldrich syndrome protein WASP¹²⁷, the WASP interacting protein WIP¹²⁸, WASP-family verprolin homologous protein WAVE1¹²⁹, the Centaurin- α family of PIP3 binding proteins¹³⁰, the p21-activated kinase PAK1¹³¹, the ϵ -chain of CD3¹³² and others.

When following FasL expression in normal activated T cells, we observed an intracellular localization within the putative secretory granules. Upon activation with TPA/ionomycin, we saw a rapid disintegration of these granules and later a diffuse surface expression of FasL. Interestingly, when analyzing the kinetics of surface expression, we detected a clear biphasic pattern in all tested T cells and clones indicating two waves of FasL expression in activated T cells. The first peak was seen after short-term stimulation (10 minutes) and most probably reflects a PKC/ Ca^{2+} induced reorganization of the cytoskeleton leading to transport of FasL to the surface. The second maximum is reached after 2 hours and is dependent on *de novo* protein synthesis and lysosomal transport (Marcus Lettau, Diploma Thesis).

To address the question whether Nck1 is involved in this process, we followed the expression pattern of both molecules in transfectants and normal T cells. Before, we proved the interaction between Nck1 and FasL using the different constructs that we obtained from our collaborators Louise Larose (Quebec) and Michael Way (London). Clearly, *in vitro* binding was seen with full length Nck1 and with the second and third SH3 domain. As had been described before¹³², all SH3 domains seem to cooperate since individual mutation in all three domains reduced the binding to FasL. We also show co-precipitation of FasL from co-transfectants and conversely co-precipitation of Nck1 with anti-FasL antibodies.

Upon transfection of 293T cells, we found a co-localization of wt Nck1 and SH2 mutated Nck1 with FasL. From parallel staining for cathepsin D, we knew that both molecules were associated with the lysosomal compartment. As expected from the *in vitro* binding studies, mutations in all three SH3 domains influenced binding and co-localization. However, all three individual mutations almost completely abrogated co-localization indicating once more that all SH3 domains cooperate for function of Nck1. Interestingly, while Nck1 was mostly expressed as a diffusely distributed cytoplasmic protein in single transfectants, in double-transfectants, it was located in part in the proximity of lysosomes also occupied by FasL (and Cathepsin D or lamp1). Since it had been reported that upon TCR stimulation, Nck1 recruits other proteins to the TCR/CD3 complex re-assembling the cytoskeleton around the immunological synapse¹³², we wanted to investigate a potential co-localization in T cells that were exposed to target cells. Before, we observed in superantigen-reactive T cell clones that FasL, Cathepsin D and Nck1 rapidly co-localized in pseudopodium-like protrusions that formed after exposure to superantigen. This process was sensitive to inhibitors of actin polymerisation (latrunculin A or cytochalasin D) indicating an major contribution of regulators of cytoskeleton dynamics. Also, we proved the synapse formation by phalloidin staining of the "actin-disk" that is seen between T cells and target cells. Once again, this synapse formation and phalloidin staining was sensitive to latrunculin A or cytochalasin D.

Ultimately, we analyzed CD8⁺ T cells and $\gamma\delta$ T cells that were incubated with their cognate target cells (EBV transformed B cells and MeWo tumor cells, respectively). In both cases, we observed a directed movement of all molecules (FasL, Nck1 and Cathepsin D) to the area of contact. This effect could also be inhibited by prevention of actin filament formation. Taken together, these data indicate that Nck1 may in fact be involved in the TCR/CD3-dependent directed movement of FasL to the immunological synapse (Fig. 5.2.). However, in the future the specificity of this interaction needs to be further addressed e.g. by siRNA approaches since other molecules (CD2BP1 and Grb2) that interact with FasL could also play a role in the context of synapse formation.

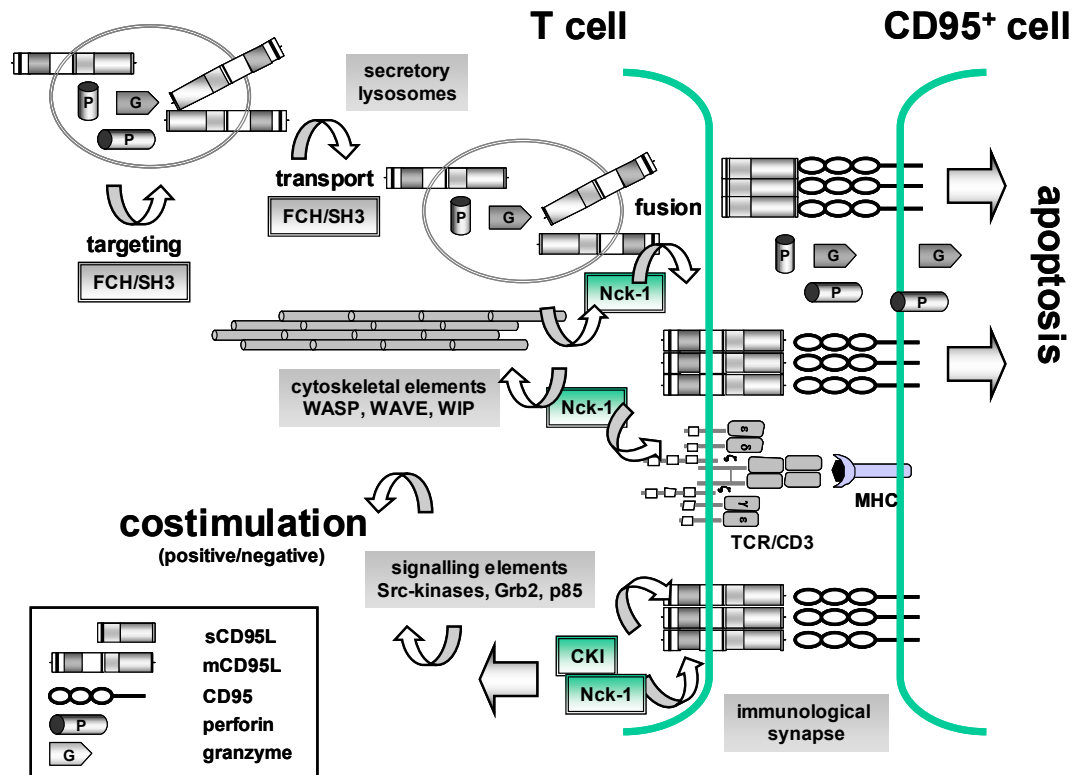


Fig. 5.2. FasL interacting proteins - from secretory granules to the immunological synapse. In cytotoxic T cells and NK cells, FasL is targeted to the so-called secretory granules/lysosomes. Besides FasL, these lysosomes contain other cytotoxic molecules such as granzymes and perforins which in concert contribute to an effective target cell lysis. Of note, targeting of FasL to these lysosomes strictly depends on the proline-rich domain (PRD) within the cytoplasmic tail of the molecule. In this context, members of the FCH/SH3 family (including FBP17, PACSINs, CD2BP1 and others) are candidates for directing the localization and transport of FasL (and/or secretory lysosomes in general). Most proteins of this family are involved in actin cytoskeleton reorganization and protein/organelle trafficking. Other interactors for FasL are the small adapter proteins Grb2 and Nck1. Therefore, an attractive model would be that the PRD is not only required for lysosomal targeting but also for transport and fusion of these lysosomes to the area where the immunological synapse is formed. This could be followed by the release of the various cytolytic factors and by FasL cleavage in the presence of a metalloproteinase (e.g. matrilysin, MMP-7). Whether the sFasL induces or inhibits apoptosis then depends on the potential to form active multimers. The complex biology of FasL is further underscored by the fact that it has been found to act as a "negative" or "positive" costimulatory molecule for T cells. Whether the same (FCH/SH3-family, Grb2 or Nck1) or other (e.g. CK1, PI 3-kinases or Src kinases) FasL- interacting molecules are involved in this aspect, is still open.

5.4. Other FasL interacting proteins: FLAFs

As part of the present work, we also demonstrated that FasL is capable of interacting with three "Fas-ligand associated factors" (FLAF1-3) that had been deposited in the NCBI database by Hachiya and coworkers in 1996 (accession numbers: AAB93495, AAB93496, AAB93497). They were identified in a yeast two-hybrid screen by using the cytoplasmic portion FasL as bait. The proteins contain either a WW domain (FLAF1) or

one or more SH3 domains (FLAF2,3). Except a note that FLAFs might regulate FasL stability, so far there are no further results published. Sequence comparison with novel entries in protein databases reveals that FLAF1 forms part of the formin binding protein 11 (FBP11, also called the huntingtin-interacting protein A, HYPA), FLAF2 is part of the c-Cbl-associated protein SH3P12 = "sorbin and SH3 domain containing 1" (containing 3 SH3 domains), and FLAF3 represents a portion of the BAI1-associated protein 2 (BAP2 β , with a single SH3 domain).

FBP11/FLAF1 is one of several very proteins that bind to formins, proteins involved in murine limb and kidney development. FBP11 contains two WW domains, which bind to proteins with proline-motifs. Recently, HYPA, the human ortholog of murine FBP11, was identified and shown to interact with the N terminus of the huntingtin protein^{153,154}. A more recent report shows that FBP11 regulates nuclear localization of N-WASP and inhibits N-WASP-dependent microspike formation¹⁵⁵. Thus, this protein might also be involved in cytoskeleton reorganization. Concerning FasL, at the moment GST "pull down" analyses with isolated WW domains confirmed that WW domains of FBP11/FLAF1 are capable of interacting with FasL. SH3P12/FLAF2 has been demonstrated in a, so far single report, as a binding partner for I-afadin and vinculin, two isoforms of a novel actin filament (F-actin)-binding protein and is localized at cell-cell and cell-matrix junctions¹⁵⁶. Concerning BAP2 β /FLAF3, it is known that the SH3 domain of BAP2 interacts with the proline-rich cytoplasmic portion of BAI1 and co-localizes it to the cytoplasmic membrane¹⁵⁷. Miki et al. found that FLAF3 (also termed insulin receptor substrate protein 53 (IRSP53) by this group) is essential for RAC-type G-proteins to induce membrane ruffling, probably due to a recruitment of WAVE2, which in turn stimulates actin-polymerization mediated by the ARP2/3 complex¹⁵⁸.

Based on RT-PCR, we found that all FLAFs or the corresponding proteins are expressed in T cell blasts and T cell lines (HUT 78). The distribution of myc-tagged SH3P12/FLAF2 and BAP2 β /FLAF3 is mainly in cytosolic with some staining in membrane ruffles in 293T transfectants. While co-expressed, they showed strong co-localization with FasL at the plasma membrane. The biological role of the interactions remains to be elucidated.

6. Summary

FasL, a type II transmembrane protein of the TNF superfamily, acts as a death factor and a costimulatory molecule. In the course of this thesis, the retrograde signaling of FasL could be demonstrated for the first time in human T cell populations. With the help of a FasFc fusion protein used as a binding partner for FasL, it was demonstrated that FasL engagement results in a severe block of T cell activation. This was reflected in reduced proliferation, a block in expression of activation markers and a marked reduction in cell-cycle progression without increased cell death. Importantly, inhibition was seen in purified whole T cells as well as in CD4⁺ and CD8⁺ subpopulations and FasL needed to be crosslinked to achieve the effects.

FasL contributes to immune selection, immune response termination and the establishment of immune privilege. FasL expression has to be tightly regulated to prevent unwanted damage within the immune system. The protein expression differs in individual immune cell subsets. In cytotoxic T cells and NK cells, FasL is targeted to and stored in so-called secretory lysosomes. This association strictly depends on the presence of a proline-rich domain (PRD) in the cytosolic part of FasL. Several putative interactors for this PRD of FasL had been identified *in vitro*. A second main focus of the present study was the detailed analyses of several of these interactions *in vitro* and *in vivo*. Starting with FBP17 and PACSIN2, two of the proteins that had been previously identified as FasL interactors, and extending the analysis to the whole FCH/SH3 family of closely related proteins, it was demonstrated that all members of this family can interact with FasL *in vitro* and *in vivo*. Furthermore, most if not all FCH/SH3 proteins tested dramatically changed the subcellular localization of FasL when co-expressed in non-hematopoietic cells indicating a major role of these interactors in guiding FasL to the lysosomal compartment.

FCH/SH3 proteins might also play a role on the way of FasL to the immunological synapse. However, in this context, it could be demonstrated that the adapter protein Nck1 co-localizes with the FasL and upon stimulation of T cells both molecules move to the area of target cell contact. Since Nck1 has been described as a direct link of actin-dependent recruitment of molecules to the immunological synapse, the present data suggest that the TCR-triggered recruitment of Nck1 also results in a directed transport of FasL and associated secretory lysosomes.

Der Fas Ligand (FasL) ist ein Transmembran-Protein der TNF-Familie und fungiert als Todesfaktor und als ko-stimulatorisches Molekül. Im Rahmen der vorliegenden Arbeit wurde seine Funktion als retrograder Signalgeber in humanen T-Zell-Populationen erstmals gezeigt. Nach Bindung eines FasFc Fusionsproteins beobachteten wir eine FasL-vermittelte Inhibition der T-Zell-Aktivierung. Dies äußerte sich in unter anderem in einem Block der Expression von Aktivierungsmarkern und einer deutlichen Reduktion der Zellzyklus-Progression ohne erhöhte Induktion von Zelltod. Im Gegensatz zu publizierten Daten aus Mausmodellen, traten die Effekte gleichermaßen in angereicherten T-Zellen wie auch in isolierten CD4⁺ and CD8⁺ T-Zellen auf. In allen Fällen war eine Kreuzvernetzung von FasL erforderlich.

FasL ist an der Selektion von Immunzellen ebenso beteiligt wie an der Beendigung der Immunantwort oder an der Etablierung von Immunprivileg. Die FasL-Expression muss wohl reguliert sein, um Störungen innerhalb des Immunsystems zu vermeiden. Die Expression des Proteins differiert in verschiedenen Zellpopulationen. In zytotoxischen T- und NK-Zellen wird der FasL zu sekretorischen Lysosomen geleitet und dort gespeichert. Die Assoziation hängt von der prolinreichen Domäne im zytoplasmatischen Anteil von FasL ab. Für diese Region wurden in Vorarbeiten eine Reihe von potenziellen Interaktionspartnern beschrieben. Im zweiten Schwerpunkt der vorliegenden Untersuchung sollten diese Interaktionen *in vitro* und *in vivo* näher analysiert werden. Beginnend mit den FasL-bindenden Proteinen FBP17 und PACSIN2 wurde letztendlich für die ganze "FCH/SH3"-Familie gezeigt, dass alle Mitglieder mit FasL interagieren können. Alle untersuchten Proteine dieser Familie beeinflussten die subzelluläre Verteilung des FasL, was die Bedeutung der FCH/SH3-Proteine für die lysosomale Lokalisation des FasL unterstreicht.

Die FCH/SH3 Proteine könnten zudem eine Rolle bei der Rekrutierung des FasL zur immunologischen Synapse spielen. Im Rahmen der Untersuchungen wurde gezeigt, dass das Adapterprotein Nck mit FasL kolokalisiert und dass beide Moleküle zusammen zur Region des Zielzell-Kontaktes verlagert werden. Da Nck kürzlich als direktes Bindeglied zwischen Aktin-Zytoskelett und der immunologischen Synapse beschrieben wurde, deuten die Befunde darauf hin, dass die TZR-induzierte Umlagerung von Nck mit einem gerichteten Transport von FasL und möglicherweise den sekretorischen Lysosomen zur immunologischen Synapse assoziiert ist.

7. References

1. Suda T, Takahashi T, Golstein P, and Nagata S (1993) Molecular cloning and expression of the Fas ligand, a novel member of the tumor necrosis factor family. *Cell*. 75: 1169-1178
2. Nagata S (1999) Fas ligand-induced apoptosis. *Annu Rev Genet*. 33: 29-55
3. Suda T, Okazaki T, Naito Y, Yokota T, Arai N, Ozaki S, Nakao K, and Nagata S (1995) Expression of the Fas ligand in cells of T cell lineage. *J Immunol*. 154: 3806-3813
4. Janssen O, Sanzenbacher R, and Kabelitz D (2000) Regulation of activation-induced cell death of mature T-lymphocyte populations. *Cell Tissue Res*. 301: 85-99
5. Brunner T, Mogil RJ, LaFace D, Yoo NJ, Mahboubi A, Echeverri F, Martin SJ, Force WR, Lynch DH, Ware CF, and . (1995) Cell-autonomous Fas (CD95)/Fas-ligand interaction mediates activation-induced apoptosis in T-cell hybridomas. *Nature*. 373: 441-444
6. Dhein J, Walczak H, Baumler C, Debatin KM, and Krammer PH (1995) Autocrine T-cell suicide mediated by APO-1/(Fas/CD95). *Nature*. 373: 438-441
7. Ju ST, Panka DJ, Cui H, Ettinger R, el Khatib M, Sherr DH, Stanger BZ, and Marshak-Rothstein A (1995) Fas(CD95)/FasL interactions required for programmed cell death after T- cell activation. *Nature*. 373: 444-448
8. Oberg HH, Lengli-Janssen B, Kabelitz D, and Janssen O (1997) Activation-induced T cell death: resistance or susceptibility correlate with cell surface fas ligand expression and T helper phenotype. *Cell Immunol*. 181: 93-100
9. Janssen O, Stocker A, Sanzenbacher R, Oberg HH, Siddiqi MA, and Kabelitz D (2000) Differential regulation of activation-induced cell death in individual human T cell clones. *Int Arch Allergy Immunol*. 121: 183-193
10. Kabelitz D and Janssen O (1997) Antigen-induced death of T-Lymphocytes. *Front Biosci*. 2: d61-d77
11. Varadhachary AS, Perdow SN, Hu C, Ramanarayanan M, and Salgame P (1997) Differential ability of T cell subsets to undergo activation-induced cell death. *Proc Natl Acad Sci U S A*. 94: 5778-5783
12. Varadhachary AS, Edidin M, Hanlon AM, Peter ME, Krammer PH, and Salgame P (2001) Phosphatidylinositol 3'-kinase blocks CD95 aggregation and caspase-8 cleavage at the death-inducing signaling complex by modulating lateral diffusion of CD95. *J Immunol*. 166: 6564-6569
13. Varadhachary AS, Peter ME, Perdow SN, Krammer PH, and Salgame P (1999) Selective up-regulation of phosphatidylinositol 3'-kinase activity in Th2 cells

- inhibits caspase-8 cleavage at the death-inducing complex: a mechanism for Th2 resistance from Fas-mediated apoptosis. *J Immunol.* 163: 4772-4779
14. Zhang X, Brunner T, Carter L, Dutton RW, Rogers P, Bradley L, Sato T, Reed JC, Green D, and Swain SL (1997) Unequal death in T helper cell (Th)1 and Th2 effectors: Th1, but not Th2, effectors undergo rapid Fas/FasL-mediated apoptosis. *J Exp Med.* 185: 1837-1849
 15. Kirchhoff S, Muller WW, Krueger A, Schmitz I, and Krammer PH (2000) TCR-mediated up-regulation of c-FLIPshort correlates with resistance toward CD95-mediated apoptosis by blocking death-inducing signaling complex activity. *J Immunol.* 165: 6293-6300
 16. Kirchhoff S, Muller WW, Li-Weber M, and Krammer PH (2000) Up-regulation of c-FLIPshort and reduction of activation-induced cell death in CD28-costimulated human T cells. *Eur J Immunol.* 30: 2765-2774
 17. Bossi G and Griffiths GM (1999) Degranulation plays an essential part in regulating cell surface expression of Fas ligand in T cells and natural killer cells. *Nat Med.* 5: 90-96
 18. Eischen CM, Schilling JD, Lynch DH, Krammer PH, and Leibson PJ (1996) Fc receptor-induced expression of Fas ligand on activated NK cells facilitates cell-mediated cytotoxicity and subsequent autocrine NK cell apoptosis. *J Immunol.* 156: 2693-2699
 19. Kashii Y, Giorda R, Herberman RB, Whiteside TL, and Vujanovic NL (1999) Constitutive expression and role of the TNF family ligands in apoptotic killing of tumor cells by human NK cells. *J Immunol.* 163: 5358-5366
 20. Medvedev AE, Johnsen AC, Haux J, Steinkjer B, Egeberg K, Lynch DH, Sundan A, and Espevik T (1997) Regulation of Fas and Fas-ligand expression in NK cells by cytokines and the involvement of Fas-ligand in NK/LAK cell-mediated cytotoxicity. *Cytokine.* 9: 394-404
 21. Blott EJ and Griffiths GM (2002) Secretory lysosomes. *Nat Rev Mol Cell Biol.* 3: 122-131
 22. Trambas CM and Griffiths GM (2003) Delivering the kiss of death. *Nat Immunol.* 4: 399-403
 23. Stinchcombe JC, Bossi G, Booth S, and Griffiths GM (2001) The immunological synapse of CTL contains a secretory domain and membrane bridges. *Immunity.* 15: 751-761
 24. Kiener PA, Davis PM, Rankin BM, Klebanoff SJ, Ledbetter JA, Starling GC, and Liles WC (1997) Human monocytic cells contain high levels of intracellular Fas ligand: rapid release following cellular activation. *J Immunol.* 159: 1594-1598
 25. Kishimoto H, Surh CD, and Sprent J (1998) A role for Fas in negative selection of thymocytes in vivo. *J Exp Med.* 187: 1427-1438

26. Matiba B, Mariani SM, and Krammer PH (1997) The CD95 system and the death of a lymphocyte. *Semin Immunol.* 9: 59-68
27. Singer GG and Abbas AK (1994) The fas antigen is involved in peripheral but not thymic deletion of T lymphocytes in T cell receptor transgenic mice. *Immunity.* 1: 365-371
28. Green DR, Droin N, and Pinkoski M (2003) Activation-induced cell death in T cells. *Immunol Rev.* 193: 70-81
29. Restifo NP (2000) Not so Fas: Re-evaluating the mechanisms of immune privilege and tumor escape. *Nat Med.* 6: 493-495
30. Stuart PM, Griffith TS, Usui N, Pepose J, Yu X, and Ferguson TA (1997) CD95 ligand (FasL)-induced apoptosis is necessary for corneal allograft survival. *J Clin Invest.* 99: 396-402
31. Griffith TS, Brunner T, Fletcher SM, Green DR, and Ferguson TA (1995) Fas ligand-induced apoptosis as a mechanism of immune privilege. *Science.* 270: 1189-1192
32. Bellgrau D, Gold D, Selawry H, Moore J, Franzusoff A, and Duke RC (1995) A role for CD95 ligand in preventing graft rejection. *Nature.* 377: 630-632
33. D'Alessio A, Riccioli A, Lauretti P, Padula F, Muciaccia B, De Cesaris P, Filippini A, Nagata S, and Ziparo E (2001) Testicular FasL is expressed by sperm cells. *Proc Natl Acad Sci U S A.* 98: 3316-3321
34. Hunt JS, Vassmer D, Ferguson TA, and Miller L (1997) Fas ligand is positioned in mouse uterus and placenta to prevent trafficking of activated leukocytes between the mother and the conceptus. *J Immunol.* 158: 4122-4128
35. Kauma SW, Huff TF, Hayes N, and Nilkaeo A (1999) Placental Fas ligand expression is a mechanism for maternal immune tolerance to the fetus. *J Clin Endocrinol Metab.* 84: 2188-2194
36. Gochuico BR, Miranda KM, Hessel EM, De Bie JJ, Van Oosterhout AJ, Cruikshank WW, and Fine A (1998) Airway epithelial Fas ligand expression: potential role in modulating bronchial inflammation. *Am J Physiol.* 274: L444-L449
37. Giordano C, Stassi G, De Maria R, Todaro M, Richiusa P, Papoff G, Ruberti G, Bagnasco M, Testi R, and Galluzzo A (1997) Potential involvement of Fas and its ligand in the pathogenesis of Hashimoto's thyroiditis. *Science.* 275: 960-963
38. Stassi G, Di Liberto D, Todaro M, Zeuner A, Ricci-Vitiani L, Stoppacciaro A, Ruco L, Farina F, Zummo G, and De Maria R (2000) Control of target cell survival in thyroid autoimmunity by T helper cytokines via regulation of apoptotic proteins. *Nat Immunol.* 1: 483-488
39. Gutierrez-Steil C, Wrone-Smith T, Sun X, Krueger JG, Coven T, and Nickoloff BJ (1998) Sunlight-induced basal cell carcinoma tumor cells and ultraviolet-B-

- irradiated psoriatic plaques express Fas ligand (CD95L). *J Clin Invest.* 101: 33-39
40. Nakajima M, Nakajima A, Kayagaki N, Honda M, Yagita H, and Okumura K (1997) Expression of Fas ligand and its receptor in cutaneous lupus: implication in tissue injury. *Clin Immunol Immunopathol.* 83: 223-229
 41. Liles WC, Kiener PA, Ledbetter JA, Aruffo A, and Klebanoff SJ (1996) Differential expression of Fas (CD95) and Fas ligand on normal human phagocytes: implications for the regulation of apoptosis in neutrophils. *J Exp Med.* 184: 429-440
 42. De Maria R, Testa U, Luchetti L, Zeuner A, Stassi G, Pelosi E, Riccioni R, Felli N, Samoggia P, and Peschle C (1999) Apoptotic role of Fas/Fas ligand system in the regulation of erythropoiesis. *Blood.* 93: 796-803
 43. Sata M and Walsh K (1999) Cyclosporine downregulates Fas ligand expression on vascular endothelial cells: implication for accelerated vasculopathy by immunosuppressive therapy. *Biochem Biophys Res Commun.* 263: 430-432
 44. Volpert OV, Zaichuk T, Zhou W, Reiher F, Ferguson TA, Stuart PM, Amin M, and Bouck NP (2002) Inducer-stimulated Fas targets activated endothelium for destruction by anti-angiogenic thrombospondin-1 and pigment epithelium-derived factor. *Nat Med.* 8: 349-357
 45. Mullauer L, Mosberger I, Grusch M, Rudas M, and Chott A (2000) Fas ligand is expressed in normal breast epithelial cells and is frequently up-regulated in breast cancer. *J Pathol.* 190: 20-30
 46. Choi C, Park JY, Lee J, Lim JH, Shin EC, Ahn YS, Kim CH, Kim SJ, Kim JD, Choi IS, and Choi IH (1999) Fas ligand and Fas are expressed constitutively in human astrocytes and the expression increases with IL-1, IL-6, TNF-alpha, or IFN-gamma. *J Immunol.* 162: 1889-1895
 47. Frigerio S, Silei V, Ciusani E, Massa G, Lauro GM, and Salmaggi A (2000) Modulation of fas-ligand (Fas-L) on human microglial cells: an in vitro study. *J Neuroimmunol.* 105: 109-114
 48. Takada T, Nishida K, Doita M, and Kurosaka M (2002) Fas ligand exists on intervertebral disc cells: a potential molecular mechanism for immune privilege of the disc. *Spine.* 27: 1526-1530
 49. Bonfoco E, Stuart PM, Brunner T, Lin T, Griffith TS, Gao Y, Nakajima H, Henkart PA, Ferguson TA, and Green DR (1998) Inducible nonlymphoid expression of Fas ligand is responsible for superantigen-induced peripheral deletion of T cells. *Immunity.* 9: 711-720
 50. O'Connell J, Houston A, Bennett MW, O'Sullivan GC, and Shanahan F (2001) Immune privilege or inflammation? Insights into the Fas ligand enigma. *Nat Med.* 7: 271-274

51. O'Connell J, O'Sullivan GC, Collins JK, and Shanahan F (1996) The Fas counterattack: Fas-mediated T cell killing by colon cancer cells expressing Fas ligand. *J Exp Med.* 184: 1075-1082
52. O'Connell J, Bennett MW, O'Sullivan GC, Collins JK, and Shanahan F (1999) Fas counter-attack--the best form of tumor defense? *Nat Med.* 5: 267-268
53. Igney FH, Behrens CK, and Krammer PH (2000) Tumor counterattack--concept and reality. *Eur J Immunol.* 30: 725-731
54. Igney FH and Krammer PH (2002) Immune escape of tumors: apoptosis resistance and tumor counterattack. *J Leukoc Biol.* 71: 907-920
55. Andreola G, Rivoltini L, Castelli C, Huber V, Perego P, Deho P, Squarcina P, Accornero P, Lozupone F, Lugini L, Stringaro A, Molinari A, Arancia G, Gentile M, Parmiani G, and Fais S (2002) Induction of lymphocyte apoptosis by tumor cell secretion of FasL-bearing microvesicles. *J Exp Med.* 195: 1303-1316
56. Rivoltini L, Carrabba M, Huber V, Castelli C, Novellino L, Dalerba P, Mortarini R, Arancia G, Anichini A, Fais S, and Parmiani G (2002) Immunity to cancer: attack and escape in T lymphocyte-tumor cell interaction. *Immunol Rev.* 188: 97-113
57. Hahne M, Rimoldi D, Schroter M, Romero P, Schreier M, French LE, Schneider P, Bornand T, Fontana A, Lienard D, Cerottini J, and Tschopp J (1996) Melanoma cell expression of Fas(Apo-1/CD95) ligand: implications for tumor immune escape. *Science.* 274: 1363-1366
58. De Maria R, Zeuner A, Eramo A, Domenichelli C, Bonci D, Grignani F, Srinivasula SM, Alnemri ES, Testa U, and Peschle C (1999) Negative regulation of erythropoiesis by caspase-mediated cleavage of GATA-1. *Nature.* 401: 489-493
59. Kaplan HJ, Leibole MA, Tezel T, and Ferguson TA (1999) Fas ligand (CD95 ligand) controls angiogenesis beneath the retina. *Nat Med.* 5: 292-297
60. Hill LL, Ouhtit A, Loughlin SM, Kripke ML, Ananthaswamy HN, and Owen-Schaub LB (1999) Fas ligand: a sensor for DNA damage critical in skin cancer etiology. *Science.* 285: 898-900
61. Rouvier E, Luciani MF, and Golstein P (1993) Fas involvement in Ca(2+)-independent T cell-mediated cytotoxicity. *J Exp Med.* 177: 195-200
62. Pinkoski MJ and Green DR (1999) Fas ligand, death gene. *Cell Death Differ.* 6: 1174-1181
63. Cohen PL and Eisenberg RA (1991) Lpr and gld: single gene models of systemic autoimmunity and lymphoproliferative disease. *Annu Rev Immunol.* 9: 243-269

64. Takahashi T, Tanaka M, Brannan CI, Jenkins NA, Copeland NG, Suda T, and Nagata S (1994) Generalized lymphoproliferative disease in mice, caused by a point mutation in the Fas ligand. *Cell*. 76: 969-976
65. Adachi M, Suematsu S, Kondo T, Ogasawara J, Tanaka T, Yoshida N, and Nagata S (1995) Targeted mutation in the Fas gene causes hyperplasia in peripheral lymphoid organs and liver. *Nat Genet*. 11: 294-300
66. Karray S, Kress C, Cuvellier S, Hue-Beauvais C, Damotte D, Babinet C, and Levi-Strauss M (2004) Complete loss of Fas ligand gene causes massive lymphoproliferation and early death, indicating a residual activity of *gld* allele. *J Immunol*. 172: 2118-2125
67. Rieux-Laucat F, Le Deist F, and Fischer A (2003) Autoimmune lymphoproliferative syndromes: genetic defects of apoptosis pathways. *Cell Death Differ*. 10: 124-133
68. Suzuki I and Fink PJ (1998) Maximal proliferation of cytotoxic T lymphocytes requires reverse signaling through Fas ligand. *J Exp Med*. 187: 123-128
69. Suzuki I and Fink PJ (2000) The dual functions of fas ligand in the regulation of peripheral CD8+ and CD4+ T cells. *Proc Natl Acad Sci U S A*. 97: 1707-1712
70. Desbarats J, Duke RC, and Newell MK (1998) Newly discovered role for Fas ligand in the cell-cycle arrest of CD4+ T cells. *Nat Med*. 4: 1377-1382
71. Suzuki I, Martin S, Boursalian TE, Beers C, and Fink PJ (2000) Fas ligand costimulates the in vivo proliferation of CD8+ T cells. *J Immunol*. 165: 5537-5543
72. Boursalian TE and Fink PJ (2003) Mutation in fas ligand impairs maturation of thymocytes bearing moderate affinity T cell receptors. *J Exp Med*. 198: 349-360
73. Oberg HH, Lengl-Janssen B, Robertson MJ, Kabelitz D, and Janssen O (1997) Differential role of tyrosine phosphorylation in the induction of apoptosis in T cells via CD95 or the TCR/CD3-complex. *Cell Death Differ*. 4: 403-412
74. Oberg HH, Sanzenbacher R, Lengl-Janssen B, Dobmeyer T, Flindt S, Janssen O, and Kabelitz D (1997) Ligation of cell surface CD4 inhibits activation-induced death of human T lymphocytes at the level of Fas ligand expression. *J Immunol*. 159: 5742-5749
75. Sanzenbacher R, Kabelitz D, and Janssen O (1999) SLP-76 binding to p56lck: a role for SLP-76 in CD4-induced desensitization of the TCR/CD3 signaling complex. *J Immunol*. 163: 3143-3152
76. Kavurma MM and Khachigian LM (2003) Signaling and transcriptional control of Fas ligand gene expression. *Cell Death Differ*. 10: 36-44
77. Brunner T, Kasibhatla S, Pinkoski MJ, Fruttschi C, Yoo NJ, Echeverri F, Mahboubi A, and Green DR (2000) Expression of Fas ligand in activated T cells is regulated by c-Myc. *J Biol Chem*. 275: 9767-9772

78. Chow WA, Fang JJ, and Yee JK (2000) The IFN regulatory factor family participates in regulation of Fas ligand gene expression in T cells. *J Immunol.* 164: 3512-3518
79. Kasibhatla S, Genestier L, and Green DR (1999) Regulation of fas-ligand expression during activation-induced cell death in T lymphocytes via nuclear factor kappaB. *J Biol Chem.* 274: 987-992
80. Latinis KM, Norian LA, Eliason SL, and Koretzky GA (1997) Two NFAT transcription factor binding sites participate in the regulation of CD95 (Fas) ligand expression in activated human T cells. *J Biol Chem.* 272: 31427-31434
81. Mittelstadt PR and Ashwell JD (1998) Cyclosporin A-sensitive transcription factor Egr-3 regulates Fas ligand expression. *Mol Cell Biol.* 18: 3744-3751
82. Mittelstadt PR and Ashwell JD (1999) Role of Egr-2 in up-regulation of Fas ligand in normal T cells and aberrant double-negative Ipr and gld T cells. *J Biol Chem.* 274: 3222-3227
83. Dzialo-Hatton R, Milbrandt J, Hockett RD, Jr., and Weaver CT (2001) Differential expression of Fas ligand in Th1 and Th2 cells is regulated by early growth response gene and NF-AT family members. *J Immunol.* 166: 4534-4542
84. Faris M, Latinis KM, Kempiak SJ, Koretzky GA, and Nel A (1998) Stress-induced Fas ligand expression in T cells is mediated through a MEK kinase 1-regulated response element in the Fas ligand promoter. *Mol Cell Biol.* 18: 5414-5424
85. Brunet A, Bonni A, Zigmond MJ, Lin MZ, Juo P, Hu LS, Anderson MJ, Arden KC, Blenis J, and Greenberg ME (1999) Akt promotes cell survival by phosphorylating and inhibiting a Forkhead transcription factor. *Cell.* 96: 857-868
86. Blott EJ, Bossi G, Clark R, Zvelebil M, and Griffiths GM (2001) Fas ligand is targeted to secretory lysosomes via a proline-rich domain in its cytoplasmic tail. *J Cell Sci.* 114: 2405-2416
87. Letourneur F and Klausner RD (1992) A novel di-leucine motif and a tyrosine-based motif independently mediate lysosomal targeting and endocytosis of CD3 chains. *Cell.* 69: 1143-1157
88. Trowbridge IS, Collawn JF, and Hopkins CR (1993) Signal-dependent membrane protein trafficking in the endocytic pathway. *Annu Rev Cell Biol.* 9: 129-161
89. Ashkenazi A (2002) Targeting death and decoy receptors of the tumour-necrosis factor superfamily. *Nat Rev Cancer.* 2: 420-430
90. Nagata S (1997) Apoptosis by death factor. *Cell.* 88: 355-365
91. Locksley RM, Killeen N, and Lenardo MJ (2001) The TNF and TNF receptor superfamilies: integrating mammalian biology. *Cell.* 104: 487-501

92. Lens SM, Drillenburg P, den Drijver BF, van Schijndel G, Pals ST, van Lier RA, and van Oers MH (1999) Aberrant expression and reverse signalling of CD70 on malignant B cells. *Br J Haematol.* 106: 491-503
93. Cerutti A, Schaffer A, Goodwin RG, Shah S, Zan H, Ely S, and Casali P (2000) Engagement of CD153 (CD30 ligand) by CD30+ T cells inhibits class switch DNA recombination and antibody production in human IgD+ IgM+ B cells. *J Immunol.* 165: 786-794
94. Wiley SR, Goodwin RG, and Smith CA (1996) Reverse signaling via CD30 ligand. *J Immunol.* 157: 3635-3639
95. van Essen D, Kikutani H, and Gray D (1995) CD40 ligand-transduced co-stimulation of T cells in the development of helper function. *Nature.* 378: 620-623
96. Cayabyab M, Phillips JH, and Lanier LL (1994) CD40 preferentially costimulates activation of CD4+ T lymphocytes. *J Immunol.* 152: 1523-1531
97. Miyashita T, McIlraith MJ, Grammer AC, Miura Y, Attrep JF, Shimaoka Y, and Lipsky PE (1997) Bidirectional regulation of human B cell responses by CD40-CD40 ligand interactions. *J Immunol.* 158: 4620-4633
98. Blair PJ, Riley JL, Harlan DM, Abe R, Tadaki DK, Hoffmann SC, White L, Francomano T, Perfetto SJ, Kirk AD, and June CH (2000) CD40 ligand (CD154) triggers a short-term CD4(+) T cell activation response that results in secretion of immunomodulatory cytokines and apoptosis. *J Exp Med.* 191: 651-660
99. Langstein J, Michel J, Fritsche J, Kreutz M, Andreesen R, and Schwarz H (1998) CD137 (ILA/4-1BB), a member of the TNF receptor family, induces monocyte activation via bidirectional signaling. *J Immunol.* 160: 2488-2494
100. Langstein J, Michel J, and Schwarz H (1999) CD137 induces proliferation and endomitosis in monocytes. *Blood.* 94: 3161-3168
101. Stuber E, Neurath M, Calderhead D, Fell HP, and Strober W (1995) Cross-linking of OX40 ligand, a member of the TNF/NGF cytokine family, induces proliferation and differentiation in murine splenic B cells. *Immunity.* 2: 507-521
102. Chen NJ, Huang MW, and Hsieh SL (2001) Enhanced secretion of IFN-gamma by activated Th1 cells occurs via reverse signaling through TNF-related activation-induced cytokine. *J Immunol.* 166: 270-276
103. Scheu S, Alferink J, Potzel T, Barchet W, Kalinke U, and Pfeffer K (2002) Targeted disruption of LIGHT causes defects in costimulatory T cell activation and reveals cooperation with lymphotoxin beta in mesenteric lymph node genesis. *J Exp Med.* 195: 1613-1624
104. Shaikh RB, Santee S, Granger SW, Butrovich K, Cheung T, Kronenberg M, Cheroutre H, and Ware CF (2001) Constitutive expression of LIGHT on T cells leads to lymphocyte activation, inflammation, and tissue destruction. *J Immunol.* 167: 6330-6337

105. Morel Y, Truneh A, Sweet RW, Olive D, and Costello RT (2001) The TNF superfamily members LIGHT and CD154 (CD40 ligand) costimulate induction of dendritic cell maturation and elicit specific CTL activity. *J Immunol.* 167: 2479-2486
106. Eissner G, Kirchner S, Lindner H, Kolch W, Janosch P, Grell M, Scheurich P, Andreesen R, and Holler E (2000) Reverse signaling through transmembrane TNF confers resistance to lipopolysaccharide in human monocytes and macrophages. *J Immunol.* 164: 6193-6198
107. Chou AH, Tsai HF, Lin LL, Hsieh SL, Hsu PI, and Hsu PN (2001) Enhanced proliferation and increased IFN-gamma production in T cells by signal transduced through TNF-related apoptosis-inducing ligand. *J Immunol.* 167: 1347-1352
108. Watts AD, Hunt NH, Wanigasekara Y, Bloomfield G, Wallach D, Roufogalis BD, and Chaudhri G (1999) A casein kinase I motif present in the cytoplasmic domain of members of the tumour necrosis factor ligand family is implicated in 'reverse signalling'. *EMBO J.* 18: 2119-2126
109. Kay BK, Williamson MP, and Sudol M (2000) The importance of being proline: the interaction of proline-rich motifs in signaling proteins with their cognate domains. *FASEB J.* 14: 231-241
110. Takahashi T, Tanaka M, Inazawa J, Abe T, Suda T, and Nagata S (1994) Human Fas ligand: gene structure, chromosomal location and species specificity. *Int Immunol.* 6: 1567-1574
111. Hane M, Lowin B, Peitsch M, Becker K, and Tschopp J (1995) Interaction of peptides derived from the Fas ligand with the Fyn-SH3 domain. *FEBS Lett.* 373: 265-268
112. Wenzel J, Sanzenbacher R, Ghadimi M, Lewitzky M, Zhou Q, Kaplan DR, Kabelitz D, Feller SM, and Janssen O (2001) Multiple interactions of the cytosolic polyproline region of the CD95 ligand: hints for the reverse signal transduction capacity of a death factor. *FEBS Lett.* 509: 255-262
113. Ghadimi MP, Sanzenbacher R, Thiede B, Wenzel J, Jing Q, Plomann M, Borkhardt A, Kabelitz D, and Janssen O (2002) Identification of interaction partners of the cytosolic polyproline region of CD95 ligand (CD178). *FEBS Lett.* 519: 50-58
114. Tomlinson MG, Lin J, and Weiss A (2000) Lymphocytes with a complex: adapter proteins in antigen receptor signaling. *Immunol Today.* 21: 584-591
115. Plomann M, Lange R, Vopper G, Cremer H, Heinlein UA, Scheff S, Baldwin SA, Leitges M, Cramer M, Paulsson M, and Barthels D (1998) PACSIN, a brain protein that is upregulated upon differentiation into neuronal cells. *Eur J Biochem.* 256: 201-211
116. Hilton JM, Plomann M, Ritter B, Modregger J, Freeman HN, Falck JR, Krishna UM, and Tobin AB (2001) Phosphorylation of a synaptic vesicle-associated

- protein by an inositol hexakisphosphate-regulated protein kinase. *J Biol Chem.* 276: 16341-16347
117. Qualmann B and Kelly RB (2000) Syndapin isoforms participate in receptor-mediated endocytosis and actin organization. *J Cell Biol.* 148: 1047-1062
 118. Modregger J, Ritter B, Witter B, Paulsson M, and Plomann M (2000) All three PACSIN isoforms bind to endocytic proteins and inhibit endocytosis. *J Cell Sci.* 113 Pt 24: 4511-4521
 119. Ritter B, Modregger J, Paulsson M, and Plomann M (1999) PACSIN 2, a novel member of the PACSIN family of cytoplasmic adapter proteins. *FEBS Lett.* 454: 356-362
 120. Wasiak S, Quinn CC, Ritter B, de Heuvel E, Baranes D, Plomann M, and McPherson PS (2001) The Ras/Rac guanine nucleotide exchange factor mammalian Son-of-sevenless interacts with PACSIN 1/syndapin I, a regulator of endocytosis and the actin cytoskeleton. *J Biol Chem.* 276: 26622-26628
 121. Tanaka K (2000) Formin family proteins in cytoskeletal control. *Biochem Biophys Res Commun.* 267: 479-481
 122. Fuchs U, Rehkamp G, Haas OA, Slany R, Konig M, Bojesen S, Bohle RM, Damm-Welk C, Ludwig WD, Harbott J, and Borkhardt A (2001) The human formin-binding protein 17 (FBP17) interacts with sorting nexin, SNX2, and is an MLL-fusion partner in acute myelogenous leukemia. *Proc Natl Acad Sci U S A.* 98: 8756-8761
 123. Haft CR, de la Luz SM, Barr VA, Haft DH, and Taylor SI (1998) Identification of a family of sorting nexin molecules and characterization of their association with receptors. *Mol Cell Biol.* 18: 7278-7287
 124. Aspenstrom P (1997) A Cdc42 target protein with homology to the non-kinase domain of FER has a potential role in regulating the actin cytoskeleton. *Curr Biol.* 7: 479-487
 125. Tian L, Nelson DL, and Stewart DM (2000) Cdc42-interacting protein 4 mediates binding of the Wiskott-Aldrich syndrome protein to microtubules. *J Biol Chem.* 275: 7854-7861
 126. Takahashi S, Inatome R, Hotta A, Qin Q, Hackenmiller R, Simon MC, Yamamura H, and Yanagi S (2003) Role for Fes/Fps tyrosine kinase in microtubule nucleation through its Fes/CIP4 homology domain. *J Biol Chem.* 278: 49129-49133
 127. Rivero-Lezcano OM, Marcilla A, Sameshima JH, and Robbins KC (1995) Wiskott-Aldrich syndrome protein physically associates with Nck through Src homology 3 domains. *Mol Cell Biol.* 15: 5725-5731
 128. Anton IM, Lu W, Mayer BJ, Ramesh N, and Geha RS (1998) The Wiskott-Aldrich syndrome protein-interacting protein (WIP) binds to the adaptor protein Nck. *J Biol Chem.* 273: 20992-20995

129. Eden S, Rohatgi R, Podtelejnikov AV, Mann M, and Kirschner MW (2002) Mechanism of regulation of WAVE1-induced actin nucleation by Rac1 and Nck. *Nature*. 418: 790-793
130. Dubois T, Kerai P, Zemlickova E, Howell S, Jackson TR, Venkateswarlu K, Cullen PJ, Theibert AB, Larose L, Roach PJ, and Aitken A (2001) Casein Kinase I Associates with Members of the Centaurin-alpha Family of Phosphatidylinositol 3,4,5-Trisphosphate-binding Proteins. *J Biol Chem*. 276: 18757-18764
131. Bokoch GM, Wang Y, Bohl BP, Sells MA, Quilliam LA, and Knaus UG (1996) Interaction of the Nck adapter protein with p21-activated kinase (PAK1). *J Biol Chem*. 271: 25746-25749
132. Gil D, Schamel WW, Montoya M, Sanchez-Madrid F, and Alarcon B (2002) Recruitment of Nck by CD3 epsilon reveals a ligand-induced conformational change essential for T cell receptor signaling and synapse formation. *Cell*. 109: 901-912
133. Lussier G and Larose L (1997) A casein kinase I activity is constitutively associated with Nck. *J Biol Chem*. 272: 2688-2694
134. Janssen O, Lengl-Janssen B, Oberg HH, Robertson MJ, and Kabelitz D (1996) Induction of cell death via Fas (CD95, Apo-1) may be associated with but is not dependent on Fas-induced tyrosine phosphorylation. *Immunol Lett*. 49: 63-69
135. Kebache S, Zuo D, Chevet E, and Larose L (2002) Modulation of protein translation by Nck-1. *Proc Natl Acad Sci U S A*. 99: 5406-5411
136. Zeng R, Cannon JL, Abraham RT, Way M, Billadeau DD, Bubeck-Wardenberg J, and Burkhardt JK (2003) SLP-76 coordinates Nck-dependent Wiskott-Aldrich syndrome protein recruitment with Vav-1/Cdc42-dependent Wiskott-Aldrich syndrome protein activation at the T cell-APC contact site. *J Immunol*. 171: 1360-1368
137. Janssen O, Qian J, Linkermann A, and Kabelitz D (2003) CD95 ligand - death factor and costimulatory molecule? *Cell Death Differ*. 10: 1215-1225
138. Kennedy NJ, Kataoka T, Tschopp J, and Budd RC (1999) Caspase activation is required for T cell proliferation. *J Exp Med*. 190: 1891-1896
139. Alderson MR, Tough TW, Davis-Smith T, Braddy S, Falk B, Schooley KA, Goodwin RG, Smith CA, Ramsdell F, and Lynch DH (1995) Fas ligand mediates activation-induced cell death in human T lymphocytes. *J Exp Med*. 181: 71-77
140. Mempel TR, Henrickson SE, and Von Andrian UH (2004) T-cell priming by dendritic cells in lymph nodes occurs in three distinct phases. *Nature*. 427: 154-159
141. Guo Z, Zhang M, An H, Chen W, Liu S, Guo J, Yu Y, and Cao X (2003) Fas ligation induces IL-1beta-dependent maturation and IL-1beta-independent

- survival of dendritic cells: different roles of ERK and NF-kappaB signaling pathways. *Blood*. 102: 4441-4447
142. Li J, Nishizawa K, An W, Hussey RE, Lialios FE, Salgia R, Sunder-Plassmann R, and Reinherz EL (1998) A cdc15-like adaptor protein (CD2BP1) interacts with the CD2 cytoplasmic domain and regulates CD2-triggered adhesion. *EMBO J*. 17: 7320-7336
 143. van der Merwe PA, McNamee PN, Davies EA, Barclay AN, and Davis SJ (1995) Topology of the CD2-CD48 cell-adhesion molecule complex: implications for antigen recognition by T cells. *Curr Biol*. 5: 74-84
 144. Dustin ML (1997) Adhesive bond dynamics in contacts between T lymphocytes and glass-supported planar bilayers reconstituted with the immunoglobulin-related adhesion molecule CD58. *J Biol Chem*. 272: 15782-15788
 145. Badour K, Zhang J, Shi F, McGavin MK, Rampersad V, Hardy LA, Field D, and Siminovitch KA (2003) The Wiskott-Aldrich syndrome protein acts downstream of CD2 and the CD2AP and PSTPIP1 adaptors to promote formation of the immunological synapse. *Immunity*. 18: 141-154
 146. Wu Y, Spencer SD, and Lasky LA (1998) Tyrosine phosphorylation regulates the SH3-mediated binding of the Wiskott-Aldrich syndrome protein to PSTPIP, a cytoskeletal-associated protein. *J Biol Chem*. 273: 5765-5770
 147. Spencer S, Dowbenko D, Cheng J, Li W, Brush J, Utzig S, Simanis V, and Lasky LA (1997) PSTPIP: a tyrosine phosphorylated cleavage furrow-associated protein that is a substrate for a PEST tyrosine phosphatase. *J Cell Biol*. 138: 845-860
 148. Wise CA, Gillum JD, Seidman CE, Lindor NM, Veile R, Bashiardes S, and Lovett M (2002) Mutations in CD2BP1 disrupt binding to PTP PEST and are responsible for PAPA syndrome, an autoinflammatory disorder. *Hum Mol Genet*. 11: 961-969
 149. Dombrosky-Ferlan P, Grishin A, Botelho RJ, Sampson M, Wang L, Rudert WA, Grinstein S, and Corey SJ (2003) Felic (CIP4b), a novel binding partner with the Src kinase Lyn and Cdc42, localizes to the phagocytic cup. *Blood*. 101: 2804-2809
 150. Holbert S, Dedeoglu A, Humbert S, Saudou F, Ferrante RJ, and Neri C (2003) Cdc42-interacting protein 4 binds to huntingtin: neuropathologic and biological evidence for a role in Huntington's disease. *Proc Natl Acad Sci U S A*. 100: 2712-2717
 151. Bossi G, Stinchcombe JC, Page LJ, and Griffiths GM (2000) Sorting out the multiple roles of Fas ligand. *Eur J Cell Biol*. 79: 539-543
 152. Russell JH and Ley TJ (2002) Lymphocyte-mediated cytotoxicity. *Annu Rev Immunol*. 20: 323-370

153. Faber PW, Barnes GT, Srinidhi J, Chen J, Gusella JF, and MacDonald ME (1998) Huntingtin interacts with a family of WW domain proteins. *Hum Mol Genet.* 7: 1463-1474
154. Passani LA, Bedford MT, Faber PW, McGinnis KM, Sharp AH, Gusella JF, Vonsattel JP, and MacDonald ME (2000) Huntingtin's WW domain partners in Huntington's disease post-mortem brain fulfill genetic criteria for direct involvement in Huntington's disease pathogenesis. *Hum Mol Genet.* 9: 2175-2182
155. Mizutani K, Suetsugu S, and Takenawa T (2004) FBP11 regulates nuclear localization of N-WASP and inhibits N-WASP-dependent microspike formation. *Biochem Biophys Res Commun.* 313: 468-474
156. Mandai K, Nakanishi H, Satoh A, Takahashi K, Satoh K, Nishioka H, Mizoguchi A, and Takai Y (1999) Ponsin/SH3P12: an I-afadin- and vinculin-binding protein localized at cell-cell and cell-matrix adherens junctions. *J Cell Biol.* 144: 1001-1017
157. Oda K, Shiratsuchi T, Nishimori H, Inazawa J, Yoshikawa H, Taketani Y, Nakamura Y, and Tokino T (1999) Identification of BAIAP2 (BAI-associated protein 2), a novel human homologue of hamster IRSp53, whose SH3 domain interacts with the cytoplasmic domain of BAI1. *Cytogenet Cell Genet.* 84: 75-82
158. Miki H, Yamaguchi H, Suetsugu S, and Takenawa T (2000) IRSp53 is an essential intermediate between Rac and WAVE in the regulation of membrane ruffling. *Nature.* 408: 732-735

8. Appendix

8.1. Publications

Original papers

Ghadimi M, Sanzenbacher R, Thiede B, Wenzel J, Qian J, Plomann M, Borkhardt A, Kabelitz D, Janssen O (2002) Identification of interaction partners of the cytosolic polyproline region of CD95 ligand (CD178). *FEBS Lett.* 519: 50-58

Published reviews

Linkermann A, Qian J, Janssen O (2003) Slowly getting a clue on CD95L Biology. *Biochem Pharmacol.* 66: 1417-1426

Janssen O, Qian J, Linkermann A, Kabelitz D (2003) CD95 Ligand - death factor and costimulatory molecule? *Cell Death Differ.* 10: 1215-1225

Linkermann A, Qian J, Kabelitz D, Janssen O (2003) The Fas ligand as a cell death factor and signal transducer. *Signal Transduction.* 3: 33-46

Book Chapters

Linkermann A, Qian J, Janssen O. Retrograde Fas Ligand signaling. in: Wajant H (Ed) *Fas Signaling*, 2004. Landes Bioscience. in press

Published abstracts

Qian J, Oberg H-H, Jakob M, Linkermann A, Plomann M, Borkhardt A, Janssen O (2002) CD95L binding proteins involved in intracellular trafficking and reverse signaling: I. Identification of a protein family that might regulate localization of transmembrane proteins to secretory lysosomes. *Immunobiology.* 206: 138

Linkermann A, Qian J, Schulze-Osthoff K, Janssen O (2002) CD95L binding proteins involved in intracellular trafficking and reverse signaling: II. Strategies, working models and first results concerning reverse signaling. *Immunobiology.* 206: 136

Linkermann A, Qian J, Schulze-Osthoff K, Janssen O (2002) Indications for Reverse Signaling through the CD95 Ligand. *Signal Transduction.* 3-4: 106

Qian J, Oberg H-H, Jakob M, Linkermann A, Plomann M, Borkhardt A, Janssen O (2002) Identification of a CD95L binding protein family that might be involved in intracellular trafficking and reverse signaling. *Signal Transduction.* 3-4: 108

Qian J, Larose L, Way M, Janssen O (2003) CD95L-interacting proteins - Nck as a potential regulator of CD95L trafficking and function. *Immunobiology.* 208: 115

Qian J, Plomann M, Borkhardt A, Janssen O (2003) CD95L-interacting proteins - Regulators of actin dynamics and vesicular transport associated with CD95L. *Immunobiology.* 208: 124

Qian J, Linkermann A, Larose L, Way W, Janssen O (2003) Role for the adaptor protein Nck in FasL trafficking and function. *Signal transduction*. 3-4: 140

Qian J, Plomann M, Borkhardt A, Janssen O (2003) Regulation of actin dynamics and vesicular transport associated with FasL. *Signal transduction*. 3-4: 141

8.2. Acknowledgements

This study was carried out in the Institute of Immunology, Medical Center Schleswig-Holstein, Campus Kiel, Germany between 2001 and 2004.

I wish to express my sincere gratitude to all who have been involved in this study and especially would like to thank the following persons:

First of all, I am really grateful to Prof. Dieter Kabelitz for giving me the opportunity to work and study in his institute.

Secondly, I thank PD. Dr. Ottmar Janssen for his great support, his scientific guidance, his valuable advice and his patient revision of my thesis.

Special thanks would be given to Mrs. Alyn Beyer and Mrs. Grazella Podda for their strong technical support and kind help in and out the laboratory.

I would like to thank Dr. Heiner Oberg, Dr. Daniela Wesch, Dr. Marie-Luise Kruse, Dipl. Biol. Marten Jakob, Richard Walther, Andreas Linkermann and all colleagues in the institute for their kindness and a lot of help to answer plenty of technical questions.

Finally, and of most importance, I would like to thank my dear parents, who always support me in every aspect. I am most grateful to my husband and our daughter, whose love and concern make me strong to cope with any frustration while I worked in Kiel.

8.3. Curriculum Vitae

PERSONAL DATA

Name: QIAN Jing

Address: Niemannsweg 15, Zi. 143, D-24105 Kiel

Date of birth: April 8, 1973

Place of birth: Hangzhou, Zhejiang, P. R. China

Nationality: Chinese

Marriage State: married, child 3 years old

WORK EXPERIENCE

2001-Present PhD student

Institute of Immunology, Medical Center Schleswig-Holstein, Campus
Kiel, Germany

Director: Prof. Dr. med. Dieter. Kabelitz

1996-2001 Research and teaching assistant

Institute of Microbiology, Medical School, Zhejiang University,
Hangzhou, Zhejiang, China

Head: Prof. Dr. Miaoquan Lu

1995-1996 Intern

First Affiliated Hospital, Medical School, Zhejiang University,
Hangzhou, Zhejiang, China

Chair: Prof. Dr. Shushen Zheng

EDUCATION

1998.9-2001.6 M.Sc. in Microbiology, Zhejiang University

1991-1996 Bachelor of Medicine, Medical School, Zhejiang University

1985-1991 Middle School, Hangzhou, Zhejiang, China

1979-1985 Primary School, Hangzhou, Zhejiang, China

8.4. Erklärung/ Statement

Hiermit erkläre ich, dass ich unter der wissenschaftlichen Leitung von PD Dr. Ottmar Janßen, ausschließlich mit der Unterstützung der Mitglieder seines Labors am Institut für Immunologie in Kiel, alle in dieser Doktorarbeit zusammengefassten Daten selbstständig erarbeitet habe. Außerdem versichere ich, dass für diese Doktorarbeit kein Dissertationsverfahren bei einem anderen Fachbereich oder einer anderen Hochschule beantragt wurde und wird.

Herewith I declare that all data presented in this thesis result from my own work that was performed under the scientific guidance of PD Dr. Ottmar Janßen with the help of members of his group at the Institute of Immunology in Kiel. I certify that I did not submit this dissertation to any other faculty or university.

Kiel, 19.04.2004

Jing Qian